NOTE TO USERS

DISSERTATION

UNRAVELING THE DIVERGENT BIOLOGICAL EFFECTS OF 3, 3',4 ,4',5-PENTACHLORO BIPHENYL (PCB 126):

TOWARD UNDERSTANDING THE ROLE OF GENE EXPRESSION

Submitted by

Mark S.V. Maier

Department of Environmental and Radiological Health Sciences

In partial fulfillment of the requirements

For the Degree of Doctor of Philosophy

Colorado State University

Fort Collins, Colorado

Spring 2005

COLORADO STATE UNIVERSITY

March 31, 2005

WE HEREBY RECOMMEND THAT THE DISSERTATION PREPARED UNDER OUR SUPERVISION BY MARK S. V. MAIER ENTITLED UNRAVELING THE DIVERGENT BIOLOGICAL EFFECTS OF 3,3',4,4',5-PENTACHLORO BIPHENYL (PCB 126): TOWARD UNDERSTANDING THE ROLE OF GENE EXPRESSION, BE ACCEPTED AS FULFILLING IN PART REQUIREMENTS FOR THE DEGREE OF DOCTOR OF PHILOSOPHY.

Committee on Graduate Work:

William H. Hanneman

John D. Tessari

Ronald B. Tjalkens

Colin M. Clay

Advisor – Marie E. Legare

Department Head – John D. Zimbrick

ABSTRACT OF DISSERTATION

UNRAVELING THE DIVERGENT BIOLOGICAL EFFECTS OF

3 ,3',4 ,4',5-PENTACHLORO BIPHENYL (PCB 126):

TOWARD UNDERSTANDING THE ROLE OF GENE EXPRESSION

Expression of genetic information encoded within DNA underpins the existence of life. Adaptive responses to chemical stressors may alter the levels and activity of gene-products and modify molecular interactions leading to downstream health effects. One mechanism by which chemicals can alter the activity of genes is by altering transcription of mRNA. Humans, in particular breast-fed infants, continue to be exposed to polychlorinated biphenyls (PCBs), specifically to the congener 3 ,3',4 ,4',5-pentachloro biphenyl (PCB 126, CAS # 57465-28-8, molecular weight 326.44) from environmental sources. PCB 126, and other related compounds such as the prototype halogenated aromatic hydrocarbon 2,3,7,8-tetrachlorodibenzo-*p*-dioxin (TCDD), are persistent environmental chemicals known to potently induce the activity of several important xenobiotic metabolizing enzymes in liver and other tissues. An important step in the cascade of events leading to enzyme induction is the transcriptional activation of genes encoding these enzymes. While it is unclear if the increased activity of these particular enzymes following transcriptional activation is directly responsible for toxicity, their induction is highly correlated with numerous toxic responses including events that increase the risk of cancer. The aim of this dissertation is to identify, on a transcriptome-wide basis, genes selectively activated or suppressed by PCB 126, and then connect these genes to previously observed biological effects of PCB 126. Knowledge of these linkages

should then provide additional weight-of-evidence for conclusions about human health risks from exposure to PCB 126 and other similar chemicals such as TCDD. Following a comprehensive literature review presented in this dissertation, it is clear that biochemical effects of PCB 126 in liver are well characterized and comparable to those of TCDD. Although epidemiological studies of PCB mixtures implicate PCB 126 as having a role in adverse neurodevelopment outcomes, experimental data to support this role are equivocal. For these reasons, it was decided to compare gene expression profiles of PCB 126 in xenobiotic-metabolizing liver and brain tissues using two methods capable of interrogating genome-wide transcriptional responses. The results of this research clearly demonstrate transcriptional responses to PCB 126 are unique between liver and brain tissues, a finding that points to the need for organ-specific risk assessment.

Research Hypothesis

Exposure of rat liver and brain tissues to PCB 126 causes changes in mRNA transcription of certain genes. These genes can be identified, and mRNA transcripts of these genes can be quantified and compared. In cases were gene ontology is defined, changes in transcription levels can be linked to biological effects and toxicity caused by PCB 126.

Mark S. V. Maier
Department of Environmental and
Radiological Health Sciences
Colorado State University
Fort Collins, CO 80523
Spring 2005

Dedication

To get one thing, one must often give up another. Economists call the thing you give up *opportunity cost*— a concept explained with words like *forgone* and *sacrifice*. When it came to raising their kids, my parents understood no such concept. Nothing done to ensure our success in life was a sacrifice; nothing was forgone; no opportunity cost. The one wish my parents held for each of us, was that we reach up and seize our grandest ambitions. Dad and Mom, your youngest child has climbed to one of those grand summits and holds dearly your single wish for me. It is to your interminable love, encouragement and support that I dedicate this achievement. I miss you.

Acknowledgements

The process of earning a doctorate of philosophy is self-seeking and abstract; it is a goal of immense endurance. It was for me, a mid-life discovery entangled with fuzzy distinctions between student and mentor. Through the haze of nontraditional roles, I extend to my mentors, my friends, to those of you who have shown the fortitude to guide me across the finish line, my heartfelt gratitude and utmost respect.

Marie Legare
Bill Hanneman
John Tessari
Ron Tjalkens
Colin Clay

Table of Contents

I. Introduction

Polychlorinated biphenyls (PCBs) are a group of persistent environmental chemicals eliciting a spectrum of toxic responses similar to those caused by the more potent aryl hydrocarbon receptor (AhR) agonist 2,3,7,8-tetrachloro-*p*-dioxin (TCDD) (van den Berg *et al.*, 1998). PCBs are fat soluble chemicals known to cross human placenta during pregnancy (Jacobson *et al.*, 1984; Wang *et al.*, 2004) and epidemiological evidence associates PCB exposures with cognitive and behavioral deficits in children (Jacobson *et al.*, 1990; Schantz *et al.*, 1996). Additionally, exposure to PCBs is associated with risk of cancers of the liver, gall bladder and biliary tract (Kimbrough, 1995). These health risks continue to be of concern because all humans have body burdens of PCBs and are continually exposed to low levels of PCB mixtures in the environment (Link *et al.*, 2005; NCEH, 2003).

PCBs occur in mixtures and there are more than 200 different PCB molecules that vary by number and arrangement of chlorine atoms around a biphenyl ring system. Quantitative structure-activity relationship (QSAR) studies indicate that 3 ,3',4 ,4'-tetrachloro (PCB 77), 3, 3'4 ,4',5-pentachloro (PCB 126), and 3, 3',4 ,4',5 ,5'-hexachloro (PCB 169) biphenyls exhibit toxic responses similar to the prototype dioxin TCDD, and PCB 126 is the most active PCB in assays developed to evaluate dioxin-like potencies (Safe, 1990; Safe, 1994). Although PCB 126 occurs at relatively low environmental concentrations, because it exhibits the most potent TCDD-like activity, this PCB congener contributes a high percentage of dioxin equivalent toxicity to exposure media.

Of particular concern are human bio-monitoring data that indicate PCB 126 contributes the most TCDD-equivalent toxicity of any PCB to foods often consumed by children such as breast milk and dairy milk, an to other foods such as fish and fats (Cramer *et al.*, 2001; Focant *et al.*, 2002; Focant *et al.*, 2003; Link *et al.*, 2005; Llobet *et al.*, 2003; Yang *et al.*, 2002; Zennegg *et al.*, 2004).

PCBs, TCDD and other halogenated aromatic hydrocarbons (HAHs) are known to alter gene expression in the liver (Vezina *et al.*, 2004). The most extensively studied gene expression changes caused by these compounds is the transcriptional activation and subsequent induction of the highly conserved xenobiotic metabolizing enzyme cytochrome P450 (CYP) gene family 1, subfamily A, members 1 and 2 (CYP1A1/2). Induction of CYP1A1/2 enzymes in the liver has been studied for decades and is regarded as a classic biomarker of exposure to HAHs (Safe, 1994). While TCDD is believed to be the most potent inducer of CYP1A1/2 activity; PCB 126 is the most potent among PCBs. Even though CYP1A1/2 induction is an exquisitely sensitive hallmark of exposure to HAHs in the liver, the toxicological consequences of CYP1A1/2 induction of itself is unclear. Despite this uncertainty, extensive mechanistic studies, primarily in liver, indicate that CYP1A1/2 induction and other forms of toxicity associated with TCDD and coplanar PCB exposure, are mediated by the AhR (Schmidt *et al.*, 1996). Because PCB 126 elicits many of the same toxic response as TCDD, and because PCB 126 and TCDD both strongly induce *CYP1A1/2* gene expression, it is commonly reasoned that both TCDD and PCB 126 interact with the AhR leading to altered expression of other important genes, and that this mechanism extends to other tissues. An essential goal of

the research presented in this dissertation, is to identify changes in gene expression caused by PCB 126, and then seek linkages between the biological role of these genes and known pathological changes caused by PCB 126. Additionally, this research tests whether extra-hepatic tissues exhibit transcriptional responses to PCB 126 that are comparable to liver.

In recent years, high-throughput screening techniques have lead to an inductive research paradigm in which theory and testable hypotheses are generated after observing and synthesizing large volumes of data. This approach is in contrast to the traditional deductive scientific method by which individual experiments are designed to test a hypothesis derived from some theory. In the present research, an inductive approach is used whereby the initial objective is to obtain quantitative, transcriptome-wide differential gene expression data after treating cells with PCB 126; and then test for both global and specific differences between treatments and controls, and between different tissues. Finally, after identifying differentially expressed genes, an attempt is made to explain observed differences within the context of gene function and observed effects of PCB 126. Afterwards, testable hypotheses are formulated from the analysis. At minimum, this endeavor necessitated the measurement of expression levels of more than 28,000 genes, which conceptually amounts to as many separate experiments. In order to assemble a context for understanding differential gene expression and to aid in experimental design, it was necessary to understand the biological effects of PCB 126. While there are several TCDD reviews (Pohl *et al.*, 2000; Schecter *et al.*, 2003), before now there was no comprehensive source of PCB 126 information despite its sentinel role

in coplanar PCB toxicity. Section II of this dissertation fulfills the need for a comprehensive review of PCB 126 and details the biological relevance of PCB 126 exposure at both the organismal and biomolecular levels.

Review of the pertinent literature afforded several observations that aided in the design of novel and relevant experiments. First, it is clear from experimental studies that PCB 126 exhibits a wide spectrum of biological effects, ranging from classic responses strongly correlated with AhR-mediated CYP1A1/2 induction such as hepatomegaly (Chu *et al.*, 1994) and thymic atrophy (Andersson *et al.*, 1991), to novel effects demonstrated in certain species such as osteolysis in mink jaws (Render *et al.*, 2000a) and hepatocarcinogenicity in rats (NTP, 2004). Second, there is epidemiological evidence linking PCB exposure to cognitive deficits in children (Seegal, 1996). Experimental data demonstrating a role for PCB 126 in neurocognitive development is equivocal and ranges from adverse effects (Bernhoft *et al.*, 1994; Holene *et al.*, 1995), to no effect (Rice *et al.*, 1998), to improved performance (Schantz *et al.*, 1996). From the literature, several important unanswered questions emerge with the potential to be addressed by comprehensive gene expression data, including:

1. Does PCB 126 cause different transcriptional responses in different tissues given the spectrum of effects observed in different organ systems in experimental studies?
2. Does the transcriptional response in brain tissue explain the variable effects of PCB 126 on neurodevelopment?
3. Does the transcriptional profile of PCB 126 in liver, reveal activated or suppressed genes that could play a role in carcinogenesis?

These questions lead to experimental designs able to observe genome-wide transcriptional effects of PCB 126 on xenobiotic metabolizing tissues of both liver and brain. This research endeavor revealed different gene expression patterns in different tissues that are both surprising and intriguing. It was demonstrated that the transcriptional response exhibited by astrocytic brain cells to PCB 126 is uniquely different from the response of hepatic cells. Furthermore, the response of astrocytic cells to PCB 126 is explained by a transcriptional activation mechanism that probably does not involve the AhR. Results of this research bring the putative role of the AhR in extra-hepatic tissues into question, and provide evidence for a novel mechanism of action for dioxin-like PCB 126. The comprehensive literature review of PCB 126 is first presented in Section II of this dissertation. The result of two experimental approaches for observing transcriptome-wide expression changes are presented in Section III, and finally, a unifying Discussion is provided.

II. PCB 126 Review

A. PCB PRODUCTION

PCB 126 is a toxicologically important member of the entirely anthropogenic polychlorinated biphenyl (PCB) family of compounds. Commercial PCBs were produced by the chlorination of biphenyl resulting in synthesis of mixtures that were marketed according to weight of chlorine content. Worldwide production of PCBs began in 1929 and has been slowly phased out over the last three decades, with PCBs being produced in Russia as late as 1992 (PCB Steering Group, 2000). Of the 1.25 billion pounds of PCBs produced between 1929 and 1977, and in the U.S. alone, at least 450 million pounds were released to the environment (ATSDR, 2000). It is estimated that 1.5 million metric tons of these environmentally persistent mixtures were produced worldwide for many purposes, but the largest quantities were used for heat transfer and dielectric fluids. PCBs released into the environment continue to be cycled globally, primarily through volatilization, and secondarily by redistribution of PCBs bound to sediments (ATSDR, 2000).

B. NOMENCLATURE

The underlying chemical structure of PCBs is the biphenyl ring system shown in Figure 2.1. Biphenyl is a dual 6-carbon aromatic (benzene) ring system linked by a carbon-carbon single bond. With two aromatic rings linked in this way, it is possible to attach chlorine atoms to ten possible carbons, numbered 2 - 6 on one ring, and 2' ("two-prime") - 6' on the other ring. By convention, the 1 and 1' positions are carbons that join the two rings.

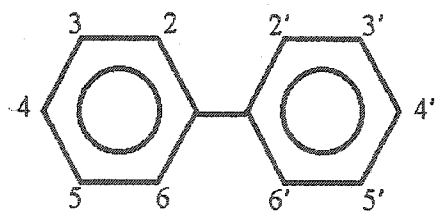

Figure 2.1. 1, 1'-Biphenyl. The underlying hydrocarbon framework for polychlorinated biphenyls (PCBs) is the biphenyl ring system. The ring positions available for chlorine substitutions are numbered 2-6 and 2'-6' for each ring, respectively.

Replacing hydrogen atoms (not shown) with chlorine atoms at available ring positions yields chlorinated biphenyl. A biphenyl species with a single chlorine substituent would be called "*mono*chlorobiphenyl", a species with two chlorines is "*di*chlorobiphenyl", and those species with three through ten chlorines, would be: "*tri*", "*tetra*", "*penta*", "*hexa*", "*hepta*", "*octa*", "*nona*", and "*deca*chlorobiphenyl", respectively. Any unique arrangement of 1-10 chlorine atoms on biphenyl is known as a PCB *congener*. The chemical name of a particular congener specifies the total number of chlorine substituents and the position of each chlorine atom. For example, the PCB congener shown in Figure 2.2A is named 3, 3',4 ,4'-tetrachlorobiphenyl. There are 209 unique chlorine arrangements, and hence 209 different PCB congeners (USEPA, 2003). In 1980, a system was proposed to identify all 209 PCB congeners with sequential numbers, whereby 3, 3',4, 4',5-pentachloro biphenyl was designated as PCB *126* (Ballschmiter *et al.*, 1980; USEPA, 2004).

Aroclors

During the PCB manufacturing era in the United States, Monsanto produced mixtures of PCB congeners called Aroclors. These mixtures were synthesized in a batch process by heating biphenyl and adding anhydrous chlorine in the presence of ferric chloride.

Different degrees of chlorination were required to synthesize Aroclors having the desired physical and thermal properties. The average degree of chlorination in an Aroclor batch is controlled mostly by reaction time. Different reaction mixtures were designated with Monsanto's *Aroclor* trademark followed by a four-digit number. The first two digits indicate a biphenyl mixture and the second pair of digits indicate the total percent weight of chlorine in the mixture. For example, Aroclor 1232 is a chlorinated biphenyl mixture with 32-percent chlorine. Aroclor 1016 is an exception to the Aroclor numbering scheme with 41-percent chlorine. As the biphenyl chlorination reaction proceeds, certain PCB congeners may continue to accept chlorine at the same rate, or at least at some predictable rate, thus the ratio of some congeners with respect to others is usually constant between batches of commercial PCB mixtures (Erickson, 1997). PCB 126 is primarily present in Aroclor 1254 (0.02% by weight) with trace amounts in Aroclor 1248 (Frame *et al.*, 1996).

C. STEREOCHEMISTRY

Different PCB congeners can interact differently with biological systems owing to unique structural and stereochemical diversity. PCB congeners are often divided into two general categories that define their biological activities and are based on properties that define the spatial configuration of the biphenyl rings; namely *coplanar* PCBs and *non-coplanar* PCBs. Respectively, Figure 2.2 depicts the coplanar PCB 3, 3',4, 4'-tetrachloro biphenyl (PCB 77) and the non-coplanar-PCB 2, 2',4, 4'-tetrachloro biphenyl (PCB 47). These two PCB congeners are structural isomers of one another and have identical empirical formulas (C_{12} H_6 Cl_4). Nonetheless, these structural isomers exhibit different toxicological properties. This difference is assumed to be related to molecular geometry

attributable to steric hindrance that prevents free ring rotation about the single carbon-carbon bond that connects the biphenyl rings.

As shown in Figure 2.2B, 2, 2',4, 4'-tetrachloro biphenyl is di-*ortho* substituted (i.e., two chlorine substituents at the 2 and 2' positions). Di-*ortho* configurations prevent free rotation of the biphenyl rings, and thus precludes the ability of both rings to exist in the same geometric plane (i.e., the rings are "non-coplanar"). Although 3, 3',4, 4'-tetrachloro

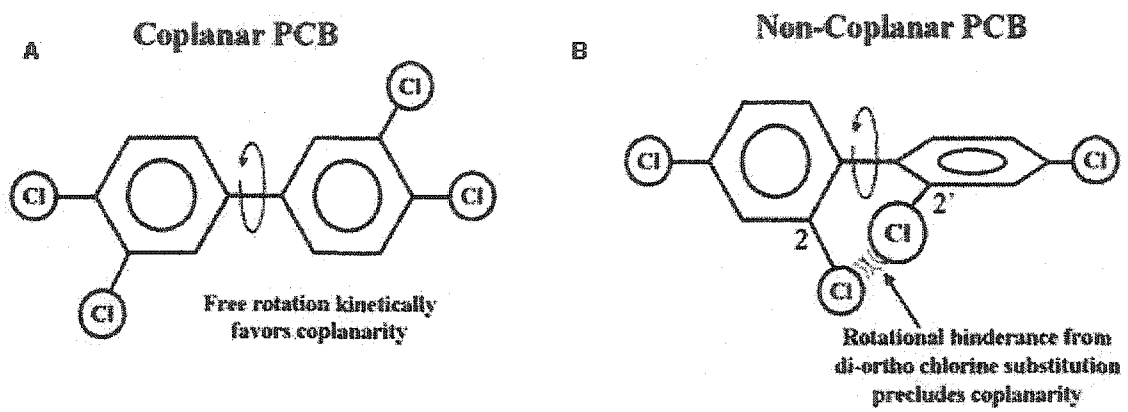

Figure 2.2. Coplanar and non-coplanar PCB congeners. Configurations exhibited by two PCB congeners with identical empirical formulas. Aromatic rings lacking di-ortho substitutions are free to rotate, kinetically favoring a flat (coplanar) configuration (A). Aromatic rings with di-*ortho* chlorine substitutions (i.e., 2, 2'-dichloro) are sterically directed into a non-coplanar configuration (B). These PCB congeners have different biochemical activity.

biphenyl (Figure 2.2A) is not strictly precluded from assuming a non-coplanar configuration, co-planarity is energetically favored, and hence this molecule exhibits coplanar properties. PCBs with mono-*ortho* chlorine substitution (i.e., 2-monochlorobiphenyl) often exhibit biochemical behavior similar to di-*ortho*, non-coplanar PCBs. Di-*ortho* substituted PCB congeners appear to have the highest bioavailable mass, principally because these congeners predominate in commercial mixtures (Frame *et al.*, 1996). Unlike most congeners, di-*ortho* congeners are slightly

soluble in the water column and thus partition into the vapor phase and hence are transported world-wide by the atmosphere (Baker *et al.*, 1990).

D. DIOXINS

PCBs co-occur with dioxin in the environment. Although there have been rare occupational and accidental exposures to PCBs only, or dioxins in the presence of chemicals other than PCBs, dioxins and PCBs always co-occur in contaminated environmental media. Similarly, human body burdens consist of both dioxins and PCBs. For this reason, it is generally difficult to distinguish the health effects of PCBs from the health effects of dioxins. Experimentally controlled studies in which animals are exposed to individual dioxins or PCB congeners provide clues that associate certain health hazards with particular PCBs. Generally, these adverse health effects are classified as either "dioxin-like" or "non-dioxin-like". In the broadest sense, dioxins and coplanar PCBs are "dioxin-like" while non-coplanar mono- and di-*ortho* substituted PCBs are "non-dioxin-like"(Safe, 1994). The PCB congener 126 studied in the present research, is a coplanar dioxin-like PCB.

In most instances, the term "dioxins" collectively refers to two chemical classes shown in Figure 2.3. These classes are the polychlorinated dibenzo-*p*-dioxins (PCDDs) and the polychlorinated dibenzofurans (PCDFs), Figures 2.3A, and 2.3B, respectively. Like PCBs, these chemicals are generically classified as halogenated aromatic hydrocarbons (HAHs). PCDDs include 75 congeners, and PCDFs include 135 different congeners. It is generally believed that only 7 PCDD congeners and 10 PCDF congeners exhibit "dioxin-like toxicity", and at minimum, dioxin-like toxicity requires chlorine and/or bromine

substitutions at the 2,3,7,8 ring positions (USEPA, 2000). The most widely studied of these compounds is TCDD (often simply called "dioxin"). TCDD represents the reference compound for PCDDs and PCDFs. Unlike PCBs, PCDDs and PCDFs do not have a single carbon-carbon bond between aromatic rings to permit ring rotation. For this reason, TCDD, like other PCDDs and PCDF, can only exist as coplanar molecules.

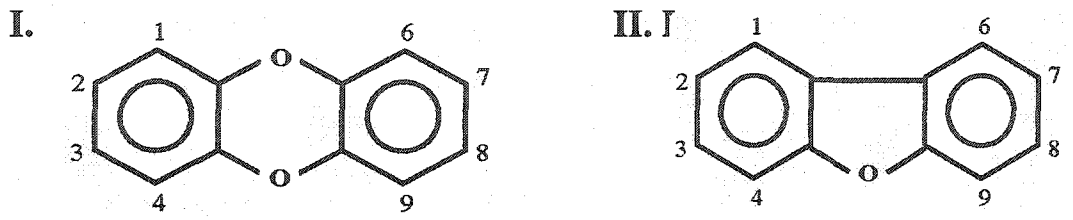

Figure 2.3 Dibenzo-*p*-dioxin (A) and dibenzofuran (B). Dioxin-like toxicity for either chemical requires halogen (chlorine or bromine) substitution in at least the 2,3,7,8 ring positions.

E. EQUIVALENT TOXICITY

TCDD and 1,2,3,7,8-pentachlorodibenzo-*p*-dioxin are commonly regarded as being the most toxic HAHs. Consequently, in risk assessments when toxicity comparisons or risk estimates associated with HAH mixtures are needed, these most toxic compounds are assigned relative toxic equivalency factor (TEF) of unity and, depending on toxicity and AhR binding affinity, less potent HAHs are assigned TEFs less than 1 and that range upward from 0.0001. PCB 126 used in this study, is unique because it has the highest TEF of any PCB and is commonly assigned a TEF value of 0.1; this indicates PCB 126 exhibits dioxin-like toxicity with $1/10^{th}$ the potently of TCDD.

There are extensive and convincing arguments for the additivity of TEFs for most toxic endpoints, and hence TEFs are widely used to assess health risks from exposure to environmental mixtures containing coplanar PCBs, PCDFs and PCDDs (Cal-EPA, 2003). On the other hand, TEFs are problematic when used to evaluate risk associated with individual or small subsets of PCB congeners because of substantially dissimilar dose-response relationships between different PCBs, PCDFs and PCDDs. Nonetheless, coplanar PCBs, PCDFs and PCDDs at minimum have the common AhR mechanism of action involving gene expression that underlies the rationale for the present differential gene expression research.

Because the toxicity of PCB 126, and certain other coplanar PCBs, have the AhR mechanism in common with TCDD for certain responses in some organs, risk assessments often apply TEFs and assume the subsequent scaled doses are additive. The underlying assumption for making these comparisons is that HAHs act via a common AhR mediated mechanism. Indeed, there is considerable scientific evidence to indicate dioxin-like coplanar PCBs exhibit dose-responses for many effects that can be scaled to TCDD toxicity using toxic equivalency factors (TEFs) (DeVito *et al.*, 2000; Safe, 1994). While numerous TCDD studies report the role of the AhR in extra-hepatic tissues, most investigations into the role of the AhR in mediating effects of PCB 126, center around the AhR's role in mediating gene expression in adult rodent liver tissues.

F. ARYL HYDROCARBON RECEPTOR (AHR)

Almost fifty years ago, it was recognized that polycyclic aromatic hydrocarbons (PAHs) induce the activity of a group of microsomal enzymes collectively referred to as

arylhydrocarbon hydroxylase (AHH) (Conney *et al.*, 1956). Data from several studies suggested the existence of a receptor encoded by the *Ah* gene locus. Poland *et al.* first identified a cytosolic protein in mouse liver that had low-capacity (~ 105 sites/mouse liver cell) and high affinity (K_d ~ 0.7 nM) for [^{3}H]-TCDD (Poland *et al.*, 1976). Subsequent studies identified this protein receptor as the AhR and confirmed its role in dioxin and coplanar PCB toxicity using mechanistic information derived from research on structure-activity relationships (reviewed in: (Pohl *et al.*, 2000)). Ultimately, it was recognized that induction of aryl hydrocarbon-metabolizing enzymes was occurring at a single genetic locus. Furthermore, this enzyme induction was adaptive because acute re-exposure to high levels of the same PAHs resulted in more rapid oxidation and less toxicity than would have occurred in the absence of prior exposure. This adaptive genetic locus became known as *Ah*, for "aryl hydrocarbon" responsiveness, since the gene responded to aryl hydrocarbons such as PAHs (Eppig, 1993; Green, 1973; Thomas *et al.*, 1973). Additionally, numerous studies support the conclusion that binding to the AhR is an essential first step for dioxin-like toxicity (Birnbaum, 1994a; Birnbaum, 1994b; Hankinson, 1995; Okey *et al.*, 1994; Safe, 1990).

The AhR protein is a cytosolic ligand-activated transcription factor involved in the regulation of cellular growth, differentiation, and metabolism. Additionally, AhR-mediated gene expression plays a role in such critical biological processes as cell differentiation, cell division, and apoptosis (Micka *et al.*, 1997). Recent investigations with *Caenorhabditis elegans* demonstrate a role for the AhR in neuronal development (Qin *et al.*, 2004). For *C. elegans* at least, the AhR is expressed only in certain neurons,

and organisms that lack AhR function have specific defects in neuronal differentiation, including altered morphology and defects in cell and axonal migration.

The AhR is conserved across species and occurs in most, but not all, tissues and organs (Carlson *et al.*, 2002). The AhR is a member of the large basic Helix-Loop-Helix (bHLH) homology domain family of transcription factors that includes the *Drosophila* circadian rhythm protein PER (period). These proteins are involved in myoblast differentiation (e.g., myogenic differentiation antigen 1) and the cellular response to hypoxia (e.g., the AhR nuclear translocator (ARNT) also know as hypoxia inducible factor (HIF)-1β), and the *Drosophila* neurogenic protein SIM (single-minded, a regulator of CNS

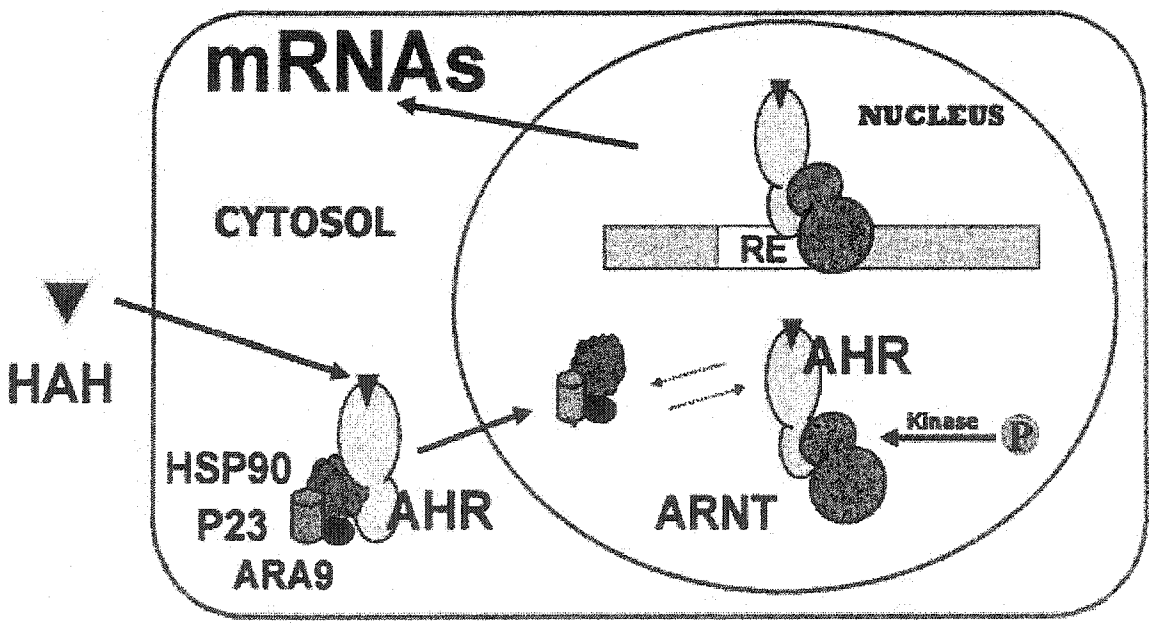

Fig 2.4 Putative mechanism for induction of cytochrome P450 1A1 by halogenated aromatic hydrocarbons (see text).

Abbreviations: AhR, aryl hydrocarbon receptor; **ARA9**, AhR-activated protein 9; **ARNT**, aryl hydrocarbon nuclear translocator basic helix-loop-helix (HLH)-periodicity/ARNT/single-minded [Per/ARNT/Sim (PAS)] transcription factor; **HAH,** halogenated aromatic hydrocarbon (e.g., TCDD or PCB 126); **HSP90**, heat shock protein, 90 kDa; **P23**, HSP90-associated co-chaperone protein, 23 kDa; **RE**, response element.

development). The "PAS" designation is derived from the first letter of the bold underlined acronyms just mentioned. The bHLH-PAS multi-domain proteins generally form heterodimeric transcription factors, of which AhR is the only member conditionally activated in response to ligand binding. In the absence of ligand, the AhR is maintained as an inactive cytosolic complex with two molecules of the 90-kDa heat-shock protein (HSP90), plus other proteins. In most species, HSP90 is needed to maintain the unliganded receptor in a ligand binding configuration (Pongratz *et al.*, 1992).

A simplified scheme for CYP1A1 induction is shown in Figure 2.4. Enzyme induction via the AhR proceeds after ligand is bound within the PAS domain of cytosolic AhR. In association with chaperone proteins such as Hsp90, p23, Ara9, and others, the AhR is translocated to the nucleus where it undergoes a conformation change, dissociates from chaperone proteins and dimerizes with the aryl hydrocarbon nuclear translocator basic helix-loop-helix (HLH)-periodicity/ARNT/ single-minded [Per/ARNT/Sim (PAS)] transcription factor (ARNT) (Carver *et al.*, 1997; Gasiewicz *et al.*, 2003; Hollingshead *et al.*, 2004). The AhR/ARNT heterodimer then interacts with DNA sequences know as response elements (REs). Few proteins can bind to the major RE-containing enhancer regions in the absence of HAH ligand; this is due to inaccessibility conferred by the configuration of nucleosomal proteins (Wu *et al.*, 1992; Wu *et al.*, 1993). REs present in the 5' regulatory regions of *CYP1A1* genes are responsible for initiating transcription (Denison *et al.*, 1988a; Denison *et al.*, 1988b). The RE consensus sequence, 5′-TNGCGTG-3′ occurs upstream of target genes and functions to activate/repress transcription of target genes. The RE upstream of the *CYP1A1* gene consists of both a

transcriptional promoter and an enhancer region. The former ensures that transcription is initiated at the correct site. Neither the enhancer nor the promoter will function in the absence of the other (Jones *et al.*, 1990).

Studies of the *CYP1A1* promoter demonstrate a proximal transcriptional promoter region spanning about 150-bp with several sites for protein binding; this region is necessary for transcriptional activation (Creasey *et al.*, 2002). This activation region includes a TATA box (consensus 5'-TATAAA-3') at about minus-25 upstream of the transcription start site. This TATA region is involved in RNA polymerase binding via a TATA-protein, a guanine rich G-box element, and two binding sites for transcription factor nuclear factor-1 (consensus 5'-TTTTGGATTGAAGCCAATATGATAA-3' (Jones *et al.*, 1990; Leegwater *et al.*, 1985). These observations lead to a model in which receptor interactions with multiple upstream REs facilitate chromatin disruption which allows downstream promoter elements to bind their respective factors and initiate transcription (Okino *et al.*, 1995; Wu *et al.*, 1992). It appears that increased production of CYP1A2, CYP1B1, glutathione S-transferase Ya subunit, NADPH quinone reductase 1 and 3, and class 3 aldehyde dehydrognease also occurs by a similar mechanism (Schmidt *et al.*, 1996).

Induction of xenobiotic metabolizing enzymes in the cytochrome P450 1 subfamily (i.e., CYP1A1, CYP1A2 and CYP1B1) is a robust response to HAH exposure and occurs in a variety of different animal species, including humans. Induction of these genes may be responsible for substantially increased rates of metabolic substrate activation to genotoxic

intermediates or carcinogens. Following AhR binding, TCDD and other HAH ligands cause alteration in transcription and translation of a number of genes including oncogenes and genes encoding growth factors, receptors, hormones and xenobiotic metabolizing enzymes (Birnbaum, 1994a; Birnbaum, 1994b). Kinases involved with various signal transduction processes and cell cycle control are also affected by ligand binding (Weiss *et al.*, 1996).

HAHs modulate signal transduction processes and gene expression by at least two pathways that include direct interaction of the AhR and its heterodimer partners with gene regulatory elements, and initiation of a phosphorylation-dephosphorylation cascade and subsequent activation of other nuclear transcription factors (Enan *et al.*, 1996; Matsumura, 1994; Pohl *et al.*, 2000). Interestingly, the prominent pathway appears to differ between acute and chronic exposure to dioxin-like compounds and during different developmental periods. Ligand binding was observed to result in rapid depletion of AhR in both cell culture and animal studies (Pollenz *et al.*, 1998; Roman *et al.*, 1998). This suggests that AhR protein may itself be important in the regulation of AhR-mediated signaling. The complexity of AhR signaling has been further complicated by a recent finding that the AhR also participates in posttranscriptional regulation of gene expression (Falahatpisheh *et al.*, 2003).

Development of AhR deficient mice, AhR(-/-), permits definitive evaluation of the role played by the AhR (Fernandez-Salguero *et al.*, 1995). Although AhR(-/-) mice are viable, they have slower growth rates, decreased fertility, and reduced liver size; expression of

these phenotypes appears related to altered vascular architecture during development (Lahvis *et al.*, 2000). Using AhR deficient mice, investigators demonstrated that many toxic effects of halogenated aromatic hydrocarbons, including PCB 126 and TCDD, depend on the AhR. For example, it was found that fetuses of TCDD-treated pregnant AhR(-/-) mice did not develop hydronephrosis or cleft palate typical of similarly treated AhR(+/+) mice (Mimura *et al.*, 1997). In another study, it was found that thymic atrophy induced by TCDD did not occur in AhR(-/-) mice (Fernandez-Salguero *et al.*, 1996).

1. AhR Polymorphisms

The AhR protein has numerous intra-species polymorphisms whereby different *AhR* alleles produce receptors with different molecular weights and different primary structures (Poland *et al.*, 1986; Poland *et al.*, 1994). Cloning studies demonstrated that differences in molecular weight result from differences in the position of the translation termination codon, but not because of differential splicing or posttranslational protein modification (Carver *et al.*, 1994; Dolwick *et al.*, 1993; Poland *et al.*, 1994; Schmidt *et al.*, 1993)

Individual AhR mediated responses exhibit a high degree of variability. In mice, a polymorphism based on a single nucleotide difference in the ligand binding domain of the AhR was sufficient to reduce ligand affinity by more than 10-fold in certain strains (Fernandez-Salguero *et al.*, 1996). Also, based on a follow-up study in humans exposed to TCDD from the Seveso accident, mean serum lipid TCDD concentrations of children with chloracne averaged 18,700 ppt (range of 1,680 to 56,000 ppt). Despite this, some

individuals with higher serum TCDD levels did not develop chloracne. Such variability in humans appears to be the result of AhR polymorphisms (Needham *et al.*, 1997).

Inter-individual variation for CYPIA1 induction may vary up to 103-fold in humans (Smart *et al.*, 2000). At least four genetic polymorphisms of the *CYP1A1* gene are known; these are termed: *CYP1A1**2A, *CYP1A1**2B, *CYP1A1**3 and *CYP1A1**4. The *CYP1A1**2A polymorphism is associated with significantly increased lung cancer in a Japanese population, but not found to be significant in a Caucasian population, possibly due to lower polymorphism frequency. The *CYP1A1**3 polymorphism is specific to African Americans, but was not associated with increased risk for an adverse health effect. The role of *CYP1A1**4 polymorphism has yet to be characterized.

2. AhR Ligands

Many anthropogenic chemicals have AhR affinity. HAHs with AhR affinity include twelve non-di*ortho* substituted, tetra-, penta- and hexa-chloro PCB congeners (including PCB 126), six polychlorinated dibenzodioxins (including TCDD), and ten polychlorinated dibenzofurans. Additionally, halogenated naphthalenes, chlorinated paraffins, and hexachlorobenzene have measurable AhR affinity (USEPA, 2000). Unsubstituted polycyclic aromatic hydrocarbons (PAHs) can also bind the AhR with moderate to high affinity (Chaloupka *et al.*, 1993; Nebert, 1989; Poland *et al.*, 1982). Many chemicals such as hexachlorobenzene and the brominated diphenyl ethers are weakly dioxin-like, but have significant toxicological effects not mediated by the AhR. Brominated homologs of dioxins, benzofurans, biphenyls and naphthalene also induce

dioxin-like effects in experimental animals (Birnbaum *et al.*, 1991; Miller *et al.*, 1986; Weber *et al.*, 1997).

In contrast to anthropogenic AhR ligands, naturally occurring AhR ligands generally exhibit little environmental persistence and are not addressed in most environmental risk assessments. Such naturally occurring AhR ligands include, indole derivatives such as indole-3-carbinol (I3C), 3,3'-diindolylmethane (DIM), and indolocarbazoles (ICZs). Heterocyclic aromatic amines and oxidized essential amino acids also have AhR affinity. Indole chemicals such as I3C and DIM are present in a variety of cruciferous vegetables. At least two secondary metabolites of these indoles are capable of inducing phase I and II metabolic enzymes (CYP1A-dependent glutathione and glucuronyl transferases, and oxidoreductases) in experimental animals (Bradfield *et al.*, 1987) and humans (Michnovicz *et al.*, 1991). The ICZ, indolo[3,2b]carbazole, exhibits high binding affinity for the rodent AhR (approximately equal 2,3,7,8-tetrachlorodibenzofuran) and can induce CYP1A1 activity in cultured cells (Chen *et al.*, 1995). Other dietary AhR ligands appear to be formed in cooked meat. Experimental animals and humans fed thermally treated meat protein exhibited CYP1A2 induction (Degawa *et al.*, 1989). The aspartate aminotransferase catalyzed tryptophan metabolite, indole-3-pyruvate, acts as a proagonist that, although not an AhR ligand itself, endogenously produces a family of metabolites that are AhR agonists; interestingly some of these agonists not only induce CYP1A1, but are metabolized by it (Bittinger *et al.*, 2003; Wei *et al.*, 2000). Taken together, there is a considerable data to support the conclusion that the AhR evolved to respond to numerous hydrophobic by-products of normal metabolism (Denison *et al.*, 2002).

3. AhR Inducible Enzyme Systems

Early animal studies found that PCB congeners could be classified into two categories based upon enzyme induction, the 3-methylcholanthrene (MC) type and the phenobarbital (PB) type (Conney, 1967; Snyder *et al.*, 1979). Concurrent with the ability to unambiguously synthesize PCB congener 126 (Saeki *et al.*, 1979), Ozawa and coworkers demonstrated that PCB 126, like TCDD, is an MC-type inducer (Ozawa *et al.*, 1979). PCB 126 is the most potent PCB congener for enhancing activity of a variety of xenobiotic enzymes including, aryl-hydrocarbon hydroxylase (AHH), ethoxyresorufin *O*-deethylase (EROD), cytochrome P450-dependent monooxygenase and benzo[a]pyrene (BP) 3-hydroxylase in liver; CYP1A1, CYP1A2 and CYP2A1 are the inducible MC-type isoforms of cytochrome P450 (Bradlaw *et al.*, 1979; Chu *et al.*, 1994; Safe, 1994; Yoshimura *et al.*, 1979).

EROD activity and acetanilide 4-hydroxylase activity (ACOH) were used as markers to evaluate PCB 126 induction of CYP1A1 and CYP1A2, respectively (DeVito *et al.*, 2000). EROD induction was evaluated in mouse liver, lung and skin, and ACOH was evaluated in mouse liver. Clearly, PCB 126 induced EROD and ACOH activities in all tissues evaluated which included liver, lung, and skin. LOAELs for both enzyme activities ranged from 0.045 µg/kg/d (EROD in lung) to 1.5 µg/kg/d (EROD in liver). Interestingly, the relative potency of PCB 126 versus TCDD, was dose-dependent for liver and lung EROD induction, while in skin, the potency for EROD induction was linear across all doses (0.015 – 1.5 µg/kg/d, 5d/wk for 13 weeks by gavage) with a

LOAEL of 8 ppb. ACOH induction by TCDD in liver was also linear with a tissue dose LOAEL of 47 ppb.

Prior to research that distinguished the cytochrome P450 isoforms, Yoshimura and colleagues, set out to compare total CYP and the acute toxicity of PCB 126 and PB-type *ortho*-substituted inducers (2,3,4,4'- and 2,2',5,5'-tetrachloro biphenyl in young male Wistar rats (Yoshimura *et al.*, 1979). They compared CYP induction and the effects of these congeners on growth rate, organ weight and liver lipid content, 5 days after an extremely large single intraperitoneal injection (100,000 μg/kg). The PB-type inducers slightly increased total CYP content in liver, but did not show any significant toxicity. In contrast, PCB 126 substantially increased total CYP in liver, and strongly reduced overall growth rate and the weights of thymus and spleen. Liver enlargement accompanied by fatty liver was also observed only with PCB 126 treatment. It is interesting to note, in contrast to PCB 126, mono-*ortho* and di-*ortho* substituted PCBs tend to be PB-like inducers for such cytochrome-P450 isoforms as CYP2B1, CYP2B2 and CYP3A (Safe, 1994); in particular, CYP2B1 induction is mediated by a nuclear receptor, different from the AhR, known as the constitutive androstane receptor (CAR) (Muangmoonchai *et al.*, 2001).

It was demonstrated by others in our laboratory that CYP1A1 induction in the liver is regional and switch-like in individual cells. In rats dosed 3 times per week for 6 wks with PCB 126, induction of CYP1A1 in the liver appeared at low dose (0.1 μg/kg/d) in the centrilobular region and progressed to panlobular regions only with higher dose (1.0

μg/kg/d) (Chubb *et al.*, 2004). The number of liver cells, exhibiting all-or-none switch-like induction of CYP1A1 following PCB 126 exposure *in vitro*, was also dose-dependent (Broccardo *et al.*, 2004; French *et al.*, 2004).

G. HUMAN EXPOSURE

Epidemiological investigations of accidental exposures to HAHs dating back to the Vietnam War era, have associated HAH exposure with overt toxicity and to increased risk of subtle adverse health effects in exposed humans. More recently, structure-activity, genetic, and molecular biological studies of HAHs were able to link many hallmark toxic responses of these compounds to AhR mediated processes (Schecter *et al.*, 2003). The relationships between HAHs, the AhR, and certain biological effects have become dogma for assessing risks of HAH exposure. Indeed, health effects connected to AhR activation are supported by hundreds of animal studies that demonstrate stereoselective interactions of diverse HAH ligands with the AhR and demonstrate rank-order correlations between molecular structure and toxicity relationships of these ligands (Safe, 1994). AhR activation by many HAHs, including PCB 126, is a hallmark for effects on vascular, renal, cardiac, skin, bone marrow, liver, eye, ovary, immune system function, and carcinogenesis (Denison *et al.*, 2003). Interestingly, there is a dearth of data implicating AhR activation in neurological effects.

Some biological effects are universal for HAHs, while other effects can only be demonstrated for TCDD, Aroclors, certain HAH mixtures, or specific PCB congeners. Mono-*ortho* substituted PCBs for example, have extremely low affinity for the AhR with extremely low dioxin equivalent toxicity; TEFs for mono-*ortho* PCBs range from

0.00005 to 0.001 (Safe, 1994). Di-*ortho* substituted PCB congeners (i.e., non-coplanar PCBs) are particularly distinctive because they do not appear to be AhR ligands at all, and they produce unique forms of neurotoxicity (Shain *et al.*, 1991; Tilson *et al.*, 1997).

Because no human data are available for the biological effects of PCB 126 alone, *in vivo* human effects of PCB 126 exposure must be inferred from epidemiological and clinical data from accidental exposure to mixtures, or extrapolated from animal or *in vitro* studies. In some cases, the effects of concurrent exposure to multiple HAHs may not be specifically relevant to PCB 126. In fact, as previously noted, some commercial mixtures contain small concentrations of PCB 126. Additionally, the presence of *ortho*-substituted PCBs is demonstrated to mute the toxicity and alter the pharmacokinetics of coplanar PCBs such as PCB 126 (Lee *et al.*, 2002).

1. Chloracne

Perhaps the most unambiguous and historically important effect in humans exposed to mixtures of dioxins and/or PCBs is the dermal disease chloracne. Because there are no cases in which humans were exposed to a single PCB congener, there are no chloracne cases specifically attributable to PCB 126. Nonetheless, given the putative role of the AhR in the toxicity of other HAHs known to cause chloracne, and given that PCB 126 is a potent ligand for the AhR in most tissues, it is likely PCB 126 alone would cause this disfiguring disease.

Chloracne manifests as an acne-like eruption of comedones, cysts, and pustules. Lesions are extremely persistent and resist usual acne treatment regimens (DermNet New

Zealand, 2004). During 1968, in northern Kyushu, Japan there was an outbreak of chloracne. Following an intensive epidemiological study it was discovered that everyone afflicted with chloracne had consumed Kanemi brand rice oil (Kuratsune *et al.*, 1969). The disease was termed Yusho ("yu" means oil and "sho" means disease in Japanese) and was found to be caused by ingesting rice oil contaminated with PCBs and dioxins (generated by PCB pyrolysis) from a leaking heating tube in a rice oil tank. In addition to chloracne in exposed individuals, Yusho neonates exposed lactationally were reported to have poor cognitive development, gingival hyperplasia and premature eruption of teeth (Yamashita *et al.*, 1985). In 1979, a similar incident occurred in Taiwan, also from rice oil contaminated with PCBs and PCB pyrolysis products. The disease associated with this incident was termed "Yucheng" ("yu" means oil and "cheng" means syndrome, in Chinese) (Hsu *et al.*, 1985). In Yusho patients, total PCB levels in liver, adipose, and blood were reported to be 18-226 ppb, 200-6,000 ppb, and 6.7 ppb, respectively (Aoki, 2001); also in Yusho patients, it was determined that the severity and rapidness of chloracne onset followed a dose response (based on amount of oil consumed). Residual chloracne may last for decades (mean duration of 26 years) and in some cases lesions persisted more than 30 years after the original exposure (Moses *et al.*, 1984). Although at the time of these accidents individual congeners could not yet be quantified, by examining contaminated rice oil samples it was later found that commercial PCB mixtures released into the rice oil, contained 68-100 ppm PCB 126 (Kannan *et al.*, 1987). Also, more than 15 years after the accident, exposed patients continued to have elevated PCB 126 concentrations in liver and small intestine (Kashimoto *et al.*, 1987; Koga *et al.*, 1990).

2. Body Burdens

Perhaps one of the most divisive issues regarding the health effects of HAHs in general, is trying to understand what body burdens of which chemicals, cause what health effects (Schecter *et al.*, 2003). Although humans are continually exposed to PCBs in the environment, body burdens of total-PCBs are generally decreasing in humans while burden trends for other HAHs are relatively constant. Trend data for PCB 126 body burdens are limited, but recent data from Germany indicate overall decreases of about 14% over the past decade (Link *et al.*, 2005). Recent cross-sectional data collected from 1999 to 2000 in the United States, show human serum concentrations of PCB 126 range from level-of-detection (≈ 9 pg/g), to 120 pg/g (ppt) on a lipid weight basis (NCEH, 2003). Interestingly, these data are highly right-skewed, indicating there is a disproportionate number of highly exposed individuals. In addition to its large contribution to TCDD equivalent toxicity, PCB 126 is a sentinel for the presence of other HAHs. In breast milk, there is a high correlation between the presence of PCB 126 and TCDD, as well as with other dioxin-like PCBs (Atuma *et al.*, 1998; Glynn *et al.*, 2001). Breast-fed infants appear to be among individuals most highly exposed to PCBs. In a 1996 New York State angler study, total PCB concentrations in samples of blood and breast milk from lactating women who routinely ate sport fish were 320-728 ng/g and 239-428 ng/g (ppb) lipid for serum and breast milk, respectively (Greizerstein *et al.*, 1999; Vena *et al.*, 1996). These levels are similar to earlier New York data where mean breast milk concentrations were 271± 116 ng/g lipid (Kostyniak *et al.*, 1999). In a recent Finnish study, breast milk from urban and rural mothers had PCB levels approximately 500 ng/g lipid and 400 ng/g lipid, respectively (Vartiainen *et al.*, 1998).

H. METABOLISM

PCB 126 is metabolized to a single hydroxy-metabolite. Using GC-ECD and GC-MS, Koga and coworkers were able to identify a hydroxy metabolite in rats dosed with PCB 126, namely the 4′-hydroxy-3, 3′, 4, 5′-pentachlorobiphenyl (HPB) (Koga *et al.*, 1990). As shown in Figure 2.5, the metabolism of PCB 126 proceeds via cytochrome P450 catalyzed 4′,5′ expoxidation, followed by rearrangement of the arene oxide intermediate (so-called "NIH shift").

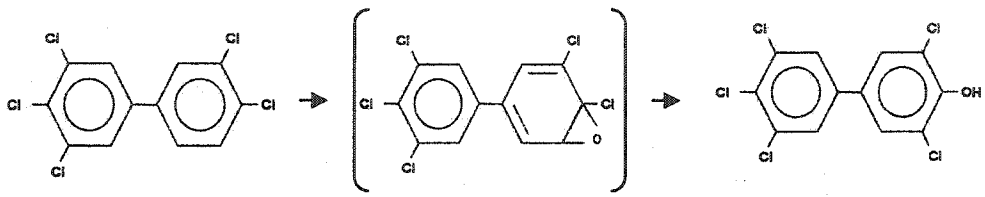

Figure 2.5. Postulated cytochrome P450 catalyzed metabolism of PCB 126 (Koga *et al.*, 1990).

While PCB 126 itself is slowly metabolized and excreted, HPB is excreted rapidly in feces and does not concentrate in the liver or elsewhere. As expected from previous studies, rats receiving intraperitoneal injections of PCB 126 (3,000 μg/kg) had significant atrophy of thymus and spleen, and hepatic hypertrophy. Conversely, rats treated with HPB (3,000 or 10,000 μg/kg) had no similar tropic effects, even at the highest dose. It was further determined that, unlike PCB 126, HPB does not exhibit classic HAH hepatic enzyme induction. In HPB treated rats, 50% of the HPB dose was excreted unchanged in feces within 24 hours, and total HPB excretion over 5 days was 60% of the total dose. In rats treated with PCB 126, fecal excretion of the HPB metabolite was greatest (0.84% of dose) during the first 24 hours, and total HPB excretion over 5 days accounted for only

1.33% of the total PCB 126 dose; only 2.8% of the total PCB 126 dose was excreted in the 5 day period and neither PCB 126 nor HPB was detected in urine.

I. PHARMACOKINETICS

Differences in the pharmacokinetics of target tissues play an extremely important role in determining the relative potency by which HAHs produce biological effects (DeVito *et al.*, 1997; DeVito *et al.*, 1998). Among HAHs there are substantial differences for structure-activity relationships that determine AhR binding characteristics (van den Berg *et al.*, 1994). PCB 126 (like TCDD) has extremely high affinity for the liver because it strongly binds to constitutively expressed hepatic CYP1A2 ($K_i \approx 3 \times 10^{-8}$ M); its pharmacokinetic behavior is also highly dose-dependent and affected by the relative abundance of other congeners (Chen *et al.*, 2001). In a 2-year rat gavage study, tissue disposition of PCB 126 was analyzed in the liver, lung, fat, and blood of controls and dosed groups. PCB 126 was detected in the blood of treated rats and liver, fat, and lung of both treated and untreated animals, albeit at low levels in untreated animals. Concentrations in treated animals generally increased with increasing PCB 126 dose (NTP, 2004).

Because PCB 126 is highly lipophilic it accumulates in fat, will cross the placenta, and is excreted by lactation in humans and other mammals(Holene *et al.*, 1995; Shain *et al.*, 1986; Takagi *et al.*, 1986). Several studies demonstrate maternal exposure to PCB 126 also results in exposed offspring. Both rat and goat offspring are observed to receive substantially more PCB 126 exposure lactationally than transplacentally (Chen *et al.*, 2001; Lyche *et al.*, 2004). Studies examining perinatal pharmacokinetics of PCB 126,

found pregnant and non-pregnant mice dosed with [^{14}C]-labeled PCB 126, exhibited concentrated liver radioactivity due to unmetabolized PCB 126. Only traces of radioactivity were found in fetal livers (Darnerud *et al.*, 1996; Wehler *et al.*, 1989).

Interestingly, the brain appears to be largely protected from PCB 126 exposure. PCB was detected in rat pup brains at weaning (postnatal day 21) when dams were dosed with 0, 0.25, or 1.0 μg/kg/day Monday to Friday beginning 5 weeks before and continuing through gestation and lactation. In this study, pup brain concentrations were 1/100th of the levels found in fat (Rice, 1999) and PCB 126 was not detected in brains of offspring from exposed dams after weaning (Bernhoft *et al.*, 1994; Holene *et al.*, 1995; Holene *et al.*, 1998; Rice *et al.*, 1999).

J. ANIMAL STUDIES

PCB 126 exhibits a spectrum of effects in numerous organ systems. This section reviews the body of literature covering these effects in whole animal studies. Table 2-1 summarizes these effects.

1. Tropic Responses

Tropic responses including both suppressed growth and hyperplastic responses have been reported in tissues of experimental animals following PCB 126 exposure. Perhaps the most classic tropic response following exposure to PCB 126 (and TCDD) is hepatomegaly (Chu *et al.*, 1994; Koga *et al.*, 1990; Yoshimura *et al.*, 1979). This response may play a role in the carcinogenicity of PCB 126 given that such mitogenic responses are thought to play an important role in carcinogenesis (Ames *et al.*, 1990).

TABLE 2-1 Biological Effects of PCB 126 (rodent studies unless otherwise stated)

Response	Reference
Tropic Responses	
hepatomegaly and fatty liver	Chu 1994; Koga 1990; Yoshimura 1979
weight loss	Chu 1994; Koga 1990; Leece 1985
increased organ/body wt. ratios	Chu 1994; Zhao, 1997
decreased bone strength	Lind, 1999, 2000
decreased organic bone matrix	Lind, 2000
squamous epithelial hyperplasia / osteolysis in jaw (mink)	Render 2000, 2001
mammary hypoplasia	Muto 2002
bronchiolar hyperplasia	Brix 2004
lesions of liver, lung, adrenal cortex, pancreas, kidney, heart, thyroid, thymus, spleen, clitoral gland, mesinteric artery	NTP 2004
Tumor Promotion	
altered hepatic foci	Dean 2002; Bager 1995; Hemming 1995a, 1995b, 1993; Flodstrom 1992
decreased hepatic connexin proteins	Bager 1995
Carcinogenicity	
liver, lung, oral mucosa	NTP 2004
Male Reproduction	
increased mounting, small prostate	Faqi 1998
decreased testosterone secretion	Desaulniers 1999
Endocrine	
anti-estrogenic effects	Krishnan 1993
decreased plasma and increased pituitary LH and FSH	Desaulniers 1999
decreased thyroxine	Rice 1998; Collins 1980
Development (pre- post-natal)	
suppressed growth	Chu 1994
increased liver / brain weights	Faqi 1998; Moore 1998
neonatal mortality, low birth weight and pup weakness	Bernhoft 1994
teratogenicity (chickens)	Brunstrom 1990, 1991
Morphogenesis	
craniofacial deformities	Zhao 1997; Mayura 1993
decreased anogenital distance	Faqi 1998
low prostate weights	Moore 1998
Neurodevelopment	
hyperactive offspring	Eriksson 1998; Bernhoft 1994; Holene 1995, 1998
improved learning	Schantz 1996
poor visual discrimination	Holene 1995
poor learning	Bernhoft 1994; Eriksson 1998
accelerated eye opening	Moore 1998
inaccurate training response	Rice 1999
low frequency hearing impairment	Crofton 1999
increased brain nicotinic receptors	Eriksson 1998
Immunity	
thymic atrophy	Andersson 1991; Koga 1990; Yoshimura 1979
suppressed cellular immunity	Mayura 1993; Harper 1994; Zhao 1997
Blood Chemistry	
decreased hematocrit	Rice 1998, 1999
increased cholesterol	Rice 1998, 1999
porphyria	Chu 1994; Sinclair 1990
altered fatty acid composition (chickens)	Stanton 2003
increased vitamin A, decreased vitamin C	Chu 1992; Chen 1994; Lind 2000
Other Organ Effects	
cardiomyopathy	Jokinen 2003
cardiomegaly	Lind 2004
arteritis	Jokinen 2003
pancreatic inflammation / atrophy	NTP 2004
Oxidative Stress	
lipid peroxidaton / DNA single strand breaks in liver and brain	Hassoun 2000, 2001, 2001, 2002
activation of NF-κB, increased IL-6 in vascular endothelium	Hennig 2002

Following dietary exposure to PCB 126 (24 ppb for 36 d) juvenile mink developed mandibular and maxillary lesions of squamous epithelium in the periodontal ligament, osteolysis in adjacent alveolar bone, and loose and displaced teeth (Render *et al.*, 2000b; Render *et al.*, 2001). These effects are consistent with observations of early tooth eruption and gingival hyperplasia seen in Yusho neonates (Yamashita *et al.*, 1985). In the mink study, TCDD also produced similar lesions when given at a 10-fold smaller dose than PCB 126 (i.e., the difference in TEF values for TCDD and PCB 126) suggesting an AhR mediated mechanism. The osteolytic effects observed in mink are also reported in marine mammals that have high body burdens of organochlorine compounds (DeGuise *et al.*, 1995). In contrast to the mink study, weanling Long Evans rats receiving a subacute exposure of 20 or 100 ppb for up to 101 days did not exhibit the jaw lesions of mink (Aulerich *et al.*, 2001). Despite this finding following subacute exposure, female rats chronically exposed to PCB 126 (2-years) developed gingival squamous cell carcinoma of the oral mucosa (NTP, 2004).

Increased incidence of nonneoplastic lesions of the liver, lung, adrenal cortex, pancreas, kidney, heart, thyroid gland, thymus, spleen, clitoral gland, and mesenteric artery have been reported in female rats exposed to PCB 126 (NTP, 2004). Lung lesions in this study included bronchiolar metaplasia of alveolar epithelium (Brix *et al.*, 2004). This finding was in contrast to alveolar epithelial hyperplasia normally observed following damage of alveolar duct epithelial cells. Interestingly, PCB 126-induced metaplastic lesions were

histologically similar to normal bronchiolar epithelium, but with abundant inflammation. Metaplastic lesions appeared to be discontinuous with neoplastic lesions also found in the PCB 126 treated group indicating different origins.

Lind and coworkers compared the effects of PCB 126 exposure (total dose 384 μg/kg by intraperitoneal injection over 3 months) and estrogen depletion (by ovariectomy) on bone strength and bone composition in the rat (Lind *et al.*, 1999; Lind *et al.*, 2000b). Decreased maximum torque, decreased torsional stiffness and increased torsion at failure were demonstrated in long bones of both groups. Additionally, there was a decrease in the amount of organic matrix, but not of inorganic components. Because there were no significant differences between ovariectomized and sham operated rats, the effects appeared to be independent of any estrogenic or antiestrogenic effects of PCB 126.
In a subsequent study it was demonstrated that decreased vitamin C levels and increased vitamin A levels noted in plasma, apparently did not mediate PCB 126 effects on bone (Lind *et al.*, 2000a). Muto *et al.*, observed that 50-day old female offspring of rats orally exposed to low levels of PCB 126 (250 ng/kg/d on gestation days 13 – 19) exhibited inhibited differentiation of mammary terminal end buds (TEBs) and larger proliferating cells. In contrast, 50-day old female offspring in a high dose group (7.5 μg kg/d on gestation days 13 – 19) showed mammary hypoplasia and low-levels of cell proliferation (Muto *et al.*, 2002). It was demonstrated in this study that estrogen receptor (ER) mRNA in TEBs increased with PCB 126 dose. This study did not provide data on concurrent circulating estrogen levels, so it is difficult to infer whether increased transcription was a

direct result of PCB 126 body burdens, or a response to decreased levels of circulating estrogen (e.g., due to a systemic endocrine-mediated PCB 126 antiestrogenic response).

2. Tumor Promotion

Chronic exposure to PCBs is associated with induction of neoplastic lesions in the liver (Silberhorn *et al.*, 1990). A important role of PCBs in the carcinogenic process appears to be tumor promotion, and PCB 126 was shown to be a potent tumor promoter when measured by increased number and area of altered hepatic foci in rats (Bager *et al.*, 1995; Dean, Jr. *et al.*, 2002; Flodstrom *et al.*, 1992; Hemming *et al.*, 1993; Hemming *et al.*, 1995). These foci are considered preneoplastic when they become enzyme-altered and stain for placental glutathione-S-transferase positive (GST-P+) or gamma-glutamyl transpeptidase (GGT) (Pitot *et al.*, 1993). Foci formation is hastened when PCB 126 was combined with an initiator such as diethylnitrosamine followed by partial hepatectomy to stimulate cell proliferation (Flodstrom *et al.*, 1992). In all studies in which an initiator was followed by partial hepatectomy, there was a dose-dependent increase in either GGT or GST-P+ foci area and number, compared to controls. PCB 126 in the absence of initiator or hepatectomy did not produce foci. Additionally, several of these studies demonstrate that *ortho*-substituted PCB congeners are antagonistic to foci formation. Consistent with the TEF approach to toxic potency assessment, PCB 126 was observed to elicit approximately 10% of TCDD's tumor promoting activity.

In the tumor promotion study, Bager *et al.* evaluated the effect of PCB 126 treatment on the expression of two major liver connexins (Cx 26 and Cx 32) (Bager *et al.*, 1994). Gap junctions formed by connexins between cells are believed to be involved in regulation of

normal cell growth and differentiation (Sohl *et al.*, 2004; Willecke *et al.*, 1991). Treatment with PCB 126 decreased levels of Cx 26 and Cx 32 proteins (but not mRNA levels) in livers of treated animals, even at low doses not producing GGT foci.

3. Carcinogenicity

Epidemiological data supporting a carcinogenic role for PCBs is equivocal since no overall increase in cancer mortality has been associated with occupational exposures. Some studies however, report nonstatistically significant increases in specific cancers of the liver, gall bladder, and biliary tract (Kimbrough, 1995). Perhaps the most compelling animal study in support of a carcinogenic role for PCB 126, comes from a recent chronic rat gavage study conducted by the National Toxicology Program (NTP, 2004). In this study, groups of 81 female Harlan Sprague-Dawley rats were administered 30, 100, 175, 300, 550, or 1,000 ng/kg body weight PCB 126 by gavage, 5 days per week, for up to 104 weeks; a group of 81 vehicle control female rats received the vehicle alone. A stop-exposure group of 50 female rats was administered 1,000 ng/kg PCB 126 by gavage for 30 weeks, then vehicle for the remainder of the study. In this 2-year study, there was clear evidence of carcinogenic activity of PCB 126 in female rats based on increased incidences of cholangiocarcinoma of the liver (doses of 300 ng/kg or greater), and squamous neoplasms of the lung (cystic keratinizing epithelioma and squamous cell carcinoma) in the 550 ng/kg and 1000 ng/kg treatment groups, and gingival squamous cell carcinoma of the oral mucosa (1000 ng/kg), similar to effects seen in mink studies. Hepatocellular adenoma was observed in all groups except the 175 ng/kg and the 1000 ng/kg stop exposure group. Hepatocholangioma of the liver in the 1000 ng/kg group was also considered to be related to administration of PCB 126. It was unclear however,

whether neoplasms of the adrenal cortex and cholangioma of the liver observed in the study were related to PCB 126 exposures.

4. Male Reproduction

Yucheng men exposed before age 20 had a substantially less likelihood of having male offspring than did age- and neighborhood-matched controls (delRio Gomez *et al.*, 2002). In 1998, semen was analyzed in young men born to mothers exposed in the Yucheng incident. These men aged 16 to 20 years, had sperm with increased abnormal morphology, reduced motility, and diminished ability to penetrate hamster oocytes (Guo *et al.*, 2000).

In contrast to human exposure to PCB mixtures in the Yucheng incident, a study to evaluate the sexual performance and behavior of male Wistar rats that were gestationally exposed to PCB 126 (single dose of 10 μg/kg PCB 126 on day 15 of gestation), showed no treatment effect on sperm morphology, sperm count or reproductive performance (Faqi *et al.*, 1998). Male offspring in this study however, exhibit increased mounting behavior and permanently reduced prostate weights.

5. Reproductive Hormones

PCB 126 exhibits the most potent antiestrogenic properties of any PCB in AhR-responsive MCF-7 human breast cancer cell lines based on inhibition of the 17β-estradiol (E2) induced secretion of procathepsin D (Krishnan *et al.*, 1993). To test whether PCB 126 also alters gonadotropin levels, Desaulniers, *et al.* evaluated the effect of PCB 126 on levels and distribution of luteinizing hormone (LH) and follicle-stimulating hormone

(FSH) (Desaulniers *et al.*, 1999). In one experiment, 5 groups of 8 rats each received two intraperitoneal injections of PCB 126, one day apart, amounting to 0, 6.25, 25, 100 or 400 μ/kg/day. Decreases in LH serum concentrations were observed beginning at doses of 25 and 100μ/kg/day, respectively, and serum FSH decreased in the high dose group. Pituitary FSH and LH content increased with PCB 126 dose. Despite changes in other reproductive hormones, PCB 126 had no effect on the androgen receptor content of the prostate. When tested in hemicastrated rats there was also evidence that PCB 126 suppressed testosterone secretion.

6. Thyroid Hormones

Reductions of circulating levels of thyroxine (T4) have been reported following gestational and lactational exposure to PCB mixtures (Collins *et al.*, 1980; Rice *et al.*, 1998). T4 and triiodothyronine (T3) have an important role in brain development, especially postnatally when a deficit or excess can have permanent adverse effects on neurological function (Davenport *et al.*, 1976). In order to determine the role of PCB 126 on thyroid hormone levels, and thus its indirect effect on development, Seo *et al.* studied the effects of PCB 126 on circulating thyroid hormone concentrations using rat dams dosed with 0.25 or 1.00 μg/kg/d PCB 126 on gestation days 10 – 16. Gestational and lactational exposure to PCB 126 in the high dose group resulted in a 20% depression in plasma T4 in female pups (Seo *et al.*, 1995). Male pups showed slight drops in plasma T4 that were not statistically significant. Additionally in this study, UDP-glucuronosyl transferase, an enzyme that catalyzes the formation of T4-glucuronide and hence leads to excretion of T4, was induced approximately 3-fold in the high dose PCB 126 group. In

light of these findings, PCB 126 appears to alter T4 levels, but at environmentally relevant doses, these changes do not appear clinically significant (Seo *et al.*, 1995)

7. Development

Possible developmental effects of PCBs are a concern in human populations based on results of numerous epidemiological studies (reviewed in (Brouwer *et al.*, 1995; Weisglas-Kuperus, 1998). Given that lipophilic PCBs cross the placenta and are excreted by lactation, there is particular concern over adverse neurodevelopment in children following *in utero* and lactational exposure to PCBs (Koopman-Esseboom *et al.*, 1997). Experimental animal studies involving *in utero* and lactational exposure demonstrate that PCB mixtures produce functional developmental effects in animal offspring that may persist into adulthood (Brouwer *et al.*, 1995).

In general, HAHs have a suppressive influence on overall growth and development, possibly due in part to altered endocrine homeostasis. As recent as 1991, serial studies on children born to women exposed during the Yucheng incident, demonstrate offspring to have shorter stature and less total lean and soft tissue mass than controls (Guo *et al.*, 2004). The gestational age-adjusted birth weight in infants delivered to Yucheng women from 1979 to 1985 was 0.5 kg lower than controls; this effect was more pronounced in children born early after maternal exposure (Guo *et al.*, 2004; Lan *et al.*, 1987). Findings for Yucheng children were similar to those for offspring evaluated in a Michigan fish eater study in cases where cord serum total PCB levels were 5.0 ng/ml or greater (Fein *et al.*, 1984).

PCB 126 appears to alter growth characteristics in experimental animals. Chu *et al.* exposed Sprague-Dawley rats to PCB 126 in food at concentrations of 0.1, 1.0, 10, or 100 ppb for 13 weeks (Chu *et al.*, 1994). Suppressed growth and decreased food consumption were observed in the highest dose groups for both genders. Increased organ and body weight ratios for liver occurred in the 10 and 100 ppb groups. (Faqi *et al.*, 1998). Pregnant Holtzman rats dosed orally with 0.5 μ/kg PCB 126 beginning on gestation day 6 and continuing daily through weaning, had 3- and 9-day old pups with increased relative liver weights (Moore *et al.*, 1998). In another study, PCB 126 was the most active coplanar PCB tested for body weight-loss (ED50 = 3.25 mmol/kg (Leece *et al.*, 1985). Male Wistar rats prenatally exposed to a single maternal oral PCB 126 dose of 10 μg/kg, exhibited significantly increased brain weights. Bernhoft *et al.* investigated the effects of pre- and postnatal exposures to PCB 126 on physical development (Bernhoft *et al.*, 1994). Twenty-four albino Lewis rats were mated and randomized into three groups. The treatment groups received 10 or 20 μg/kg oral doses of PCB 126 during the organogenesis and fetal suckling periods. Exposure to PCB 126 resulted in reduced body weight, which persisted into adulthood. The number of live pups per litter was also reduced in a dose-dependent manner and live pups were generally weaker.

8. Morphogenesis

PCB 126 caused dose-dependent fetal cleft palate (<25, 44.3, 56.3 and 100%) in offspring of C57BL/6 mice receiving a single dose (522, 783, 1044 or 2088 μg/kg, respectively) on gestation day 10. Mice treated similarly with PCB 126 plus a di-*ortho* congener, exhibited significantly less incidence of cleft palate (Zhao *et al.*, 1997),

possibly due to competitive inhibition of PCB 126 AhR-binding by the di-*ortho* congener.

Pregnant Wistar rats treated orally with a single dose 10 µg/kg PCB 126 on day 15 of gestation produced male offspring with decreased anogenital distance (versus body length) at postnatal day 65 (puberty) and on postnatal day 140 (adulthood). Additionally, female offspring exhibited significantly delayed vaginal opening (Faqi *et al.*, 1998). In another study, male offspring of Long-Evans rat dams receiving 1.0 µg/kg/d (Monday-Friday from conception through lactation) also exhibited a decrease in anogenital distance normalized for weight (Rice, 1999). At postnatal day 63, pregnant Holtzman rats dosed orally with 0.5 µ/kg PCB 126, had lower weight ventral and dorsolateral prostate glands than controls. By postnatal day 161, dorsolateral prostate weight was normal, but ventral prostate weight was still reduced (Moore *et al.*, 1998).

9. Neurodevelopment

Yucheng children assessed for cognitive development from 1985 to 1990 consistently scored lower than matched controls on cognitive tests and boys consistently scored lower on spatial acuity indices in these tests (Chen *et al.*, 1992; Guo *et al.*, 1995). Rats exposed to commercial PCB mixtures during development demonstrate impaired learning in water maze tests, decreased performance in avoidance response tests, and gender-specific learning deficits (Pantaleoni *et al.*, 1988; Shiota, 1976; Widholm *et al.*, 2001). Another common finding in animals exposed to PCB mixtures during development is hyperactivity during adolescence; an effect observed in monkeys, rats and mice (Bowman *et al.*, 1978; Lilienthal *et al.*, 1990). Hyperactivity is consistent with findings in Yucheng

offspring. Testing for hyperactivity, where higher scores represent more problems, revealed individuals exposed to *in utero* and lactationally scored 8-53% higher than controls at each of six age groups tested (Chen *et al.*, 1994; Guo *et al.*, 2004). Neurological testing also indicated Yucheng offspring exhibited slowed cognitive processing and attention deficit (Finley *et al.*, 1985; Guo *et al.*, 2004). These cognitive deficits in offspring were not associated with exposure by male parents (Guo *et al.*, 1994). Based on several studies, it appears much, but not all, of the potency for neurotoxic effects following exposure to PCB mixtures is attributable to the presence of di-*ortho* substituted PCBs (Maier *et al.*, 1994; Shain *et al.*, 1991; Tilson *et al.*, 1997). Altered calcium homeostasis and interference with oxidative energy metabolism appear to be significant contributors to di-*ortho* substituted PCB neurotoxicity; effects not produced by PCB 126, even at high dose, and also not observed with AhR activation (Kodavanti *et al.*, 1993; Maier *et al.*, 1994; Mundy *et al.*, 1999).

There is some evidence that perinatal exposure to PCB 126 alone results in hyperactive offspring with poorer visual discrimination and poorer discrimination learning(Bernhoft *et al.*, 1994; Brouwer *et al.*, 1995; Holene *et al.*, 1995; Holene *et al.*, 1998). In a subsequent study, dams dosed with 2 μg/kg/d between postnatal days 10 and 20 produced offspring with impaired visual discrimination and hyperactivity (Holene *et al.*, 1995). In contrast, rat dams dosed with 10 or 20 μg/kg/d between gestation days 9 and 19, exhibited no effect for visual discrimination, while pups in this study did exhibit delayed onset of spontaneous movement, delayed neuromuscular maturation and dose-dependent body weight reduction up to 18 weeks postpartum (Bernhoft *et al.*, 1994). Hyperactivity

was again observed in male offspring of mothers dosed with 2 μg/kg/d PCB 126 every second day from postnatal day 3 to 13 (Holene *et al.*, 1998). Pregnant Holtzman rats dosed orally with 0.5 μ/kg PCB 126 beginning on gestation day 6 and continuing daily through weaning also exhibited accelerated eye opening (Moore *et al.*, 1998).

In a series of studies, Rice *et al.* evaluated the possible effects of PCB 126 on attention and learning in offspring of Long-Evans rats receiving an environmentally relevant dose of 0, 0.25, or 1 μg/kg/d, Monday to Friday beginning 5 weeks before mating and continuing through gestation and lactation (Bushnell *et al.*, 1999; Rice *et al.*, 1998; Rice, 1999; Rice *et al.*, 1999). In a spatial delayed alternation testing battery, one 60-day old male and female from each litter were tested for their ability to press a lever for food reward that varied from right to left, and progressed through longer scheduled delays between lever pressing and reward (Rice, 1999). The testing battery ended in a variable delay test. No convincing evidence was found for performance differences between treated and control offspring. Similarly, a 200-day old male and female from each litter were tested on complex multiple mixed interval-fixed ratio reinforcement delay schedules, followed by performance on DRL (differential reinforcement of low rates of behavior) schedules in which only one lever had a scheduled reward delay (Rice *et al.*, 1998). No compelling evidence for treatment related effects was observed on either schedule. In a third behavior testing battery, male offspring were trained as adults to perform two behaviors for food reward. One test was intended to assess visuospatial attention, the other to assess sustained attention. In neither case did PCB 126 treatment affect acquisition or performance of tasks. Interestingly, PCB 126 treatment was

protective in visuospatial and sustained attention tests against the effects of chlordiazepoxide; a compound previously shown to reduce the accuracy with which rats perform tests (Bushnell *et al.*, 1999). Finally, 400-day old male and female offspring from each litter were tested under a series of random interval—random interval (RI-RI) schedules of reinforcement delay for pressing right and left levers for food at about 400 days of age, followed by assessment under a progressive ratio (PR) reinforcement schedule (Rice *et al.*, 1999). During the RI-RI schedule, the high dose group apportioned responses less accurately than controls; in more complex RI-RI schedules, exposed rats also required more repetitions to perform reward tasks. Other measures were not different between treatment and control offspring.

To evaluate whether neurotoxic effects could be detected in adult animals, NMRI mice were given a single oral dose of PCB 126 (46 or 460 μg/kg) on postnatal day 10 (Eriksson *et al.*, 1998). Two months after exposure, pairwise comparisons showed significant changes in spontaneous behaviors, including locomotion, rearing and total activity variables; effects that amplified with age. Learning and memory deficits were also apparent for adult mice in Morris water maze testing. Moreover, high dose mice exhibited decreased density of nicotinic binding sites in the hippocampus. Conversely, in another study where Sprague-Dawley rats received a lower dose, (0.25 or 1.0 μg/kg/d PCB 126 by gavage on gestation days 10 – 16), individual males or females from each of 8 litters, actually exhibited better performance in the radial arm maze than controls (Schantz *et al.*, 1996).

Low-frequency hearing loss was demonstrated in adult offspring of rats exposed to Aroclor 1254 during gestation and lactation (Herr *et al.*, 1996). To test the role of PCB 126 in hearing loss, Crofton and Rice dosed nuliparous Long Evans rats with 0, 0.25, or 1.0 μg/kg/d PCB 126 5-days/week for 35 days prior to breeding and throughout gestation and lactation (Crofton *et al.*, 1999). This exposure caused gender-independent low-frequency hearing deficits in offspring when evaluated from postnatal days 76 - 90. Additionally, elevated auditory thresholds occurred in the high dose group for 0.5 and 1 kHz tones, but not at higher frequencies. Recent data demonstrate that thyroxine (T4) replacement during the postnatal period blocks the ototoxicity of perinatal Aroclor 1254 exposure (Goldey *et al.*, 1998); this suggests the hypothyroxinemia observed following PCB 126 exposure could be responsible for altered hearing acuity.

10. Neurochemistry

Acute exposure to PCB mixtures is known to cause non-specific effects on neurotransmitter levels. Chronic exposure affects dopaminergic neurochemistry to a greater degree than other neurotransmitter systems (Tilson *et al.*, 1997). There is evidence that developmental exposure to PCBs increases dopamine concentrations in the substantia nigra and caudate nucleus, while dopamine levels decrease in the caudate nucleus in exposed adults (Seegal, 1994). While decreases in dopamine were seen in numerous brain regions of rats exposed to di-*ortho* substituted hexachloro biphenyls, at a comparable dose (9.0 μg /kg/d) PCB 126 did not alter dopamine levels. NMRI mice were given a single oral dose of PCB 126 (46 or 460 μg/kg) on postnatal day 10 to evaluate whether neurotoxic effects could be detected in adult animals (Eriksson *et al.*, 1998). High-dose mice exhibited decreased density of nicotininc cholinergic receptors in the

hippocampus, creating a plausible biochemical linkage to behavioral and cognitive effects of PCB 126 observed in the same study.

11. Effects on the Immune System

Lymphocytes originating in the bone marrow enter the thymus gland where they mature and develop into activated T-lymphocytes. Thymic atrophy occurs normally with age, during which the effectiveness of cellular immunity also diminishes. One hallmark response of prenatal PCB 126 exposure is decreased thymus weight in perinatally exposed offspring. Pregnant Holtzman rats dosed orally with 0.5 μ/kg PCB 126 beginning on gestation day 6 and continuing daily through weaning had substantially decreased relative thymus weights in 3- and 9-day old pups (Moore *et al.*, 1998). Such decreases in thymus weight appear to have an adverse effect on cellular immunity. Treating C57BL/6 and DBA/2 mice with PCB 126 followed by immunization with the T-cell independent antigen trinitrophenyl-lipopolysaccharide (TNP-LPS), resulted in a dose-dependent decrease in serum IgM and diminished cellular immunity indicated by a reduced splenic plaque-forming cell (PFC) response (Harper *et al.*, 1994; Mayura *et al.*, 1993). The ED50 values for these PCB 126-induced effects were approximately one order of magnitude higher than for TCDD, and also substantially higher in AhR responsive mice, suggesting an AhR mediated response. These results were similar to a subsequent study where the presence of a di-*ortho* substituted PCB congener inhibited thymic atrophy by PCB 126 (Zhao *et al.*, 1997).

12. Blood Chemistry

During behavioral studies, Rice and coworkers dosed Long-Evans rats with PCB 126 at 0, 0.25, or 1 μg/kg/d Monday to Friday beginning 5 weeks before mating and continuing through gestation and lactation (Rice *et al.*, 1998; Rice *et al.*, 1999). Offspring of these rats exhibited reduced hemoglobin levels and decreased hematocrit, while cholesterol levels were elevated. Increased serum cholesterol was also found in female rats following intraperitoneal injections totaling 224 μg/kg of PCB 126 given every second week over 10 weeks (Lind *et al.*, 2004). Although the relevance to mammals is unknown, pre-incubation chickens exposed to PCB 126 *in ovo* (0.1 μg PCB 126 per egg) exhibit altered plasma fatty acid composition at 21 days of age (Stanton *et al.*, 2003). In this study, PCB 126 treated eggs exhibited increased 22:1n9 fatty acids and decreased total phospholipids, saturated plasmogen and 24:6n3 fatty acids.

13. Cardiovascular Effects

Most studies of PCB 126 effects on specific organs have focused on the liver because of its pivotal role in xenobiotic metabolism. There is however, considerable evidence that HAH exposure increases the risk of cardiovascular disease in humans. Increased mortality from cardiovascular disease was noted for capacitor manufacturing and power workers exposed to PCBs and for persons exposed to TCDD during a Seveso, Italy industrial accident (Bertazzi *et al.*, 1998; Gustavsson *et al.*, 1997; Hay *et al.*, 1997). Administration of PCB 126 to Sprague-Dawley rats by gavage 5 d/wk up to 1000 ng/kg, or up to 100 ng/kg for up to 2 years, significantly increased the incidence of cardiomyopathy and chronic active arteritis in a dose-dependent manner (Jokinen *et al.*,

2003). Myocardial degeneration in these animals consisted of multiple focal lesions scattered within ventricular walls. The arteritis was progressive with inflammation and occasional endothelial cell proliferation. Increased heart weight was also found following PCB exposure (Lind *et al.*, 2004). Hennig *et al.* concluded cardiotoxicity may be linked to inflammation caused by oxidative stress from PCB 126 exposure (Hennig *et al.*, 2002).

14. Pancreatic Effects

There is evidence also from the Seveso incident, that TCDD exposure increases the risk for developing diabetes mellitus in females (Bertazzi *et al.*, 1998). In a rat 2-year chronic toxicity study, oral PCB 126 treatment resulted in exocrine pancreatic changes including cytoplasmic vacuolation, chronic active inflammation, atrophy, and arteritis (NTP, 2004). This finding raises particular concern because pancreatitis is linked to increased risk of pancreatic cancer (Lowenfels *et al.*, 1999). While similar inflammatory responses were observed for TCDD and PCDF, these compounds but not PCB 126, produced low incidence of pancreatic acinar adenoma and carcinoma independent of degeneration and inflammation levels (Nyska *et al.*, 2004).

15. Oxidative Stress

Oxidative stress leading to tissue damage results from an imbalance between production of reactive oxygen species (ROS) and antiantioxidant defense (Halliwell, 1994). Cellular ROS includes superoxide anion ($O_2^{\bullet -}$), hydroxyl radical ($^{\bullet}OH$), hydroperoxyl radical ($HO^{\bullet}_2$) and hydrogen peroxide (H_2O_2) (Betteridge, 2000). ROS are produced by normal metabolic processes and by xenobiotic metabolism including oxidative phosphorylation, P450 metabolism, and activation of inflammatory responses (Klaunig *et al.*, 2004).

Tissue damage resulting from ROS includes lipid peroxidative membrane damage, inactivation of sulfhydryl-containing enzymes and cross-linking of proteins. The ability of a cell to detoxify ROS depends on the efficiency of metabolic pathways that utilize enzymes such as superoxide dismutase, catalase and glutathione peroxidase and small molecule antioxidants such as glutathione, ascorbate and tocopherols, β-carotene, and coenzyme Q (Betteridge, 2000; Ramos *et al.*, 2001).

Of particular interest in the current context is the observation that chronic exposure to PCB 126 leads to oxidative damage, including lipid peroxidation and DNA single-strand breaks in both rat brain and hepatic tissue (Hassoun *et al.*, 2000; Hassoun *et al.*, 2001; Hassoun *et al.*, 2002). Additionally, PCB 126 causes more superoxide anion production and lipid peroxidative injury in the brain than in liver.

Lipid peroxidation and superoxide anion production, concomitant to suppression of glutathione and alpha tocopherol levels, was demonstrated in mice following acute exposure to a mixture of TCDD and PCB 126. This exposure caused a dose-dependent increase in the production of superoxide anion, lipid peroxidation and DNA single-strand breaks in liver and brain tissues of rats (Hassoun *et al.*, 2001; Slezak *et al.*, 2000). Similarly, increased lipid peroxidation and decreased glutathione peroxidase activity occurred in liver and adipose of chicken embryos following *in ovo* exposure to PCB 126 (Jin *et al.*, 2001).

Hennig *et al.*, recently demonstrated PCB 126, and other coplanar PCB AhR agonists, cause oxidative stress that is both proinflammatory and atherogenic through activation of nuclear factor-κB (NF-κB) and by increased production of interleukin-6 (IL-6) in vascular endothelial cells; these effects do not occur with PCB 153, a non-coplanar PCB (Hennig *et al.*, 2002). Consistent with the inability of PCB 153 to elicit inflammatory responses, it was further demonstrated that inflammation resulting from PCB 126 exposure requires a functional AhR. Schlezinger *et al.*, demonstrated that PCB 126, and structurally similar PCB 77 (3,3',4,4'-tetrachlorobiphenyl), uncouple the catalytic cascade of CYP1A1 resulting in formation of ROS in liver microsomes of the teleost fish scup (Schlezinger *et al.*, 2001). Although PCB 77 but not PCB 126, was tested on rat microsomes, PCB 77 produced ROS in rat microsomes just as it had done in scup microsomes; this suggests PCB 126 would probably have a similar uncoupling effect on rat cytochrome (Schlezinger *et al.*, 1999; Schlezinger *et al.*, 2001).

K. SUMMARY

Concern for human health risk from PCB exposures originated primarily form observations of toxicity and morbidity from accidental oral exposures to large doses of PCB mixtures in the Yusho and Yucheng incidents. Environmental and occupational studies of human exposure to PCBs however, are inconclusive and generally inconsistent with biological effects observed in laboratory animal studies (Swanson *et al.*, 1995). In this context, it seems unlikely that the small amount of PCB 126 remaining in the environment, poses a health risk to environmentally exposed adults. On the other hand, recent prospective epidemiologic studies demonstrate subtle effects from exposure to background levels of HAHs on physical development (Brouwer *et al.*, 1995; Weisglas-

Kuperus, 1998) and neurodevelopment (Vreugdenhil *et al.*, 2004) of children. Because numerous animal studies indicate that PCB 126 partitions to the brain at exceeding low levels, and because *ortho*-substituted PCBs appear to be most neurotoxic, PCB 126 is likely to play a secondary role in neurodevelopmental deficits that might be caused by environmental exposure to PCBs. Animal data in this review however, indicate perinatal exposure to PCB 126 could play a role in slowing physical development.

Numerous PCB 126 studies reviewed in this section were done in parallel with TCDD to validate dose-additivity using TEFs with the underlying assumption that effects of TCDD and PCB 126 are AhR mediated and that TCDD is ten times more potent than PCB 126. This assumption holds for hallmark effects such as thymic atrophy, and liver effects including hepatomegaly and CYP1A1 induction. Conversely, it is clear from this literature review that the assumption of TEF additivity does not hold for some extrahepatic effects including neurodevelopment. This observation, in conjunction with recent convincing evidence that PCB 126 is a liver carcinogen in rats, leads to a study designed to compare the gene expression effects of PCB 126 on hepatic and neurological tissues; with the aim of determining if differences in gene expression are reflected in different biological effects observed between organ systems. The following section details the rationale, experimental design, and results of a differential gene expression study to accomplish this aim.

III. Effects of PCB 126 on Gene Expression

A. PROJECT BACKGROUND

The central dogma of molecular biology says that messenger RNA (mRNA) is transcribed from DNA and subsequently translated into protein. It is mRNA that reflects regions of DNA that make up genes. The levels and composition of mRNAs at any given time, is a direct reflection of the state of gene expression in the cell and hence a snapshot of how a cell is responding to its environment. Cellular gene expression can change very rapidly in response to toxicant exposures and can be a much more sensitive endpoint than overt toxicity (Harries *et al.*, 2001).

Prior to development of genome-wide methods, gene expression could only be studied using gene-by-gene techniques such as real-time reverse transcription polymerase chain reaction (RT-PCR) (Johnson *et al.*, 2004). While sensitive and quantitative, PCR methods are not comprehensive and hence not amenable to simultaneous detection of transcriptome-wide changes. To address the hypothesis and experimental design of this research project, it is necessary to use high throughput methods able to simultaneously interrogate transcription of more than 30,000 genes.

The differential gene expression research presented in this dissertation was conducted over the past three years (2002-2004), during a period when techniques for observing transcriptome-wide changes were rapidly evolving. Based on the literature review

provided in Section I, it is apparent that most toxicity data for PCB 126 is derived from rat models. It was thus appropriate to study gene expression in the rat in light of expected future work needing to be done *in vivo*. As it turned out, the rat genome was not sequenced and mapped until 2004 (Gibbs *et al.*, 2004), which in 2002, precluded the ability to capitalize on genome-wide microarrays, that are now available.

When this project began, there were two candidate methods for simultaneously observing differential gene expression namely, suppression-subtractive hybridization (SSH) (Diatchenko *et al.*, 1996) and Serial Analysis of Gene Expression (SAGE) (Velculescu *et al.*, 1995). SSH uses proprietary, difficult to synthesize DNA constructs manufactured by a vendor from whom we previously received poor technical support. We chose to use SAGE because the constructs can be synthesized and purchased from numerous vendors. This source flexibility made SAGE the preferred method. In the end, technical problems with SAGE led to finalizing this research project using newly developed genome-wide microarray technology. Both SAGE and microarray protocols and results are detailed in this section.

B. EXPERIMENTAL DESIGN

In principle, either SAGE or microarray technology can be used with any tissue or cell exposed to PCB 126 *in vitro* or *in vivo*. Cultured cells were chosen in this project for several reasons. First, interpreting *in vivo* gene expression studies is inherently problematic because of biological variability. Whole tissue preparations simultaneously contain diffuse stem cells, progenitor cells, and terminally differentiated cells and mRNA transcripts from each cell type will be present in different proportions in different tissue

samples, and each will have different constitutive gene expression profiles (Trosko, 2004). Biological variability of whole tissues, even between inbred rodents, necessitates use of relatively large animal numbers or tissue replicates to address large statistical variance.

Finally, controlling *in vivo* experiments is difficult because PCB 126 is believed to have systemic anti-estrogenic effects (Safe *et al.*, 1993). Since animal-wide hormonal interactions may exert profound effects on gene expression creating large variability between responsive and unresponsive tissues, particularly during development, it is problematic to use *in vivo* experiments for differentiating direct and indirect gene expression effects of a toxicant. Use of an *in vitro* system mitigates the problem of systemic endocrine effects. Additionally, near-passage clones from immortalized cell lines, cultured under identical conditions should have nearly identical genetic composition and expression levels, and thus require less replicate treatments to address biological variability and statistical variance (Speed, 2003).

1. Cultured Cells

In this project, for reasons discussed below, rat H4IIE hepatoma and rat C6 glioma cells were used, cognizant that effects observed in cultured transformed cells may not be directly comparable to effects observed *in vivo*. While transformed hepatocytes, such as H4IIE cells, may not be an ideal model for observing pre-carcinogenic processes, transformed H4IIE cells should provide a good model for observing expression changes related to tumor promoting effects exhibited by PCB 126 in liver. Additionally, because H4IIE hepatoma cells have been used extensively for aryl hydrocarbon bioassays, the

response of these cells to PCBs is well known and characterized (Broccardo *et al.*, 2004; Sawyer *et al.*, 1982; Tillitt *et al.*, 1991). C6 glioma cells were chosen to represent brain astrocytes because aryl-hydrocarbon responsiveness was previously demonstrated for these cells (Geng *et al.*, 1993; Geng *et al.*, 1995; Geng *et al.*, 1998; Takanaga *et al.*, 2001).

2. H4IIE Rat Hepatoma Cell Biology

H4IIE cells were originally derived from the Ruber hepatoma H-35 and demonstrated excellent growth characteristics (Pitot *et al.*, 1964). Later it was also found that, like primary liver cells, H4IIE hepatoma cells express low constitutive levels of CYP1A1. Following the original work on inducible aryl hydrocarbon hydroxylase (AHH) enzyme activity in H4IIE cells (Benedict *et al.*, 1973), it was further demonstrated that AHH is potently induced in H4IIE cells, and when used for HAH bioassay, Niwa and coworkers were able to detect TCDD at concentrations down to 10 fmol based on induction (Niwa *et al.*, 1975). Furthermore, strong correlations ($r > 90$) were identified between enzyme induction in H4IIE cells by PCBs, and the potency of PCBs to cause effects such as wasting and thymic atrophy *in vivo* (Safe, 1987). High correlation was found for both *in vivo* enzyme induction (-log ED_{50}) versus toxic potency (-log ED_{50}) in liver cells, and *in vitro* enzyme induction (-log EC_{50}) potency versus toxic potency *in vivo* (-log ED_{50}). The ED_{50} values established in immature male Winstar rats for inhibition of weight gain and thymic atrophy by PCB congener 126 (3.3 and 0.95 μmol/kg, respectively) were lowest (i.e., most potent) of any PCB congener, and an order of magnitude higher (i.e., less potent) than TCDD (0.05 and 0.09 μmol/kg, respectively). EC_{50} values of H4IIE cells for AHH and ethoxyresorufin O-deethylase (EROD) induction, and aryl hydrocarbon

receptor binding affinity by PCB 126 (2.40E-10, 2,48E-10, and 1.2E-7 M, respectively) were also lowest of any PCB congener, and at least an order of magnitude higher than for TCDD (7.23E-11, 1.85E-10, and 1.0E-8 M, respectively).

Since the work of Niwa and coworkers, EROD bioassay using the rat hepatoma H4IIE cell line has been used extensively for measuring dioxin-like activity (Behnisch *et al.*, 2001; Behnisch *et al.*, 2002; Engwall *et al.*, 2000; Gale *et al.*, 2000; Hanberg *et al.*, 1991; Li *et al.*, 1999; Petrulis *et al.*, 1999; Safe, 1993; Sanderson *et al.*, 1996; Schmitz *et al.*, 1996; Schramm *et al.*, 2001; Schrenk *et al.*, 1991; Schwirzer *et al.*, 1998; Till *et al.*, 1997). Because H4IIE rat hepatoma cells are known to be exquisitely sensitive to induction by TCDD, and since PCB 126 induction occurs at comparable concentrations, these cells should provide a good *in vitro* model for AhR-mediated gene expression changes in liver. Additionally, correlations between adverse effects in rats and enzyme induction in H4IIE cells, adds credibility to the possible relationship between changes in gene expression sought in the present research, as well as the potential for ontological linkage of these genes to biological manifestations observed *in vivo*.

3. C6 Rat Glioma Cell Biology

Normal glial cells provide a structural matrix for neurons (Bixby *et al.*, 1991), regulate extracellular ion concentrations, metabolize neurotransmitters and xenobiotics, and mediate healing and repair functions for neurons (Geng *et al.*, 1998). Although brain cytochrome P450 activity is thought to be 1-10% of the activity found in liver, it was demonstrated that, like normal glial cells and liver cells, C6 glioma cells express CYP 1A1, 1A2, 2A1, 2B1/2, 2C7, 2D subfamily, 2E1 and P450 reductase (Geng *et al.*, 1993;

Geng *et al.*, 1995). Individually or in combination, these enzymes are known to have roles in neurotransmission (Tyndale *et al.*, 1991), neuroendocrinology and neurotoxicity (Warner *et al.*, 1995), and neurodevelopment and behavior (Naftolin, 1994).

The C6 (clonal cell strain 6) rat glioma cell line was established from a tumor induced with N-nitrosomethyl urea (Benda *et al.*, 1968). C6 cells exhibit biological characteristics of both astroglia and oligodendroglia, and are bipotential for either; this behavior suggests C6 cells resemble glial progenitor cells (Lee *et al.*, 1992). Additionally, C6 cells are used extensively as a sensitive experimental model for studying mechanisms of neurotoxicity (Tang *et al.*, 2003) and specifically, for examining mechanisms of HAH neurotoxicity (Takanaga *et al.*, 2001).

Work by Takanaga *et al.* in C6 cells, demonstrated the presence of the AhR and induction of CYP1A1 by TCDD (Takanaga *et al.*, 2001). Although experimental data from this dissertation ultimately suggested otherwise, it was originally reasoned that the dioxin-like PCB congener 126 would also induce CYP1A1 in C6 cells via the AhR. C6 cells were thus chosen for studying the effects of PCB 126 on gene expression in the central nervous system, and for making comparisons to the effects of PCB 126 in hepatic H4IIE cells.

4. Exposure Concentration and Duration of Exposure

In order to obtain meaningful differential gene expression results, two criteria are important with regard to dose and duration. The dose of PCB 126 should be just high enough to ensure maximal induction of CYP1A1, yet be as low a possible to minimize overt toxicity, and the exposure duration should be sufficient to achieve steady-state

induction. Induction of CYP1A1 by PCB 126 in H4IIE hepatoma cells was examined previously in our laboratory (Broccardo *et al.*, 2004). Both concentration-response and time course analyses of CYP1A1 mRNA induction were performed by real time RT-PCR. CYP1A1 protein induction was analyzed by fluorescence flow cytometry. For both mRNA (Fig. 3.1A) and protein (Fig. 3.1B), maximal induction occurred at PCB 126 concentrations greater than 10^{-8} M. Time-course analysis revealed maximal CYP1A1 mRNA induction occurred at 16 h (2,000-fold) then dropped to 1,000-fold, remaining relatively constant from 24 h to 48 h (Fig. 3.1C). Based on these findings, H4IIE cells were dosed with PCB 126 using a culture medium concentration of 2.5×10^{-7} M ($\approx$ 80 ppb), which is a concentration approximately one-order of magnitude higher than was observed to cause maximal induction. The exposure duration of 24 hours should be sufficient to reach steady state mRNA induction. No overt toxicity was seen at this concentration. To facilitate comparison between H4IIE and C6 cells, both cell lines were dosed at the same PCB 126 concentration for the same duration. Both SAGE and microarray analyses requires cell culture, PCB 126 treatment, and total RNA isolation. The following methods for these initial steps are the same for both SAGE and microarray protocols, and are discussed here.

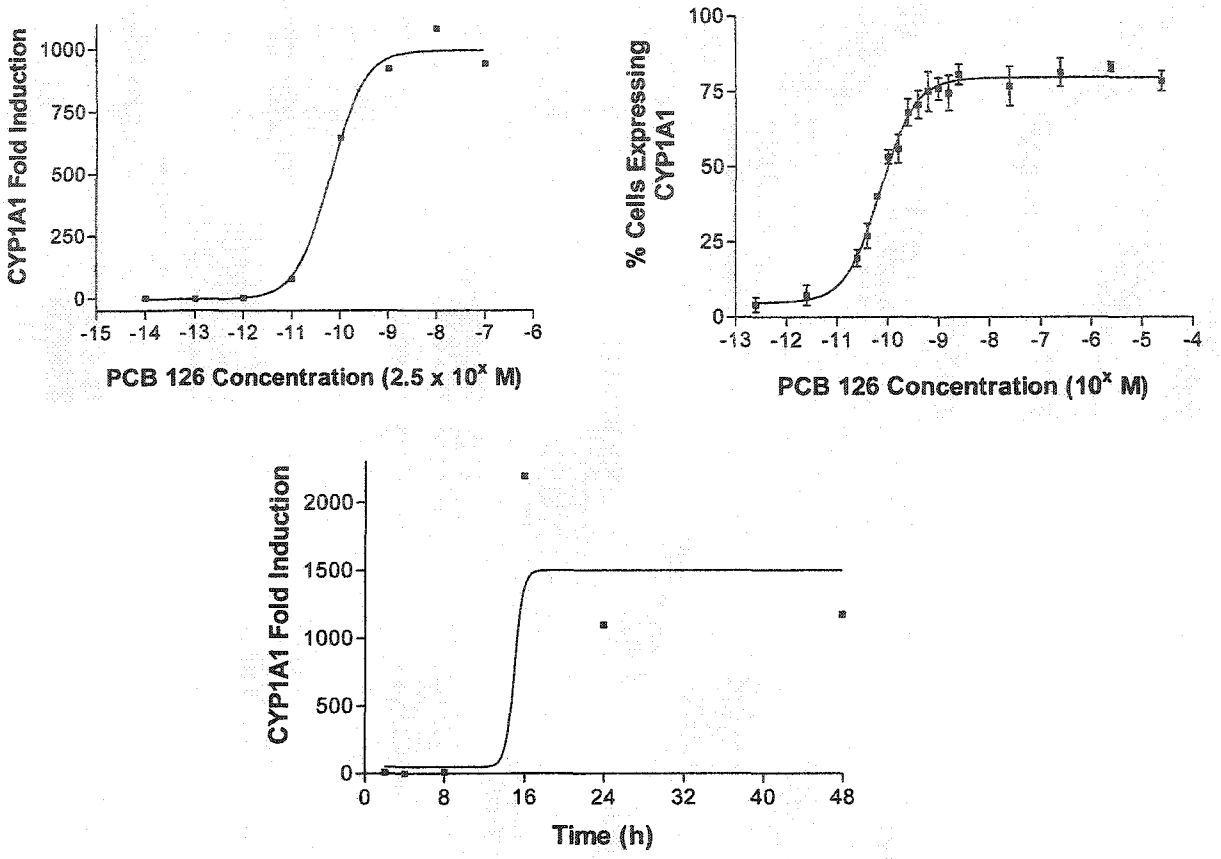

Figure 3.1. A.) CYP1A1 mRNA fold induction levels in H4IIE cells; quantification via real time RT-PCR using primers specific for CYP1A1 and the β-actin housekeeping. **B.)** 24 h treatment with PCB 126 with concentrations ranged 10-fold from 2.5 x 10^{-14} to 2.5 x 10^{-7} M. **C.)** Treatment with 2.5 x 10^{-8} M PCB 126 for 2, 4, 8, 16, 24, 48 h. *Source*: Broccardo, *et. al.* (2004).

5. Growth conditions, PCB 126 treatments and RNA isolation

Control and treated rat H4IIE hepatoma and rat C6 glioma cells (ATCC) were cultured in DMEM supplemented with 10% FBS (Hyclone) and 100 units/ml penicillin/100 μg/ml streptomycin and maintained at 37°C in a 5% CO_2 atmosphere. 3.2 x 10^6 cells were plated onto 100 mm dishes for 24 h and allowed to plate down. PCB 126 (3, 3′,4 ,4′,5-pentachlorobiphenyl) was obtained from AccuStandard (New Haven, CT) and confirmed by GCMS to be pure and free of other congeners. Cells were treated with 2.5 x 10^{-7} M (80 ppb) PCB 126 for 24-hours. Control cells in the present study were treated with DMSO vehicle equivalent to 0.2% DMSO (which was equivolume to the PCB 126 treatment), and each treatment was performed in biological triplicate, (i.e., 3 plates per treatment). For SAGE, replicate treatments or controls were pooled; for microarray analyses each biological replicate was analyzed individually using replicate arrays. Following treatment, cells were directly lysed on the dish with 600 μl of lysis buffer RLT (Qiagen) containing 10 μl/ml β-mecraptoethanol and removed with a cell scraper. A Qiagen mini-kit (Valencia, CA) protocol was followed for isolating total RNA. Briefly, lysed cells were homogenized by passing the lysis mixture through a QIAshredeer (Qiagen) spin column. One volume of 70% ethanol was added to the eluate. This mixture was applied to a RNeasy (Qiagen) affinity spin column and centrifuged for 15 seconds at 8,000 x g. Columns were washed by passing low stringency (RWI) buffer and high stringency (RPE) buffer through the column by centrifuging 15 seconds at 8,000 x g for each buffer. Total RNA was eluted from the column by passing 25 μl of RNase free water through the column twice at 8,000 x g for 1 minute. Resulting RNA was quantified with a Beckman DU640B spectrophotometer which indicated total RNA yields averaging

8 µg in 25 µl of water. Total RNA quality was visualized using a 1% agarose gel (Figure 3.2). Good quality RNA is indicated by an upper 28S rRNA band (4.5 kb) that is twice the intensity of the lower 18S rRNA band (1.9 kb) and by the absence of smearing near the bottom of lanes due to degraded RNA.

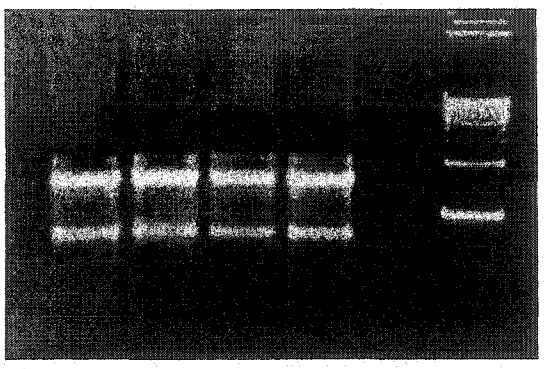

Figure 3.2 Total RNA. Isolated from C6 cells (lanes 1-2) and H4IIE cells (lanes 3-4). Top bands are 28S rRNA, lower bands are18S rRNA. 1% aragorse; molecular mass-marker far right.

C. SERIAL ANALYSIS OF GENE EXPRESSION

Serial analysis of gene expression (SAGE) was developed in the mid-90s and is based on the identification of short pieces of mRNA transcripts know as expressed sequence tags (ESTs) (Velculescu *et al.*, 1995). SAGE is the only method currently available that, in principle, can detect every expressed mRNA transcript, quantify transcript levels, and do so without any *a priori* knowledge of transcript sequence. SAGE is based on these principles:

- A short piece of mRNA (i.e., an EST of approx. 14-21 bp) obtained from a defined region within a transcript contains sufficient information to uniquely identify a transcript and hence its gene.
- ESTs can be obtained using restriction endonuclease excision from parent mRNA transcripts, can then be amplified by large scale PCR, and subsequently ligated to form long DNA polymers (concatemers) that can be cloned and sequenced.

- Because ESTs are randomly positioned in concatemers, the expression levels of each transcript is quantified by the number of times a particular tag is observed through repeated sequencing of cloned concatemers.
- With sufficient concatemer sequence data in hand, bioinformatics software and the National Center for Biotechnology Information (NCBI) SAGE database can identify genes containing sequences represented an EST.

The SAGE method is summarized in Figure 3.3. The following steps are necessary to complete the method:

1. Total RNA is isolated and incubated with magnetic beads containing oligo(dT) surface ligands that bind poly-adenylated mRNA tails.
2. Solid phase synthesis of cDNA (using bead-bound mRNA as a template) is carried out using reverse transcriptase and *E. coli* DNA polymerase.
3. Double stranded cDNA is digested with *Nla* III restriction endonuclease (known as the anchoring enzyme). Because *Nla*III sites are known to occur approximately every 250-bp, most transcripts are cleaved at least once.
4. Magnetic beads with attached cDNA are divided into two fractions and ligated to two different adapter constructs (Adapter A and Adapter B, ~40-bp each). The adapter constructs contain cohesive 4-bp overhangs that are complementary to *Nla*III digested cDNA at one end, and a Type IIS restriction site (i.e., *Mme*I) at the 3'-end. Additionally, the adapter constructs have priming sites for PCR amplification.

5. *Mme*I (known as the tagging enzyme) will bind to a recognition sequence in the adapter adjacent to the site complimentary to the 4-bp overhang remaining after *Nla*III digestion (CATG). *Mme*I possesses a subunit capable of cleaving the cDNA 21-bp downstream of the adapter and thus releases a 60-bp tag with a 4-bp overhang. At this stage, the tag consists of 40-bp of adapter sequence and 21-bp of unique sequence from a single transcript.

6. Fraction A and B are ligated to form 130-bp constructs know as ditags. Adapters A and B are now present at the 5' and 3' ends of the ditag, respectively.

7. The 130-bp ditags are PCR amplified using primers specific for the primer binding sites on the adapters; this step produces large quantities of ditags for subsequent joining into polymeric concatemers. Because the ditags are of short, uniform size and the majority of sequence is similar between amplicon, there is no significant PCR amplification bias.

8. Following amplification, the 130-bp ditags are digested with the anchoring enzyme (*Nla*III) that was used to cleave the original cDNA, resulting in the release of 34-bp ditags. These ditags consist entirely of sequence derived from transcript cDNAs, and end with the *Nla*III recognition sequence (CATG). The 34-bp ditags are now gel purified away from the adapters by polyacrylamide gel electrophoresis.

9. The 34-bp ditags are ligated into concatemers and 500–800-bp concatemers are gel isolated. Each ditag within a concatemer is punctuated with the *Nla*III recognition sequence (CATG).

10. Concatemers are inserted into a linearized cloning vectors and electroporated into bacteria that are grown on agar plates containing an antibiotic selective for bacteria expressing vector inserts. Clones containing inserts are picked from agar plate, grown in selective media and sequenced. With each transcript tag delineated by CATG punctuation, sequence data can be analyzed and compared to sequence databases for gene identification. Quantitative information is obtained from relative abundance of a particular tag sequence.

11. Sequence data are analyzed with SAGE software (Invitrogen, 2003b). The software extracts tag sequences from concatemer sequences, tabulates the occurrence of each tag, and creates a report of each tag and its abundance.

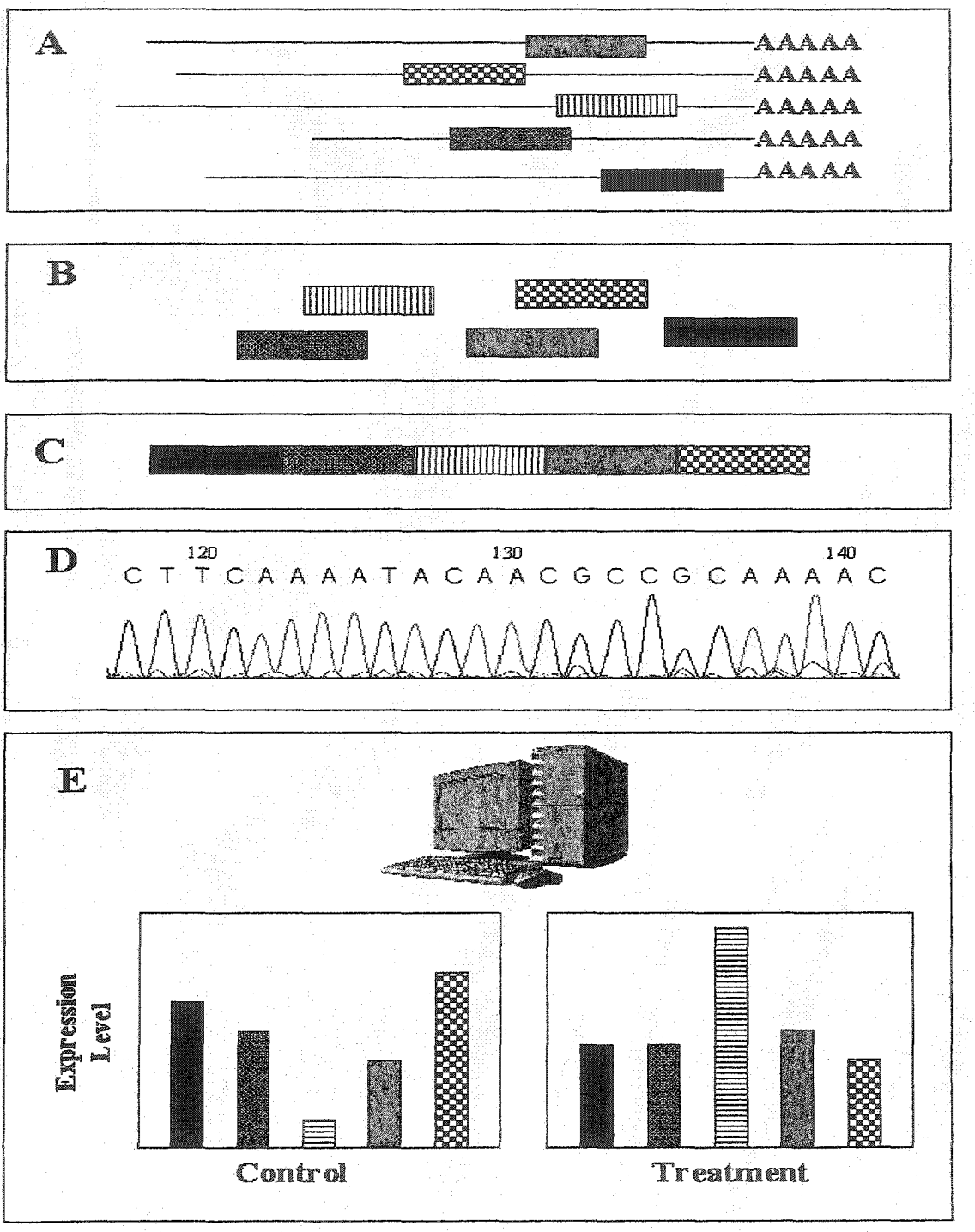

Figure 3.3 Overview of the serial analysis of gene expression (SAGE) method for analyzing differential gene expression. A) Polyadenylated mRNA is isolated and attached to biotinylated magnetic beads. B) Expressed sequence tags (ESTs) are clipped out using a series of restriction endonucleases. C) Thousands of EST fragments (14-20 bp) are ligated to form contatemers. D) Concatemers are sequenced. E) Sequence data are computationally analyzed to identify genes and transcript abundance then compared between treatments and controls.

1. Isolating Messenger RNA

Messenger RNA was isolated from total RNA using Dynabeads® magnetic separation technology (Dynal Biotech, Brown Deer, WI). This technology is based on super-paramagnetic polystyrene beads with oligo$(dT)_{25}$ covalently bound to the surface. Since most mRNA transcripts have poly(A) 3' tails, as depicted in Figure 3.4, through complementary base pairing transcripts will anneal to the oligo$(dT)_{25}$ attached to the beads. Up to 2 µg polyA^+ mRNA can be isolated per 200 µl of oligo$(dT)_{25}$ bead suspension depending on tissue and cell type and the expression level of the mRNA (Dynal, 2004). Once annealed, mRNA bound to the beads is magnetically separated from cellular debris and contaminants are removed through successive washing steps.

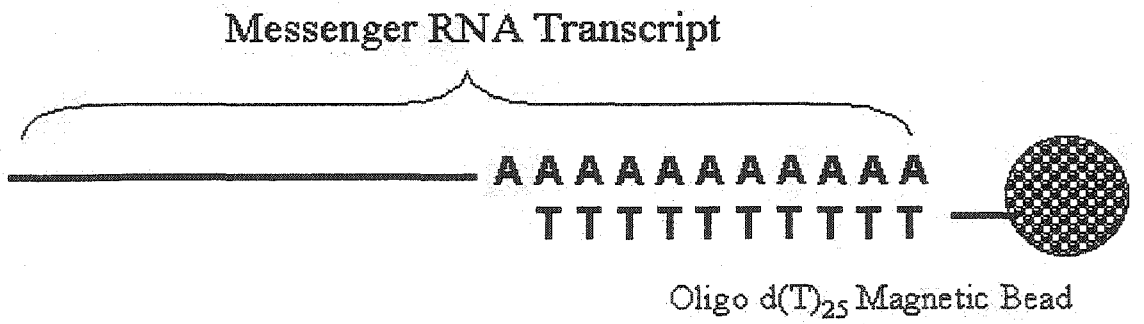

Figure 3.4. Messenger RNA transcript bound to Oligo $d(T)_{25}$ magnetic bead.

Washing Procedure

For each washing step, the tube containing beads is placed on a magnetic stand for 2 minutes. During this time the magnetic beads migrate to the wall of the tube adjacent to the magnet. A 200 µl pipette tip is then slid to the bottom of the tube, without disturbing the beads, and the buffer is aspirated. The next wash buffer is added, tubes are removed

from the magnetic stand and the beads are resuspended. Again the tube is returned to the magnetic stand and the process is repeated for each wash cycle.

2. Binding mRNA to Magnetic Beads

Beads were equilibrated and washed twice with 1 ml of lysis/binding buffer containing 100mM Tris-HCl (pH 7.5), 500 mM LiCl, 10 mM EDTA, 1% lithium dodecyl sulfate and 5 mM dithiothreitol (DTT). Approximately 8 µg of total RNA in 25 µl of water was added to the magnetic beads and adjusted to 1 ml with lysis/binding buffer. Beads and RNA were then placed on a rocking platform at room temperature for 30 minutes. Tubes were subsequently placed on the magnetic stand and washed twice with wash buffer *A* (10 mM Tris-HCl (pH 7.5), 0.15 M LiCl, 1 mM EDTA, 0.1% lithium dodecyl sulfate and 10 µg/ml glycogen) and once with 1 ml of wash buffer *B* (10 mM Tris-HCl (pH 7.5), 150 mM LiCl, 1 mM EDTA, and 10 µg/ml glycogen). Finally, the beads were washed three times and equilibrated in 1ml of 1X first strand synthesis buffer (50 mM Tris-HCl (pH 8.3), 75 mM KCl, 3 mM $MgCl_2$ and 10 µg/ml mussel glycogen).

3. First Strand cDNA Synthesis

As depicted in Figure 3.5, first strand complimentary DNA (cDNA) was synthesized using mRNA transcripts attached to beads as templates. The synthesis reaction was carried out in 18.0 µl 5X first strand buffer (250 mM Tris-HCl (pH 8.3), 375 mM KCl, 15 mM $MgCl_2$), 54.5 µl RNase free water, 4.5 µl dNTP mix (IDT, Coralville, IA) consisting of 10 mM each of dGTP, dCTP, dATP, and dTTP, in the presence of 9 µl of 0.1 M DTT

and a trace (1 µl) of RNaseOUT (Invitrogen). 3 µl (600 U) of reverse transcriptase (RT) (SuperScript II, Invitrogen) was used to catalyze the reaction for 1 hour at 42°C.

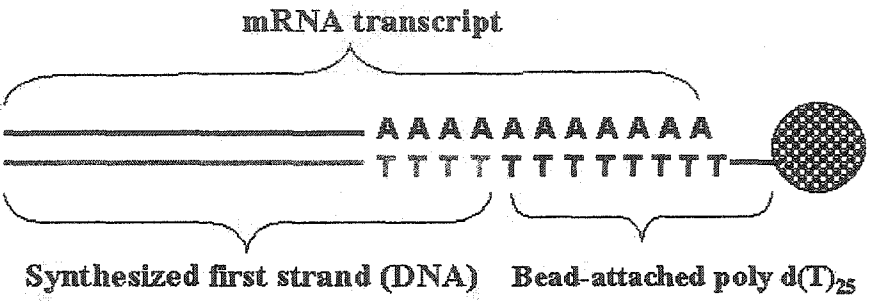

Figure 3.5. First strand synthesis. The mRNA transcript paired to poly $d(T)_{25}$ attached to the bead is used as a template for first strand cDNA synthesis.

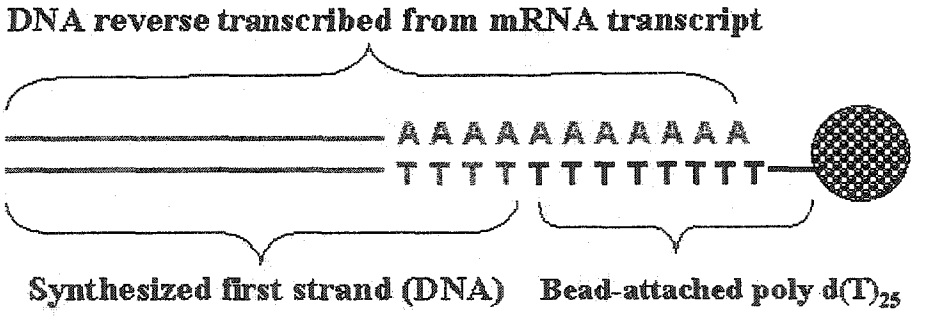

Figure 3.6. Second strand synthesis. The mRNA transcript is reverse transcribed leaving double stranded cDNA attached to the magnetic bead.

4. Second Strand cDNA Synthesis

As depicted in Figure 3.6, second strand cDNA was reverse transcribed from the first strand in 150 µl of 5X second strand buffer (100 mM Tris-HCl (pH 6.9), 450 mM KCl, 23 mM $MgCl_2$, 0.075 mM β-NAD^+, and 50 mM ammonium sulfate), 465 µl of RNase

free water, 5 µl (50 U) *E. coli* DNA ligase, 20 µl (200 U) *E. coli* DNA polymerase, and 5 µl (10 U) of *E. coli* RNase H (Invitrogen). The reaction was conducted with gentle mixing every 15 minutes at 16°C. After two hours, 45 µl of EDTA was added to sequester magnesium ion and stop the reaction. Tubes were placed on the magnetic stand, the reaction mixture was removed and 750 µl of hot (75°C) wash buffer *C* (5 mM Tris-HCl (pH 7.5), 1 M NaCl, 0.5 mM EDTA, 1% dodecyl sulfate (SDS) and 10 µg/ml mussel glycogen) was used to wash the beads three times using the magnetic washing method previously described. A 5 µl aliquot of resuspended beads was removed to verify cDNA synthesis in a later step (Figure 3.8A). The beads were then washed once with 1X buffer 4 (20 mM Tris-acetate (pH 7.9), 10 mM magnesium acetate, 50 mM potassium acetate, 1 mM DTT, and 200 µg/ml BSA) then resuspended in 1X buffer 4 and transferred to a new tube to avoid traces of *E. Coli* DNA polymerase exonuclease activity that might remain on tube walls.

5. Digesting cDNA with the Anchoring Enzyme

The recognition site of the restriction endonuclease *Nla*III (isolated from *Neisseria lactamica*) is known to occur approximately every 250-bp in most transcribed regions of DNA. Digestion with this enzyme should therefore, cleave most transcript cDNA at least once. To accomplish this, cDNA attached to beads was digested at 37°C for 1 hour in 174 µl of LoTE buffer (3 mM Tris-HCl (pH 7.5) and 0.2 mM EDTA), 20 µl buffer 4 with 6 µl (60U) of *Nla*III (New England BioLabs, Beverely, MA). After digestion, beads were washed twice with wash buffer *C* and three times with wash buffer *D* (5 mM Tris (pH 7.5), 0.5 mM EDTA, 1 M NaCl, 200 µg/ml BSA). As shown in Figure 3.6, double

stranded cDNA attached to the magnetic beads would be cleaved at *Nla*III restriction sites, leaving the 3'-most end of cDNA attached to the bead while cleaved 5'-cDNA is cleaved and removed by washing. In order to verify cleavage, a 5 µl aliquot of suspended beads was removed for subsequent PCR along with the aliquot removed prior to digestions.

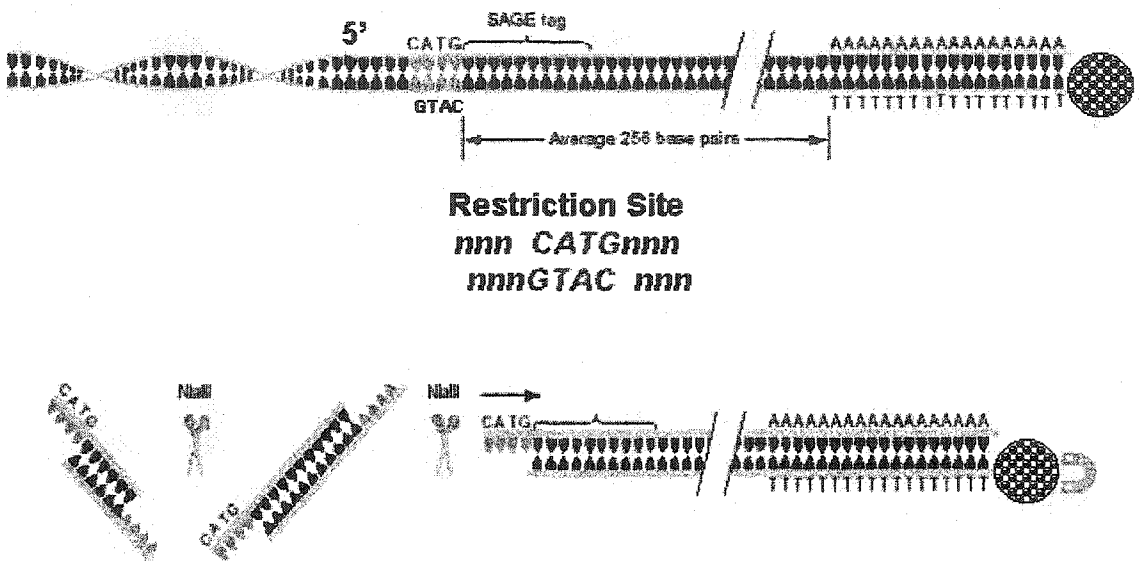

Figure 3.7. Cleavage with *Nla*III (anchoring enzyme). This step leaves the 3'-most end of cDNA attached to the magnetic bead along with a short piece of DNA representing the original transcript (i.e., the "SAGE tag").

6. Verifying cDNA Synthesis and *Nla*III Digestion

To verify cDNA synthesis and *Nla*III digestion, the 5 µl aliquots of suspended beads previously removed were amplified by PCR. The housekeeping genes, elongation factor-1-α (EF) and glyceraldehyde-3-phosphate dehydrogenase (GAPDH) were chosen to verify cDNA synthesis and *Nla*III digestion because both are constitutively expressed, and the location of *Nla*III restriction sites in mRNA transcripts are known. Primers were

designed for EF to amplify a section of the 3'-most region (i.e., toward the bead) that does not contain an *Nla*III recognition site. As depicted in Figure 3.8, successful PCR amplification of this region is a positive control for cDNA synthesis. Primers for GAPDH were selected to bracket a known *Nla*III recognition site. Successful *Nla*III cleavage is indicated when the undigested cDNA aliquot is amplified and the *Nla*III digested aliquot is not.

PCR reactions mixtures are provided in Table 2-1. Cycling began with an extended 2 minute denaturing step at 95°C, followed by 32 repeated cycles consisting of a 1 minute denaturing step at 95°C, cooling to 55°C for 1 minute to anneal double strands, and heating to 72°C for 2 minutes for extension (DNA synthesis). Finally, the mixture was held at 72°C for 5 minutes to complete DNA synthesis, then held indefinitely at 4°C. A 4% agarose gel showing successful solid phase cDNA synthesis (i.e., synthesis on the magnetic bead) and subsequent *Nla*III cleavage is shown in Figure 3.9.

7. Ligating Adapters to cDNA

Two different nucleic acid "adapter" constructs (Figure 3.10) were ligated to separate aliquots of *Nla*III-digested transcripts still attached to magentic beads. The adapters are 3'-amino-protected constructs containing a recognition site for the *Mme*I restriction endonuclease at 3'-ends, a cohesive overhang at the 3'-end complementary to the *Nla*III restriction overhang, and a PCR priming site. The 3'-amino group protects against self ligation, and use of non-complementary adapters them from annealing to each another during PCR. Once adapters become ligated, subsequent cleavage with the *Mme*I tagging

enzyme will release the adapters and a short piece of cDNA (*tag*) from the magnetic beads.

Following ligation, beads were washed twice with 150 µl of 1X ligase buffer diluted from 10X stock (60 mM Tris-HCL (pH 7.5), 60 mM $MgCl_2$, 50 mM NaCl, 1 mg/ml BSA, 70 mM β-mercaptoethanol, 1 mM ATP, 20 mM DTT, 10 mM spermidine) and then resuspended in 100 µl of 1X ligase buffer. The 100 µl bead suspension was split into two 50 µl aliquots and the 1X ligase buffer was removed. Adapters A or B (1.5 µl of 20 ng/µl) in each aliquot were ligated in 14 µl of LoTE and 2 µl of 10X ligase buffer for 2 hours at 16°C with mixing every 15 minutes. After 2 hours, beads in each aliquot were washed three times with 500 µl of wash buffer *D*.

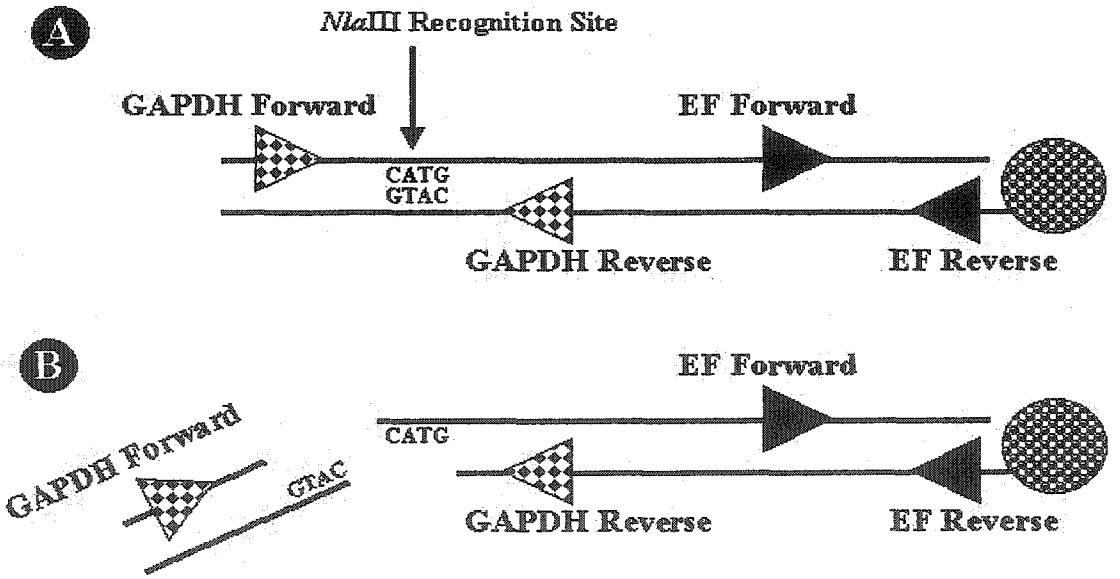

Figure 3.8. Verification of cDNA synthesis and *Nla*III cleavage. A.) If cDNA synthesis has occurred, the segment between the elongation factor-1-α (EF) forward primer and EF reverse primer will amplify by PCR. B.) If *Nla*III cleavage has occurred, the cDNA segment between the glyceraldehyde-3-phosphate dehydrogenase (GAPDH) forward primer and GAPDH reverse primer will amplify only in the cDNA aliquot removed before digestion (A) but, due to cleavage between priming sites, the segment will not amplify after digestion (B).

Table 3-1. PCR mixtures (μl) to verify cDNA synthesis and *Nla*III digestion

Reagents	GAPDH/cDNA Template	GAPDH/*Nla*III Template	EF/cDNA Template	EF/*Nla*III Template
10X BV Buffer	5	5	5	5
DMSO	3	3	3	3
dNTP Mix (10 mM each)	5	5	5	5
GAPDH Primer Set	4	4	-	-
EF Forward Primer	-	-	2	2
EF Reverse Primer	-	-	2	2
Taq Polymerase (hot start)	0.5	0.5	0.5	0.5
cDNA Template (pre digestion)	0.5	-	0.5	-
cDNA Template (post *Nla*III digestion)	-	0.5	-	0.5
RNase Free Water	to 50	to 50	to 50	to 50

BV buffer: 166 mM NH_4SO_4, 670 mM Tris-HCl (pH 8.8), 67 mM $MgCl_2$, 100 mM β-mercaptoethanol
DMSO (dimethyl sulfoxide); dNTP mix (10 mM each of dATP, dGTP, dCTP, dTTP)
GAPDH forward: 5'-TTAGCACCCCTGGCCAAGG-3'; reverse: 5'-CTTACTCCTTGGAGGCCATG-3'
EF forward: 5'-CATGTGTGTTGAGAGCTTC-3'; reverse: 5'-GAAAACCAAAGTGGTCCAC-3'
Taq hot start polymerase (Bio-Rad)

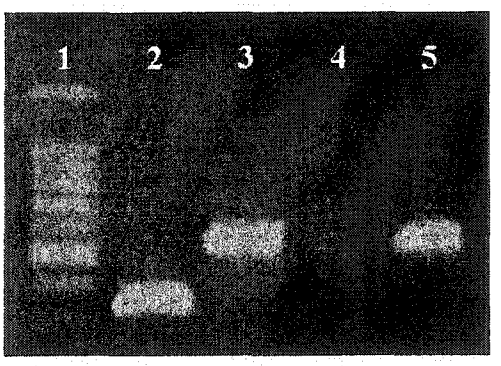

Figure 3.9. Verification of cDNA synthesis and cleavage by *Nla*III. 1) 100 bp ladder (most intense band is 500 bp); 2) EF amplicon from aliquot taken before *Nla*III digestion; 3) GAPDH amplicon from aliquot taken before *Nla*III digestion; 4) GAPDH after digestion (no amplification); 5) EF amplicon of aliquot taken after *Nla*III digestion. Starting mRNA was obtained from M059K cells. PCR was conducted using cDNA attached to magnetic beads. See text for rationale.

8. Cleaving with *Mme*I Tagging Enzyme

*Mme*I is a type IIS restriction endonuclease. Type IIS endonucleases recognize asymmetric DNA sequences and cleave both trands of DNA at fixed positions, typically several base pairs away from the recognition site (Roberts *et al.*, 1993). *Mme*I is obtained from the obligate methylotroph *Methylophilus methylotrophus*. As shown in Figure 3.10, *Mme*I is capable of cutting 18 to 20 nucleotides away from its recognition site toward the 3' (magnetic bead) end of the cDNA. This endocuclease activity results in release of the adapter and a 18 – 20 base pair SAGE tag. For this reason, *Mme*I is known as the "tagging" enzyme. Tags are later ligated to form chains called *concatemers* that are sequenced. Each tag sequence uniquely identifies a transcript, and hence identifies the gene from which it was transcribed.

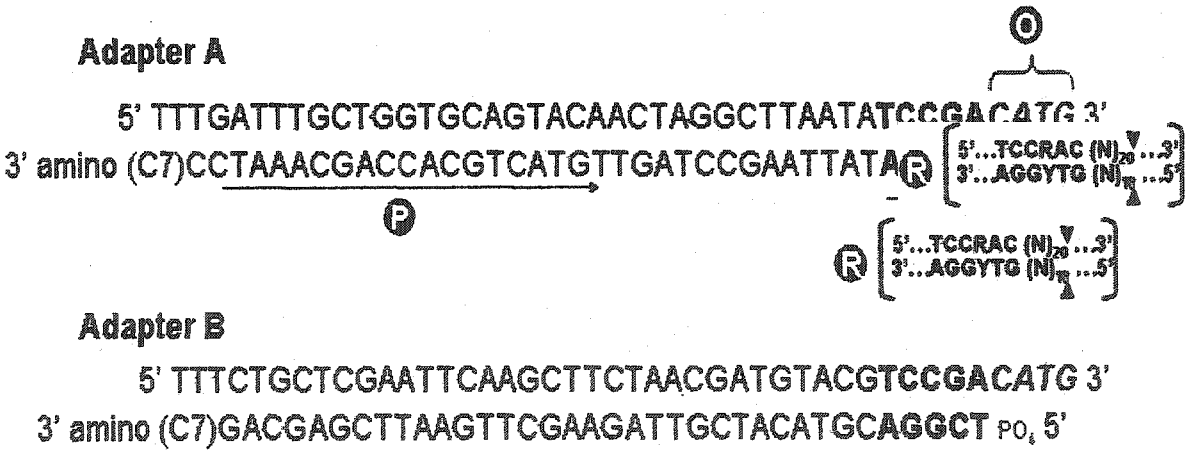

Figure 3.10. Adapter constructs for creating SAGE ditags. Adapters contain a cohesive overhang for ligation to the "sticky" end of bead-bound cDNA generated by *Nla*III digestion (O), a *Mme* I recognition and restriction site (R), and a priming site for amplification (P). In the restriction site sequence (R), Y indicates the nucleotides C or T may be present and R indicates A or G.

Before digestion, each aliquot of suspended beads is washed twice with 1X buffer *4*/1X SAM diluted from 10X buffer *4* + 10X SAM (200 mM Tris-acetate (pH 7.9), 100 mM magnesium acetate, 500 mM potassium acetate, 10 mM DTT + 400 µM S-adenosyl methionine). Cleavage is accomplished by digesting bead aliquots in 70 µl LoTE, 10 µl 10X buffer *4* + 10X SAM with 10 µl (2 U/µl) *Mme*I (New England BioLabs) at 37°C for 2.5 hours.

9. Creating SAGE Ditags

Following *Mme*I digestion, adapter A-tags and adapter B-tags, now present in the liquid phase, were separated from the beads, pooled together, and cleaned up with phenol/chloroform extraction and ethanol precipitated. Although total volumes from this cleanup procedute vary, proportions are constant. This method of clean up is used extensively throughout the rest of the SAGE procedure and is detailed here.

Phenol/chloroform-ethanol precipitation

Phenol/chloroform/isoamyl alcohol (25:24:1) is added in equal volume to the aqueous solution of DNA and thouroughly mixed and centrifuged at room temperature for 5 minutes at 14,000 x g. This step produces 2-phase system with a top aqueous phase containing nucleic acid, an interphase containing protein residues (e.g., endonucleases) and a lower chloroform phase containing hydrophobic contaminants. After centrifuging, the top aqueous phase containing DNA is transferred to a clean tube by pipetting and the interphase and chloroform phases are discarded. To the aqueous phase, two-thirds volume of 7.5M ammonium acetate (saturated) is added with a small volume of mussel glycogen (co-precipitate to improve yields) and three volumes of cold ethanol. After 20

minutes on dry ice, tubes are centrifuged at 14,000 x g for 40 minutes at 4°C. This procedure results in a visible DNA/glycogen pellet at the bottom of the tube. After carefully removing the supernatant, the pellet is washed with 70% ethanol:water to remove salt residues, and the pellet is air dried for 20 minutes to eliminate residual ethanol. The dried pellet is then redissolved in appropriate buffer or water.

In the present SAGE step, pooled tags+adapters (now in 200 µl of *Mme*I digestion mixture), were cleaned up with 300 µl phenol/chloroform and ethanol precipitated as described above. The pellet was dissolved in 6 µl of LoTE at 37°C for 15 minutes. After dissolving the pellet, the tags were ligated at their 3'-ends to form ditags (i.e., *AdapterA+Tag—Tag+AdapterB*). Ligation was accomplished with 1.8 µl (7.2 Weiss units) of T4 DNA ligase (Invitrogen), in 1.25 µl 3 mM Tris-HCl (pH 7.5), 13.5 µl 10X ligase buffer and 13.5 µl of RNase free water at 16°C overnight.

10. Amplifying SAGE Ditags

Successful SAGE requires large-scale PCR to produce approximately 200 µg of ditags (Powell, 1998). Prior to PCR on this scale, PCR conditions were optimized using a primer set complementary to a portion of each DNA adapter construct; ditag primer sequences are detailed in Table 2-2. Conditions for ditag amplification using these primers were optimized for annealing temperature, ditag dilution, dNTP concentration, and PCR cycling parameters. Temperature optimizaton experiments were run on an Mastercycler gradient thermocycler (Eppendorf, Westbury, NY). PCR products produced with various annealing temperatures are show in Figure 3.11. Additionally, as shown in

Figure 3.12B, ditag dilutions greater than 1:1000 produced the best amplification results and both Bio-Rad I-Taq® and Invitrogen Platinum® hot-start polymerases produced comparable results. Standard *Taq* polymerases (i.e., not protected for hot-start) resulted in no visible amplification when visualized on a 4% agarose gel.

Large scale PCR was conduced using a Gene Amp 9600 PCR system (Perkin-Elmer, Wellesley, MA). Because 96-well plates performed poorly due to fluid volatilization, twelve 8-well PCR tube strips with tight caps were used for amplification batch. The optimized cycling program began with an extended 2 minute denaturing step at 95°C, followed by 30 repeated cycles consisting of a 30 second denaturing step at 95°C, cooling to 54°C for 1 minute to anneal double strands, and heating to 70°C for 90 seconds for DNA synthesis. Finally, the mixture was held at 70°C for 15 minutes to complete DNA synthesis, and then held indefinitely at 4°C. When amplified by large scale PCR, ditags derived from PCB 126 treated cells produced 10 ng ditags/µl and controls produced 6 ng ditags/µl (i.e., 50 ng/5 µl and 30 ng/5 µl, respectively). These concentrations were determined using spectrophotometry verified by comparison to a DNA mass standard (*Precision Molecular Mass Ruler*, Bio-Rad, Hercules, CA) as shown in Figure 3.12A. In order to produce approximately 200 µg of ditags, PCB 126 treatment ditags were amplified in four batches of 96 x 50µl (expected yield 232 µg) and controls were amplified in seven batches (expected yield 196 µg).

Table 3-2. Optimized PCR reaction mixture for amplifying SAGE ditags

Reagents	GAPDH/cDNA Template
10X BV Buffer	5
DMSO	3
dNTP Mix (10 mM each)	7.5
Ditag Primer A (175 ng/µl) [1]	2
Ditag Primer B (175 ng/µl) [2]	2
Taq Polymerase (hot start) [3]	0.5
Ditag Template (1:1000)	1
RNase Free Water	29

1 - DiTag primer A: 5'-GTGCTCGTGGGATTTGCTGGTGCAGTACA-3'
2 - DiTag primer B: 5'-GAGCTCGTGCTGCTCGAATTCAGCTTCT-3'
3- *Taq* hot start polymerase (Bio-Rad)

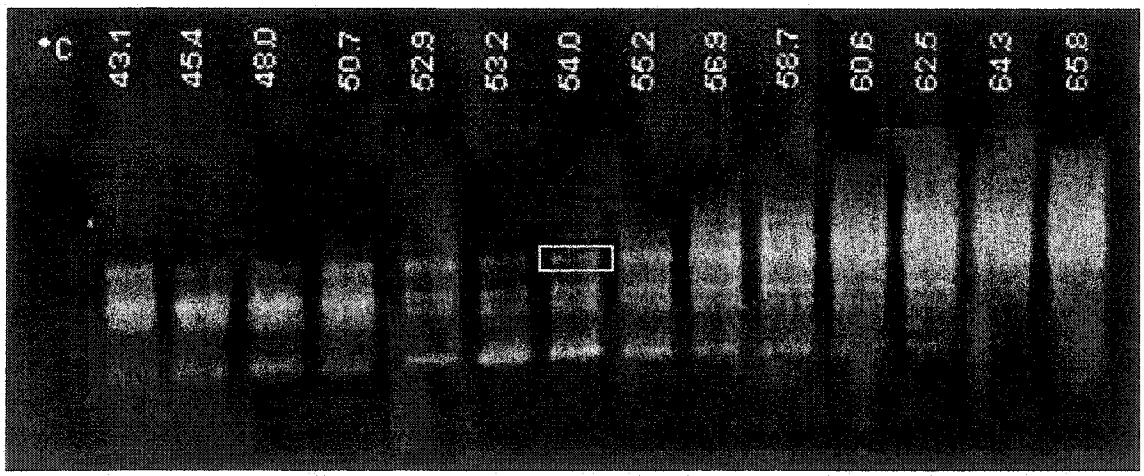

Figure 3.11. PCR annealing temperature optimization for amplification of SAGE ditags. An annealing temperature of 54°C was chosen for large scale PCR amplification of the 130 bp band (rectangle). At high temperatures mis-pairing occurs and at low temperatures, amplification of adapter dimers (i.e., no ditags) is favored.

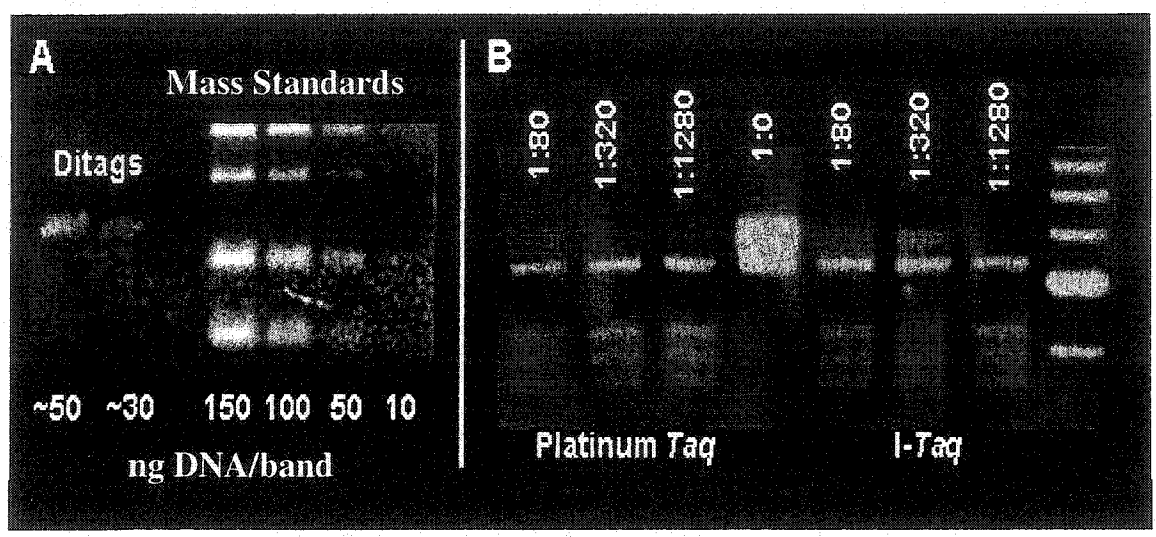

Figure 3.12. (A). Ditag yield for 5 µl of PCR reaction mixture from PCB 126 ditags (lane1) and controls (lane 2) compared to DNA mass standards (lanes 4-6); lane 3 is a blank. (B). Ditag dilution optimization and comparison of hot-start DNA polymerases. Dilution of approximately 1:1000 produced the cleanest product and little difference was observed between Platinum *Taq* (Invitrogen) and I-taq (Bio-Rad) polymerases.

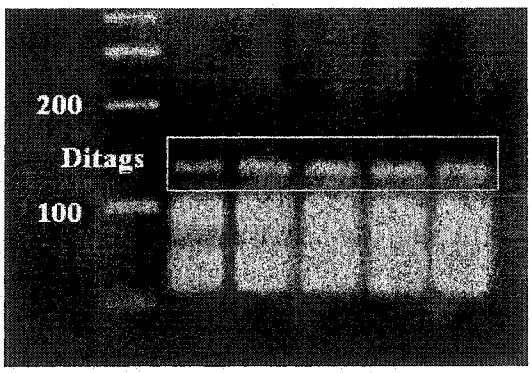

Figure 3.13. 130-bp ditag+adapters produced by large scale PCR amplification. 4% agarose with ethidium bromide staining. Ditag bands (rectangle) are recovered by excising from large-format acrylamide gels. Lower bands are amplified adapter dimmer and and adapter monomer contaminants.

11. Gel Isolating 130-bp Ditags

The large-scale PCR amplification, discussed above, yielded DNA bands of sizes shown in Figure 3.13. In order to proceed with the SAGE protocol it is necessary to isolate the 130-bp ditags from adapter dimers (~ 100-bp) and other smaller contaminants. Because ditags are similar in size to the contaminants, high resolution large-format (40 x 40 cm), high density (12%) polyacrylamide gels were needed to isolate target 130-bp ditags. In order to load relatively large volumes (20 µl) of ditag mixtures, it was also necessary to cast double-thickness gels (0.5 mm) using double spacers/combs between plates. Increased spacing necessitated a viscous gel mixture to prevent bubbles and leakage during casting. SequaGel (National Diagnostics, Atlanta, GA) mixtures produced the best large-format gels with minimal leakage. 12% acrylamide: bisacrylamide monomer gels were cast using a mixture of 40 µl TMED, 800 µl freshly prepared 10% ammonium persulfate and SequaGel components including 48 ml concentrate, 42 ml diluent, 10 ml buffer. A 0.5X TBE running buffer was used, diluted from 10X stock TBE (178 mM Tris-base, 178 mM boric acid, and 4mM EDTA).

Products from up to two (96 x 50µl) large-scale PCR runs were combined in a 50 ml *Oak Ridge* centrifuge tube and phenol/chloroform-ethanol precipitated as previously described. In this case, an equal volume of phenol/chloroform/isoamyl alcohol was used, followed by precipitation with 3.2 ml of 7.5 M ammonium acetate, 72 µl of mussel glycogen and 34 ml of 100% ethanol. Samples were centrifuged at 12,000 x g for 30 minutes at 4°C and the resulting pellet was resuspended in 300 µl of LoTE and allowed

to dissolve for 10 minutes at 37°C. After dissolution, 72 µl of 5X TBE *sample buffer* (18 mM Tris base, 18 mM boric acid, 0.4 mM EDTA free acid, 3% ficoll, 0.02% bromophenol blue and 0.02% xylene cyanol) was added. This mixture was loaded into wells of a 12% acrylamide gel (40 µl per well) and electrophoresed at 120v until the bromophenol blue dye ran out of the gel and the xylene cyanol dye front reached 1 cm from the bottom (approximately 5 hours). After electrophoresis, the gel was carefully released into an aquous solution of 2 mg/l ethidium bromide for 10 minutes then transferred to a ultra violet transilluminator.

Target 130-bp bands were visualized by transillumination and gel areas containing bands were excised using a razor blade. Electroelution turned out to be the most efficient way to extract DNA from the excised gel pieces bands. In this method, gel pieces removed from gels are placed in an electro-dialysis capsule (BioLine, Dublin, OH). Capsules are constructed with dialysis membranes on opposite sides of an internal chamber. The membranes permit current to flow through the capsule, while retaining large molecules. Excised gel pieces are placed inside the capsule's chamber, the chamber is filled with water, sealed, and placed in an agarose gel electrophoresis cell containing 1X TBE buffer. Current is applied perpendicular to the dialysis membranes (120v), causing DNA in the gel piece to be electrophoresed into surrounding water and onto the dialysis membrane adjacent to the anode. After 15-minutes of electrophoresis, the polarity is reversed briefly (40 sec) to remove DNA trapped on the dialysis membrane, and water containing eluted DNA is recovered from the capsule by pipetting.

Solutions containing DNA recovered by electroelution were combined, ethanol precipitated as previously described an dissolved in dissolved in 12 ml LoTE. Ethidium

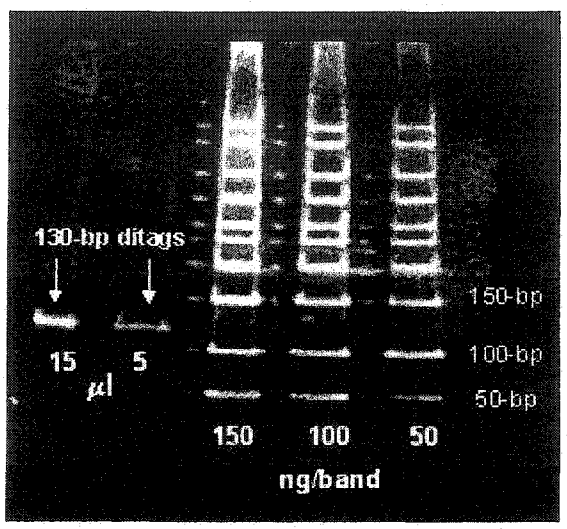

Figure 3.14. Quantification of 130-bp PCB 126 treatment ditags isolated by gel electrophoresis and removed from gels by electroelution. Trans-illuminated 12% polyacrylamide mini-gel stained with ethidium bromide.

bromide fluoresence was no longer visible after ethanol precipitation. Agarose electrophoresis of recovered DNA produced a single, sharp 130-bp band by electrophoresis in 8% polyacrylamide (Figure 3.15). Quantification using DNA mass standards and spectrophotometry, as previously described, demonstrated approximately 120 µg (10 ng/µl in 12 ml) of PCB 126 treatment ditags and 108 µg (9 ng/µl in 12 ml) of control ditags were recovered from polyacrylamide gels.

12. Digesting 130-bp Ditag/Adapters to Release Ditags

Soluble contaminants generated during the SAGE protocol are known to inhibit the activity of *Nla*III (Angelastro *et al.*, 2000). Contaminants are particularly problematic in this step because 130-bp ditags are no longer attached to magnetic beads (as they were

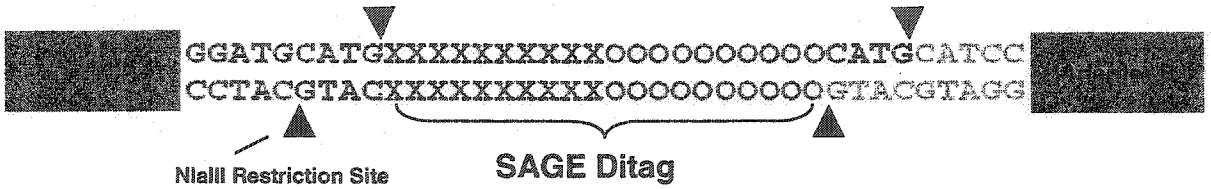

Figure 3.15. SAGE ditags+adapters. These constructs were isolated from polyacrylamide gels, purified, and digested with *Nla*III restriction endonuclease, releasing SAGE ditags with CATG 3'-sticky ends.

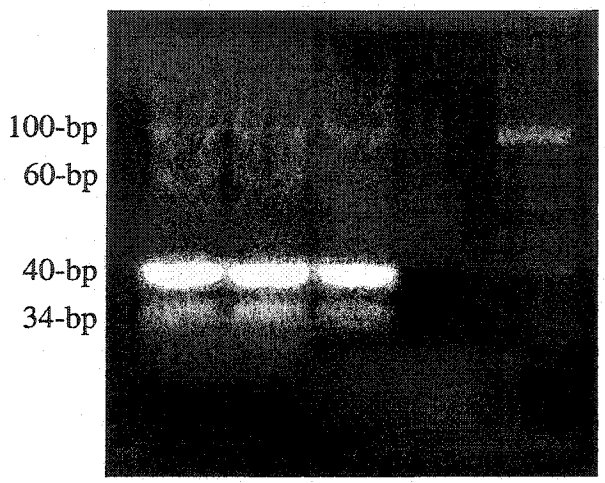

Figure 3.16. Products produced by *Nla*III-digested ditags+adapters. 34-bp bands (bottom most) are SAGE ditags, 40-bp bands are ligated di-adapters, and 60-100-bp bands result from incomplete *Nla*III digestion. 4% agarose.

during the prior anchoring digestion) which makes separation from soluble contaminants more difficult. To address this issue, affinity spin columns (Qiagen, Qiaquick kit) were used. This method is identical to the protocol previously described for isolating total RNA using affinity spin columns. Each ditag solution (12 ml) was processed through 18 affinity columns and after washing with chaotropic solvents in the kit, DNA was eluted from affinity membranes with LoTE. The *Nla*III digestion was then carried out as previously described for the anchoring step. Digesting 130-bp ditags with *Nla*III releases

34-bp ditags with CATG 3'-sticky ends (Figure 3.16). As visualized on 4% agarose, the *Nla*III digestion yielded bands shown in Figure 3.17.

13. Gel Purifying 34-bp Ditags

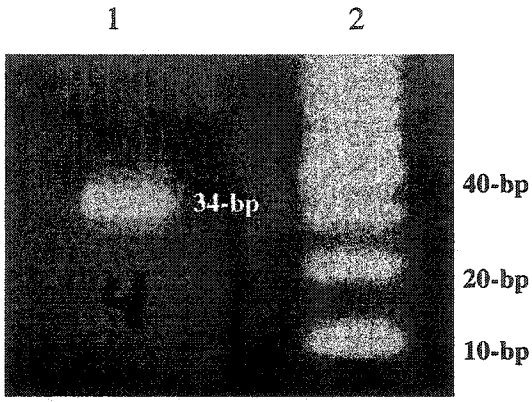

Figure 3.17. Isolated and purified 34-bp ditags (lane 1); 10-bp ladder (lane 2). 4% agarose gel with ethidium bromide staining.

In a manner identical to the gel isolation steps previously described for 135-bp ditags, 34-bp ditags were ethanol precipitated, dissolved in LoTE, combined with 5X TBE *sample buffer* and electrophoresed on large format 12% acrylamide gels until the xylene cyanol dye front reached 20 cm from the bottom (about 4 hours). 34-bp SAGE tags were excised, electroeluted and ethanol precipitated in the same manner as 134-bp ditags. Pellets were resuspended in 7.75 µl LoTE and 1µl of 10X ligase buffer. The isolated product produced a single 34-bp band when electrophoresed and visulized with a 4% agarose gel (Figure 3.18).

14. Ligating Ditags to Form Concatemers

In this step, 34-bp ditags, which now have 5'-CATG-3' "sticky" overhangs (see Figure 3.16), are ligated to form polymeric constructs called *concatemers*. This ligation reaction was carried out by incubating 8.75 µl of 34-bp DNA (from above) with 1.25 µl (5 Weiss units) of T4 DNA ligase (Invitrogen) for 3 hours at 16°C. This step is the most critical stage for constructing SAGE libraries (Mathupala *et al.*, 2002), and it is at this step that two separate attempts to construct SAGE concatemer libraries appeared to fail. Although

34-bp DNA bands were seen with 4% agarose gels prior to the ligation reaction, no DNA of any size, was seen after the ligation reaction. Possible reasons will be explored later in the discussion section of this dissertation. In hopes that some concatemers may have formed despite an ability to visualize them, in the final attempt to construct SAGE libraries, concatemer ligation reaction products were carried through to electroporation, cloning and sequencing.

15. Isolating Concatemers

The ligation reaction mixture was ethanol precipitated in the usual manner, and electrophoresed on a 12% mini-polyacrylamide gel (Bio-Rad). The 300 to 1000-bp regions expected to contain the concatemers (Invitrogen, 2003a), were excised electroeluted and ethanol precipitated. The pellet was subsequently dissolved in 6 µl of LoTE.

16. Cloning With pZErO-1 Vector

The pZEro-1 vector (Invitrogen) was used to clone putative concatemers. This cloning construct is based on the lethal *E. coli* gene *ccd*B (Bernard *et al.*, 1992; Bernard *et al.*, 1993; Bernard *et al.*, 1994; Jaffe *et al.*, 1985; Karoui *et al.*, 1983; Miki *et al.*, 1984; Ogura *et al.*, 1983; Van Melderen *et al.*, 1994). In pZEro-1, the *ccd*B gene is fused to the C-terminus of *lacZ*α. Insertion of concatemers should disrupt expression of the *lacZ*α-*ccd*B gene fusion, permitting growth of only successful recombinants. The CcdB protein acts by poisoning bacterial DNA-gyrase (i.e., topoisomerase II), an essential enzyme for catalysis of ATP-dependent negative DNA supercoiling. Other features include a Zeocin

resistant gene for selection of competent *E. coli* and universal M13 priming sites for sequencing.

Before use, the pZEro-1 vector must be linearized. 2 µg (2 µl) of vector was linearized using 1.4µl (7 U) of *Sph*1 endonuclease (New England Biolabs), 2.5 µl 10X buffer *2* (100 mM Tris-HCl (pH 7.0), 10 mM $MgCl_2$, 50 mM NaCl, 1 mM DTT) and 19.1 µl of RNase free water at 37°C for 30 minutes. After linearization 175 µl of LoTE was added to the mixure and it was phenol/chloroform extracted and ethanol precipitated in the usual manner. The pellet was dissolved in 60 µl of LoTE. 2 µl of this linearized vector was compared to native vector by 1% agarose electrophoresis. Figure 3.19 shows the result of linearization whereby the linearized vector electro-phoreses more slowly than the more compact native vector.

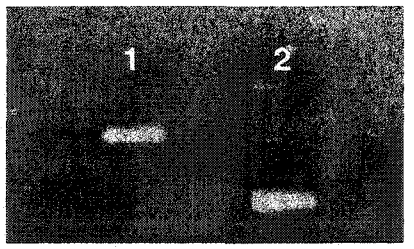

Figure 3.18. Linearized pZEro-1 vector (lane 1). Native vector (lane 2). 1% agarose gel electrophoresis with ethidium bromide staining.

17. Transforming Electrocompetent *E. Coli*

New electro-competent *E. coli* (EP-Max 10B, BioRad), were tested for viability on low-salt LB plates without antibiotic and confluent bacterial lawns were noted in two days. After confirming cell viability, ice-cold EP-Max 10B *E. coli* were electroporated (600v) with the putative concatemers. After electroporation, SOC medium was added and shaken at 37°C for 1 hour. LB/Zeocin (50 µg/ml) plates were innoculated and incubated overnight at 37°C.

18. Screening Transformants

When plates were removed from the incubator, innoculated plates produced about 150 colonies per plate. From these plates, approximately 90 colonies were picked and innoculated into SOB medium containing 50 μg/ml Zeocin and grown overnight at 37°C. Plasmid DNA was then isolated using a plasmid mini-prep kit (Bio Rad) and digested with *Xba*I and *Hind*III to release any inserted concatemers. A representative example of the digested DNA is shown in Figure 3.20; inserts ranged in size from 150- to 300-bp. If concatemers were present, the estimated lenghth of inserts would be at least 400-bp. Transformants were also analyzed by PCR utilizing M13 primer sites that flank the insertion site of the cloning vector. Unfortunately, amplicons of identical size indicate the absence of concatemer inserts (Figure 3.21).

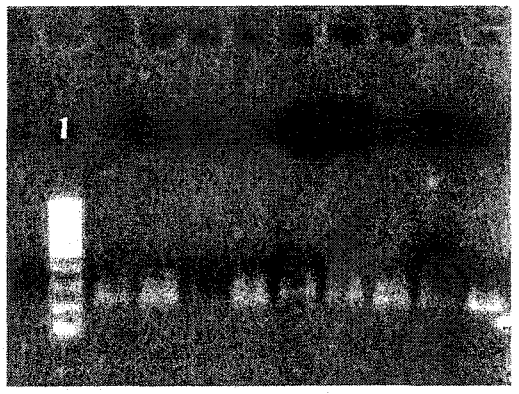

Figure 3.19. Representative example of *Xba*I and *Hind*III digested plasmid DNA from cloned recombinants. 100-bp ladder (lane 1). 1% agarose, ethidium bromide staining.

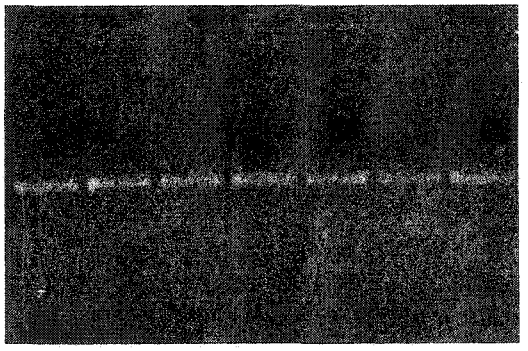

Figure 3.20. Transformants analyzed for size difference by PCR utilizing M13 priming sites on pZEro-1 cloning vector. Obseving amplicons of identical size indicates the absence of concatemer inserts. 1% agarose, ethidium bromide staining.

19. Sequencing

Six samples of intact plasmid DNA that appeard to contain the largest inserts based on *Xba*I and *Hind*III digestions (Figure 3.19), were sequenced with M13 forward primer by high throughput automated sequencing. ABI Prism Sequencer data were nearly identical between samples, no unique sequences were found, and BLAST analysis returned ~100% match to the pZEro-1 cloning vectro

D. MICROARRAY ANALYSIS

Microarray technology was pioneered by the semiconductor industry and uses solid phase chemical techniques that are able to apply hundreds of thousands of oligonucleotide probes representing different genes onto a single wafer about the size of a microscope slide. Like semi-conductor memory chips, each probe spot on a microarray is placed in an orderly addressable arrangement (Pasanen *et al.*, 2003).

Affymetrix (Afx) technology was used in this experiment (Affymetrix, 2004b). Afx uses RNA oligonucleotide probes that are similar in concept to SAGE tags, in that each probe represents a portion of the transcribed sequence of a particular gene. Unlike SAGE, where cDNA tags are generated without any a prior knowledge of sequence, Afx RNA probes are synthesized to represent five regions of the transcribed sequence of each gene, hence the sequence must be known *a priori*. In the Afx system, each gene is represented by 5 oligonucleotide pairs (probe pairs), one that has a perfect match to the sequence of a transcribed region (perfect match, PM), and a second oligonucleotide having one nucleotide mismatch in the middle (mismatch, MM). Probes are chosen within 500-bp of

the 3'-end of each gene and designed to hybridize under the same physical conditions. Control probes are designed from housekeeping genes in sets of three. One set is designed to match the 5'-end of the gene, as second set the middle, and a third set to match the 3'-end. Additionally, there are probe sets for spiked-in control RNAs corresponding to up- and down-regulated prokaryotic genes. The actual RNA hybridized to Afx microarrays is first biotin-labeled and after hybridization, stained with phycoerythrin-conjugated streptavidin for illumination and visualization with the array laser scanner. Computational details will follow. The rat genome arrays used in this experiment were comprised of about 31,000 probe sets representing approximately 28,700 well-substantiated rat genes. Array sequences were selected from GenBank, dbEST, and RefSeq.

20. Materials and Methods

Cells, growth conditions, treatments and RNA isolation

Triplicate control and treated rat H4IIE hepatoma and rat C6 glioma cells (ATCC) were cultured in DMEM supplemented with 10% FBS (Hyclone) and 100 units/ml penicillin/100 μg/ml streptomycin and maintained at 37°C in a 5% CO_2 atmosphere. 3.2 x 10^6 cells were plated onto 100 mm dishes for 24 h and allowed to plate down. PCB 126 (3,3′,4,4′,5-pentachlorobiphenyl) was obtained from Accustandard (New Haven, CT) and confirmed by GCMS to be pure and free of other congeners. Cells were treated with 2.5 x 10^{-7} M PCB 126 for 24 h. This exposure concentration and duration was selected to ensure maximal CYP1A1 induction in H4IIE cells at a low, non-toxic concentration. This dose and duration was based on concentration-response and time course analyses of

CYP1A1 mRNA and protein induction in our laboratory using real time RT-PCR and fluorescence flow cytometry, respectively (Broccardo *et al.*, 2004). We found for H4IIE cells, maximal induction of both mRNA and protein occurred at PCB 126 concentrations greater than 10^{-8} M, and time-course analysis revealed maximal *CYP1A1* mRNA induction occurred at 16 h (+2,000) then dropped to +1,000-fold, remaining relatively constant from 24 h to 48 h. Control cells in the present study were treated with DMSO vehicle equivalent to 0.2% DMSO (which was equivolume to the PCB 126 treatment). PCB 126 and DMSO control treatments were performed in biological triplicate, (i.e., 3 plates per treatment). Cells were directly lysed on the dish with 600 µl Buffer RLT and removed with a cell scraper. A Qiagen mini-kit (Valencia, CA) protocol was followed for isolating total RNA. Resulting RNA was quantified with a Beckman DU640B spectrophotometer and quality was visualized using a 1% agarose gel. RNA quality was comparable to that shown in Figure 3.2. Total RNA yields averaged 13 µg per plate in a final elution volume of 20µl.

cDNA Microarray Hybridization

A total of twelve arrays (i.e., biological triplicates of treatments and controls for C6 and H4IIE cell-lines) were hybridized to Affymetrix Rat Genome 230 2.0 arrays (Affymetrix, Inc., Santa Clara, CA) and analyzed. Experimental procedures consisting of double-strand cDNA synthesis, in vitro cRNA transcription, and biotinylation were conducted as recommended by the manufacturer (Affymetrix, 2004b). Target biotin-labeled cRNA for hybridization was prepared using a One-Cycle cDNA synthesis kit (Affymetrix). Starting with total RNA, cDNA was synthesized in the initial reverse transcription reaction using T7-oligo(dT) promoter primers followed by cleanup with a GeneChip Sample Cleanup

(GCSC) module (Qiagen, Inc.). Purified cDNA was then used as a template for in vitro transcription of cRNA in the presence of natural ribonucleotides and a biotinylated ribonucleotide analog. Cleanup of biotinylated cRNA was also done with a GCSC module, and 15 µl (0.5 µg/µl) cRNA was subsequently fragmented by metal-induced hydrolysis using 8 µl of 5X fragmentation buffer (Affymetrix) at 94°C for 35 minutes; this procedure is optimized to produce 35-200-bp cRNA fragments. After labeling and fragmentation, 15 µg of cRNA was hybridized for 16 hours according to manufacturer's instructions, to the Rat 230 2.0 GeneChips in 300 µl (final volume) of hybridization cocktail. After hybridization, automated washing and streptavidin phycoerythrin (SAPE) staining steps were instructed by GCOS-Microarray Suite (MAS) 5.0, running wash/stain fluidics script EukGE-WS2v5 on a GeneChip Fluidics Station 450 (Affymetrix). This fluidics script runs 16 post hybridization washes, 3 SAPE staining cycles, followed by 15 final washes at 35°C (Affymetrix, 2004b). Probe arrays were scanned with a GeneChip 3000 scanner (Affymetrix) running the rat230_2 library file. Images were inspected and found to be free of artifacts, debris or visible defects.

Data Analysis

The Afx system determines expression levels from microarray data using a series of computational algorithms. A qualitative value known as a *detection call* (DC) is computationally generated for each scanned image of each spot. The DC indicates whether a transcript is reliably detected (present) or not detected (absent). Each DC is determined by comparing the detection p-value generated in the analysis against user-defined cut-offs. The relative transcript abundance is quantitatively determined by the amount of fluorescent signal from each probe.

The detection algorithm uses a two-step procedure to determine the detection p-value. First, a discrimination score (R) is calculated for each probe pair. The discrimination score measures the target-specific intensity difference of the probe pair relative to its overall hybridization intensity:

$$R = \frac{PM - MM}{PM + MM}$$

Second, the discrimination score (R) is tested against the user-defined threshold value τ, which is a small positive number (by default 0.015). Those probe pairs with discrimination scores higher than τ, vote for the presence of the transcript, while scores lower than τ vote for the transcript being absent. The voting results of all probe pairs are summarized as a p-value, which is generated using the one-sided Wilcoxon's signed rank test. The greater the discrimination score is above τ, the smaller the p-value and the more likely the transcript is present. Conversely, as scores become lower than τ, a larger p-value results, and the more likely a transcript is absent. Additionally, prior to calculating the detection p-value, photomultiplier saturation is evaluated for each probe pair. If all probe pairs in a probe set are saturated, the corresponding transcript is given a present call. If the MM probe is similarly saturated, that probe pair receives an absent vote.

The DC is a qualitative value determined by comparing the detection p-value with the user-defined cut-offs, $\alpha 1$ and $\alpha 2$ (0.04 and 0.06 by default). Any p-value smaller than $\alpha 1$, is assigned a present call, and p-values larger than $\alpha 2$ are assigned an absent call.

Marginal calls (M) are given to values between $\alpha 1$ and $\alpha 2$. The p-value cut-offs can also be adjusted to change specificity or sensitivity thresholds.

Signal is a quantitative value calculated for each probe set and represents the relative level of expression of a corresponding transcript. Signal is calculated as a weighted mean using the one-step Tukey's biweight estimate. The specific signal for a probe pair is estimated by taking the log of the PM intensity after subtracting the stray signal estimate. Because it would not make biological sense to have MM probe intensity higher than PM intensity, an imputed value called change threshold (CT) can be used instead of the MM intensity. Although the computational details are omitted, three rules apply to deriving stray signal estimates:

1. If MM < PM, the MM is considered informative and the intensity is used directly to estimate stray signal;
2. If the MM probes are generally informative across the probe set except for a few mismatches, an adjusted MM value is used for uninformative mismatches based on the bi-weight mean of the PM:MM ratio;
3. If the MM probes are generally uninformative, the uninformative mismatches are replaced with a CT value slightly smaller than the PM. The transcripts represented by these probe sets are generally voted absent by the Afx detection algorithm.

Each probe pair is considered to have a potential vote in determining the signal value. The probe pair is weighted more strongly if the signal of the probe pair is closer to the median value for that probe set. Once the weight of each probe pair is determined, the mean of the weighted intensity values for that probe set is determined. This mean is reported as the signal value for each probe pair and exported from the Afx system in a compressed text format known as a .CEL file.

Differential Expression Analyses

Affymetrix MAS 5-derived signal and detection calls (.CEL files) for each array were uploaded to the GeneSifter internet-based microarray data analysis system (VizXLabs, Seattle, WA). Initial filtering criteria of log-transformed, global mean normalized data was by all MAS 5 present calls in at least one treatment group, and by p-value for unpaired two sample t-test (false discovery rate less than 5%). These criteria resulted in a starting dataset of differentially expressed genes numbering 1560 (up = 1559, down = 1) for C6 cells, and 4608 (up = 1745, down = 2863) for H4IIE cells. Meta-analysis was conducted after eliminating genes differentially expressed less than two-fold (up or down), resulting in a working dataset of 1529 (up = 1528, down =1) for C6 cells and 248 (up = 77, down = 171) for H4IIE cells. Interestingly, few C6 genes (< 30) were differentially expressed less than 2-fold. Meta analysis included intensity scatter plots of scanner data (Figures 3.21 and 3.22) and z-score analysis (Tables 3-5 and 3-6). The z-score analysis provides statistical ratings for the presence of genes in a functional category (term) established by the Gene Ontology (GO) Consortium in LocusLink (Ashburner *et al.*, 2000). The z-scores indicate whether a gene occurs more frequently than expected, and amounts to a standardized difference score calculated by subtracting the observed number genes in a GO term and dividing by standard deviation of the observed number of genes (Doniger *et al.*, 2003). Finally, a short list of genes for individual examination was chosen based on magnitude of fold-change and measurement precision (p-value). For inclusion in the short list, genes required adequate annotation (GO or primary literature) and progressively higher measurement precision for smaller fold-changes. Significance plots indicating selected genes are shown in Figures 3.21.

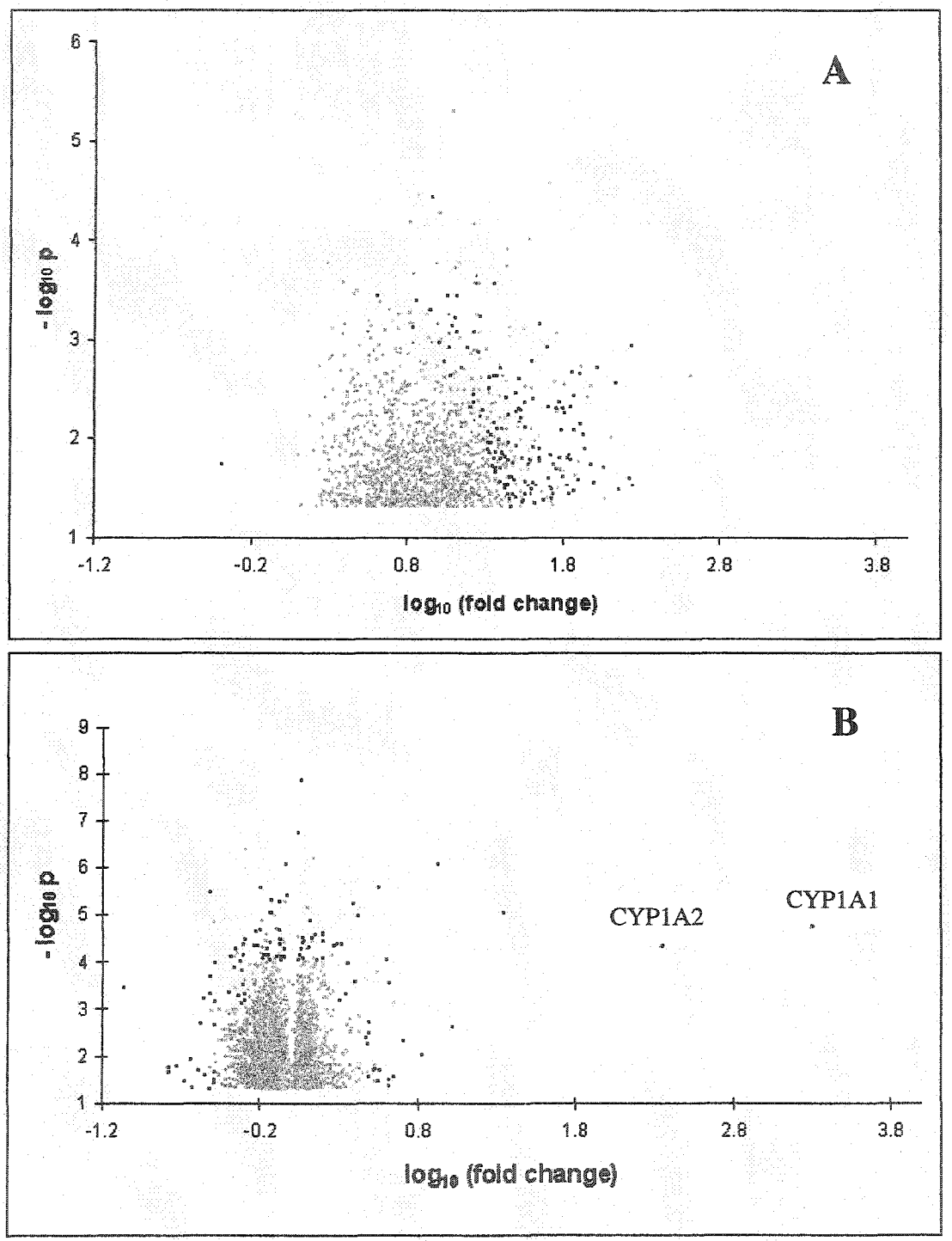

Figure 3.21 Significance plots for PCB 126-induced differential expression of C6 genes (A), and H4IIE genes (B). z-scores were calculated using genes shown ($p < 0.05$). Genes represented by black points were chosen for individual examination based on magnitude of fold-change and/or precision of measurement. For inclusion, decreasing fold-change incrementally required greater precision (i.e., larger $-\log_{10} p$).

21. Results

The results of this investigation reveal surprising transcriptional activation of C6 astrocytic cells by PCB 126, and we clearly demonstrate that the affect of PCB 126 on transcription is very different between H4IIE hepatic and C6 astrocytic cells. We also identify novel genes that tend to explain the transcriptional activation observed in C6 cells, the neuro-cognitive effects observed *in vivo*, and the hepatocarcinogenicity of PCB 126.

Treatment of rat C6 glioma or rat H4IIE hepatoma cells with 2.5×10^{-7} M PCB 126 resulted in substantially different transcriptional responses. In the original working dataset of 1,560 differentially expressed C6 genes and 4608 differentially expressed H4IIE genes, there are only six genes in common. Of these, three common genes are differentially expressed in the same direction and NAD(P)H dehydrogenase quinone 1 (*Ngo1*, GenBank J02679) is the only annotated gene in common that is differentially expressed in the same direction. In the broadest sense, PCB 126 treatment caused transcriptional activation of C6 astrocytic cells (only 1 suppressed gene), while transcriptional changes in H4IIE hepatic cells were generally weaker and balanced between activation and suppression. When interpreting gene expression data obtained by measuring mRNA transcript levels, it is important to emphasize that differential expression is reflected as mRNA accumulations from both transcriptional activity and post-transcriptional mRNA stability, and does not necessarily reflect gene product levels or activity (Vezina *et al.*, 2004).

C6 Cells

The array intensity scatter plot of C6 treatments versus controls (Figure 3.21) clearly demonstrates C6 cells are transcriptionally activated by PCB 126 treatment and, unlike differentially expressed H4IIE genes, many C6 genes (> 50) were found to be included in Kyoto Encyclopedia of Genes and Genomes (KEGG) molecular interaction networks (Table 3-2). Because most KEGG molecular interaction networks are comprised of gene products with described interactions, KEGG genes are not novel. Indeed a large percentage of C6 genes transcriptionally activated by PCB 126 are involved in

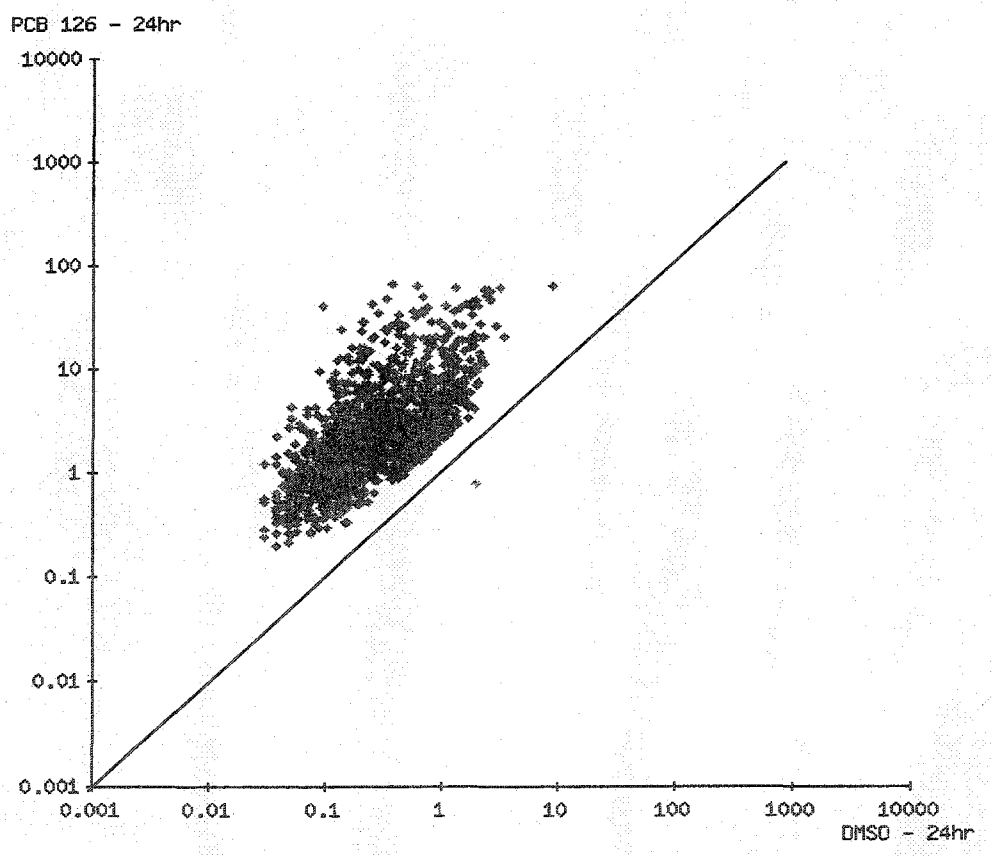

Figure 3.22. C6 rat glioma cells: Scatter plot of scanned microarray intensities for differentially expressed gene transcripts following PCB 126 treatment ($p < 0.05$, fold-change > 2).

intermediate metabolism and other known pathways. A representative list of differentially expressed C6 genes is presented in Table 3-3 and includes 130 annotated genes identified by significance plotting (Figure 3.21) that exhibit high-fold differential expression and/or high measurement precision (i.e., large $-\log_{10} p$ value).

Despite previous PCR evidence for modest increases in AhR expression and induction of *CYP1A1* by TCDD in C6 cells (Takanaga *et al.*, 2001), no transcripts for AhR or *CYP1A1/2* were detected. Despite generalized transcriptional activation of C6 cells, z-scores (Table 3-4) suggest genes associated with signal transduction and ion transport are generally under-represented. One prominent feature of PCB 126 induced differential gene expression in C6 cells was robust induction of genes encoding ribosomal protein subunits (6 – 410 fold). This finding is reflected by high z-scores for genes associated with protein biosynthesis and metabolism. Transcription of genes for mitochondrial ribosome protein subunits was also enhanced, but at relatively lower levels (2–17 fold). Activated genes associated with protein biosynthesis appear to be balanced by over-represented genes for protein catabolism (i.e., proteosomes). Expression levels of genes for ribosomal proteins and proteosome subunits are listed in Table 3-5. Pleiomorphic adenoma gene-like 1 (*PLAGL1*, syn. *LOT1/ZAC1*), involved with apoptosis and cell-cycle arrest, was the only significantly suppressed C6 gene (- 2.2). For genes associated with nerve function, the most highly expressed transcript was a Ca^{2+}-independent soluble galactose binding lectin associated with nerve regeneration, *LGALS1* (+174). As shown in Table 3-3, other known neurotropic genes transcriptionally activated by PCB 126 include *EEF1G* (+61.6) and *SERPINE2* (+13.0). *S100B*, linked to cognitive function and observed to be released at

comparable levels from both C6 cells and normal astrocytes (Van Eldik *et al.*, 1987), was transcriptionally activated (+8.9). Finally, neuroacitve genes up-regulated by PCB 126 include nerve transmission genes *NEDD4A* (+59.5), *RAB14* (+41.9) syntaxin 4 (+11.9) and the neuronal transcription regulator *NEDD8* (+17.5).

Table 3-3 (page 1 of 2). **C6 cells: Activated genes in KEGG* molecular interaction pathways**

KEGG Pathway	KEGG ID	Gene ID	Dir	Ratio	p-value	Accession	Gene Name
Amyotrophic lateral sclerosis (ALS)	mo05030	Ssr4	Up	55.08	0.01833	NM_017199	signal sequence receptor 4
ATP synthesis	mo00193	Atp5b	Up	35.04	0.04298	M19044	ATP synthase, H+ transprtg, Mt F1 complex
		Atp5a1	Up	31.05	0.02580	J05266	Mt ATP synthase, H+-ATP synthase alpha subunit
		Atp5o	Up	27.12	0.01554	D13127	oligomycin sensitivity conferring protein
Benzoate degradation via CoA ligation	mo00632	Hadhsc	Up	38.72	0.01656	AA799574	hydroxyacyl-CoA dehydrogenase, short chain
Biosynthesis of steroids	mo00100	Sqle	Up	73.56	0.03505	NM_017136	squalene epoxidase
		Fdps	Up	23.42	0.01359	NM_031840	farensyl diphosphate synthase
Butanoate metabolism	mo00650	Hadhsc	Up	38.72	0.01656	AA799574	hydroxyacyl-CoA dehydrogenase, short chain
		Hmgcs1	Up	28.39	0.01651	NM_017268	3-hydroxy-3-methylglutaryl-CoA synthase 1
Cadherin-mediated cell adhesion	mo04520	Cdc42	Up	79.10	0.02645	AA925473	cell division cycle 42 homolog
		Rhoa	Up	59.67	0.01582	AI408053	plysia ras-related homolog A2
Calcium signaling pathway	mo04020	Gnas	Up	54.43	0.03739	BI277035	GNAS complex locus
		Vdac2	Up	11.97	0.00230	AF268468	voltage-dependent anion channel 2
Carbon fixation	mo00710	Pkm2	Up	104.72	0.00198	NM_053297	pyruvate kinase, muscle
		Aldoa	Up	79.41	0.00729	NM_012495	aldolase A
		Pgk1	Up	68.97	0.01459	NM_053291	phosphoglycerate kinase 1
Citrate cycle (TCA cycle)	mo00020	Sdhd	Up	27.73	0.00385	AI410703	succinate dehydrogenase subunit D
Cysteine metabolism	mo00272	Ldha	Up	54.19	0.03384	NM_017025	lactate dehydrogenase A
		Ldhb	Up	18.41	0.00132	AA848319	lactate dehydrogenase B
Cytokine-cytokine receptor interaction	mo04060	Il6st	Up	41.45	0.00396	BM383427	interleukin 6 signal transducer
Fatty acid biosynthesis (path 2)	mo00062	Hadhsc	Up	38.72	0.01656	AA799574	hydroxyacyl-CoA dehydrogenase, short chain
Fatty acid metabolism	mo00071	Hadhsc	Up	38.72	0.01656	AA799574	hydroxyacyl-CoA dehydrogenase, short chain
Fructose and mannose metabolism	mo00051	Aldoa	Up	79.41	0.00729	NM_012495	aldolase A
Glycerolipid metabolism	mo00561	Akr1a1	Up	25.25	0.00198	NM_031000	aldo-keto reductase family 1, member A1
Glycolysis / Gluconeogenesis	mo00010	Pkm2	Up	104.72	0.00198	NM_053297	pyruvate kinase, muscle
		Aldoa	Up	79.41	0.00729	NM_012495	aldolase A
		Pgk1	Up	68.97	0.01459	NM_053291	phosphoglycerate kinase 1
		Ldha	Up	54.19	0.03384	NM_017025	lactate dehydrogenase A
		Akr1a1	Up	25.25	0.00198	NM_031000	aldo-keto reductase family 1, member A1
		Ldhb	Up	18.41	0.00132	AA848319	lactate dehydrogenase B
GPI-anchor biosynthesis	mo00563	Pigs	Up	23.19	0.00027	BI284221	phosphatidylinositol glycan class S
Huntington's disease	mo05040	Clta	Up	39.29	0.03690	M19261	clathrin, light polypeptide (Lca)
Jak-STAT signaling pathway	mo04630	Il6st	Up	41.45	0.00396	BM383427	interleukin 6 signal transducer
		Ccnd1	Up	18.79	0.00060	AW143798	cyclin D1
Lysine degradation	mo00310	Hadhsc	Up	38.72	0.01656	AA799574	hydroxyacyl-CoA dehydrogenase, short chain
MAPK signaling pathway	mo04010	Cdc42	Up	79.10	0.02645	AA925473	cell division cycle 42 homolog
		Dusp6	Up	39.95	0.03382	NM_053883	dual specificity phosphatase 6
		Hspa8	Up	37.67	0.03003	NM_024351	heat shock protein 8
		Atf4	Up	29.03	0.02456	NM_024403	activating transcription factor ATF-4
		Map2k2	Up	17.11	0.00665	D14592	mitogen activated protein kinase kinase 2
N-Glycan biosynthesis	mo00510	Rpn2	Up	30.02	0.03682	NM_031698	ribophorin 2
Oxidative phosphorylation	mo00190	Atp5b	Up	35.04	0.04298	M19044	ATP synthase, H+ transprtg, Mt F1 complex
		Atp5a1	Up	31.05	0.02580	J05266	Mt ATP synthase, H+-ATP synthase alpha subunit
		Sdhd	Up	27.73	0.00385	AI410703	succinate dehydrogenase subunit D
		Atp5o	Up	27.12	0.01554	D13127	oligomycin sensitivity conferring protein
		Cox4i1	Up	23.04	0.00708	NM_017202	cytochrome c oxidase, subunit 4a
		Ndufs7	Up	21.38	0.01390	AI231358	NADH dehydrogenase (ubiQ) Fe-S protein 7

Table 3-3 *(page 2 of 2).* **C6 cells: Activated genes in KEGG* molecular interaction pathways**

KEGG Pathway	KEGG ID	Gene ID	Dir	Ratio	p-value	Accession	Gene Name
Pentose phosphate pathway	mo00030	Aldoa	Up	79.41	0.00729	NM_012495	aldolase A
Prion disease	mo05060	Lamr1	Up	70.50	0.01661	BG153272	ribosomal protein laminin receptor 1
Propanoate metabolism	mo00640	Ldha	Up	54.19	0.03384	NM_017025	lactate dehydrogenase A
		Ldhb	Up	18.41	0.00132	AA848319	lactate dehydrogenase B
Proteasome	mo03050	Psmb3	Up	63.45	0.02415	AI169273	proteasome, macropain, beta type 3
		Psmb1	Up	39.63	0.01713	NM_053590	proteasome, macropain subunit, beta type 1
		Psmd4	Up	24.26	0.00811	NM_031331	proteasome, macropain 26S, non-ATPase,4
		Psmb4	Up	13.10	0.00037	NM_031629	proteasome, macropain subunit, beta type 4
Purine metabolism	mo00230	Pkm2	Up	104.72	0.00198	NM_053297	pyruvate kinase, muscle
Pyruvate metabolism	mo00620	Pkm2	Up	104.72	0.00198	NM_053297	pyruvate kinase, muscle
		Ldha	Up	54.19	0.03384	NM_017025	lactate dehydrogenase A
		Ldhb	Up	18.41	0.00132	AA848319	lactate dehydrogenase B
Regulation of actin cytoskeleton	mo04810	Pfn1	Up	85.07	0.01298	NM_022511	profilin
		Cdc42	Up	79.10	0.02645	AA925473	cell division cycle 42 homolog
		Itgb1	Up	62.87	0.00500	AI177366	integrin beta 1
		Rhoa	Up	59.67	0.01582	AI408053	plysia ras-related homolog A2
		Arpc1b	Up	32.73	0.00247	NM_019289	actin related protein 2/3 complex, subunit 1B
		Map2k2	Up	17.11	0.00665	D14592	mitogen activated protein kinase kinase 2
Ribosome	mo03010	Rpl29	Up	171.80	0.00115	NM_017150	ribosomal protein L29
		Rpl13	Up	143.37	0.03382	NM_031101	ribosomal protein L13
		Rpl4	Up	79.49	0.00222	NM_022510	ribosomal protein L4
		Rpl24	Up	72.58	0.00216	BI297634	ribosomal protein L24
		Lamr1	Up	70.50	0.01661	BG153272	ribosomal protein laminin receptor 1
		Rpl6	Up	68.20	0.03742	NM_053971	ribosomal protein L6
		Rpl10a	Up	67.71	0.01613	NM_031065	ribosomal protein L10a
		Arbp	Up	57.09	0.00499	NM_022402	acidic ribosomal protein P0
		Rps15	Up	53.01	0.01492	NM_017151	ribosomal protein S15
		Rpl18	Up	50.89	0.02497	NM_031102	ribosomal protein L18
		Rps10	Up	36.04	0.00792	NM_031109	ribosomal protein S10
		Rpl10	Up	23.82	0.00233	NM_031100	ribosomal protein L10
		Rps2	Up	23.65	0.02049	AA944861	ribosomal protein S2
		Rps11	Up	23.18	0.00232	NM_031110	ribosomal protein S11
Synthesis / degradation of ketone bodies	mo00072	Hmgcs1	Up	28.39	0.01651	NM_017268	3-hydroxy-3-methylglutaryl-CoA synthase 1
Terpenoid biosynthesis	mo00900	Sqle	Up	73.56	0.03505	NM_017136	squalene epoxidase
		Fdps	Up	23.42	0.01359	NM_031840	farensyl diphosphate synthase
TGF-beta signaling pathway	mo04350	Rhoa	Up	59.67	0.01582	AI408053	plysia ras-related homolog A2
		Id2	Up	23.39	0.01931	AI008792	Inhibtr DNA bindng 2, neg helx-loop-helx
Tryptophan metabolism	mo00380	Hadhsc	Up	38.72	0.01656	AA799574	hydroxyacyl-CoA dehydrogenase, short chain
Valine, leucine and isoleucine degradation	mo00280	Hadhsc	Up	38.72	0.01656	AA799574	hydroxyacyl-CoA dehydrogenase, short chain
		Hmgcs1	Up	28.39	0.01651	NM_017268	3-hydroxy-3-methylglutaryl-CoA synthase 1
Wnt signaling pathway	mo04310	Rhoa	Up	59.67	0.01582	AI408053	plysia ras-related homolog A2
		Ccnd1	Up	18.79	0.00060	AW143798	cyclin D1

* Kyoto Encyclopedia of Genes and Genomes (KEGG)

Table 3-4 (pg 1 of 3). **C6 cells: Annotated genes with high-fold differential expression and/or small p-value.**

	Dir	Ratio	p-value	Accession	Gene ID	Gene Name	Activity
Protein Metabolism* (ribosomal proteins and proteasome subunits are provided in Table X)							
	Up	70.50	0.01661	BG153272	Lamr1	ribosomal protein laminin receptor 1	biosynthesis
	Up	51.27	0.00483	AI411531	Cops4	COP9 signalosome subunit 4	catabolism
	Up	45.20	0.01564	NM_017236	Pbp	phosphatidylethanolamine binding protein	catabolism
	Up	39.63	0.01713	NM_053590	Psmb1	proteasome, macropain subunit beta type 1	catabolism
	Up	23.72	0.02168	NM_021989	Timp2	tissue inhibitor of metalloproteinase 2	catabolism
	Up	21.57	0.00313	NM_019237	Pcolce	procollagen C-proteinase enhancer protein	catabolism
	Up	21.06	0.00854	NM_031721	Prss11	protease, serine, 11	catabolism
	Up	7.22	0.00041	NM_080394	Reln	reelin	catabolism
Nerve Function							
	Up	61.57	0.00830	BM391203	Eef1g	eukaryotic transln elongtn factor 1 gamma	neuron outgrowth and migration
	Up	59.51	0.00434	BM389736	Nedd4a	neural precrsr cell expresd, develpmt dn-reg 4A	neuron signal transduction channel regulator
	Up	41.90	0.04644	BE097926	Rab14	GTPase Rab14	nerve transmission
	Up	17.49	0.00023	AF095740	Nedd8	neural precrsr cell expresd, develpmt dn-reg 8	neuronal transcription regulator
	Up	13.00	0.00083	BI275818	Serpine2	ser/cys proteinase inhibitor, clade E, member 2 (protease nexin 1)	neurogenesis, pos. regulation
	Up	11.85	0.00121	NM_031125	Stx4a	syntaxin 4	neurotransmitter transport
*	Up	8.89	0.00051	NM_013191	S100b	S100 protein, beta polypeptide	neurogenesis/pos. reg apoptosis/memeory
Transcription/Translation/Repair							
*	Up	174.04	0.02971	NM_019904	Lgals1	lectin, galactose binding, soluble 1	chromosome HDAC inhibitor, nerve regeneration
	Up	48.02	0.04292	U17565	Mcmd6	mini chromosome maintenance deficient 6	replication, up-regulation
	Up	45.39	0.01265	NM_033539	Eef1a1	eukaryotic transln elongation factor 1 alpha 1	translation elongation
	Up	45.02	0.00069	BM385924	Rpa2	p32-subunit of replication protein A	DNA base-excision repair
	Up	37.64	0.01816	BI287960	Re1	epididymal secretory protein 1	transcription suppression
	Up	35.78	0.02651	NM_031129	TCEB2	transcrptn elongtn factr B (SIII), polypeptide 2	transcription, up-regulation
	Up	35.55	0.03771	AF242550	Cnbp	cellular nucleic acid binding protein	RNA binding
	Up	34.51	0.04405	J04943	Npm1	nucleophosmin 1	RNA binding
	Up	34.12	0.01601	K01677	Eif5	eukaryotic initiation factor 5 (eIF-5)	translation initiation
	Up	33.16	0.00673	NM_053563	Ddxl	RNA helicase, DECD variant of DEAD box family	RNA helicase
	Up	31.68	0.04029	NM_053707	Hdgf	hepatoma-derived growth factor	DNA mismatch repair
	Up	31.66	0.00349	AW252511	Ddx24	DEAD (Asp-Glu-Ala-Asp) box polypeptide 24	RNA helicase
	Up	29.03	0.02456	NM_024403	Atf4	activating transcription factor ATF-4	transcription activator
	Up	28.04	0.02890	BG666846	Wbscr1	eukaryotic translation initiation factor 4H	mRNA initiation codon locator
	Up	25.08	0.01563	AI408157	Sirt6	sirtuin silent mating reg 2 homolog 6	DNA histone deacetylase
	Up	18.71	0.00591	NM_053531	Sybl1	synaptobrevin-like 1	sex chromosome inactivation
	Up	17.70	0.00027	BG666659	MGC106007	transcription factor BTF3 (similar)	transcription factor
	Up	16.89	0.00361	AI228548	S100a1	S100 calcium binding protein A1	negative regulation of transcription
	Up	10.27	0.00108	NM_012887	Tmpo	thymopoietin	transcription regulation
Morphogenesis/Organogenesis/Differentiation							
	Up	39.95	0.03382	NM_053883	Dusp6	dual specificity phosphatase 6	differentiation
	Up	36.03	0.00425	BI285635	Edf1	endothelial differentiation-related factor 1	differentiation, suppression
	Up	31.70	0.00523	NM_022297	Ddah1	dimethylarginine dimethylaminohydrolase 1	morphogenesis
	Up	9.23	0.00004	NM_022391	Pttg1	pituitary tumor-transforming 1	DNA repair, proliferation arrest
Cell Growth and Proliferaton							
	Up	79.10	0.02645	AA925473	Cdc42	cell division cycle 42 homolog	establish cell polarity
	Up	59.67	0.01582	AI408053	Rhoa	plysia ras-related homolog A2	proliferation, vascular
	Up	28.13	0.01627	AA943837	Calm2	calmodulin 2	proliferation
	Up	23.39	0.01931	AI008792	Id2	inhibtr DNA bindng 2, neg helx-loop-helx	proliferation, up-regulation
	Up	18.79	0.00060	AW143798	Ccnd1	cyclin D1	re-entry to mitosis

Table 3-4 (pg 2 of 3). **C6 cells: Annotated genes with high-fold differential expression and/or small p-value.**

Dir	Ratio	p-value	Accession	Gene ID	Gene Name	Activity
Immune Function						
Up	166.71	0.02501	NM_017125	Cd63	CD63 antigen (Lamp3)	endocytosis, up-regulation
Up	64.42	0.00554	BI277043	Mcam	I-gicerin	immunoglobin adhesion
Up	42.92	0.02949	NM_022536	Ppib	cyclophilin B (peptidylpropyl isomerase B)	chemotactic for neutorphils and T-cells
Up	41.45	0.00396	BM383427	Il6st	interleukin 6 signal transducer	hormone secretion regulation
Up	29.99	0.01778	AI012221	RT1-CE5	RT1 class Ib, locus Aw2	antigen presenting protein
Up	28.15	0.03732	AW525776	Laptm4a	lysosomal-assoc prot. transmembrane 4 alpha	cancer cell line drug resistance
Up	26.66	0.02854	M24024	RT1-Aw2	RT1 class Ib, locus Aw2	antigen presenting protein
Up	25.93	0.01374	AI235510	Bcap37	B-cell receptor-associated protein 37	B-cell receptor
Up	25.11	0.01957	NM_012857	Lamp1	lysosomal assoc. membrane glycoprotein 1	vacuole associated protein
Up	21.81	0.01118	BI285440	Tubb5	tubulin, beta 5	NK cell-mediated cytotoxicity
Up	11.49	0.00037	AI598391	Siahbp1	siah 1;pyr tract bindg splicng factr; Ro rib binding 1	autoantigenic particles of unknown function
Cytoskeleton						
Up	95.30	0.01809	BG665035	Cct2	chaperonin containing TCP-1 beta subunit	actin / tubulin folding
Up	85.07	0.01298	NM_022511	Pfn1	profilin	cytoskeleton organization and biogenesis
Up	32.73	0.00247	NM_019289	Arpc1b	actin related protein 2/3 complex, subunit 1B	cytoskeleton
Up	23.19	0.00027	BI284221	Pigs	phosphatidylinositol glycan class S	membrane anchoring protein
Up	22.67	0.01893	NM_031819	Fat	FAT tumor suppressor homolog	cell-cell adhesion
Up	21.18	0.01093	BM384017	Mpzl1	myelin protein zero-like 1; protein zero related	myelin protein
Up	16.75	0.00435	BI279735	Ubqln1	ubiquilin 1	binding protein, cytoplasm
Up	10.89	0.00173	NM_019195	Cd47	integrin-associated protein	migration
Up	7.22	0.00041	NM_080394	Reln	reelin	cell-cell adhesion
Apoptosis						
Up	57.71	0.02035	AI178772	Ptma	prothymosin alpha	apoptosis, suppression
Up	45.27	0.01680	BE108192	Gspt1	G1 to phase transition 1	apoptosis & translation
Up	25.94	0.01423	NM_022526	Dap	rap7a	apoptosis
* Dn	2.44	0.01798	NM_012760	Plagl1	pleiomorphic adenoma gene-like 1 (Lot1/Zac1))	apoptosis, cell cycle arrest
Stress Response						
Up	67.50	0.02983	BG671521	Hspca	heat shock protein 86	heat shock
Up	57.33	0.02019	NM_057114	Prdx1	peroxiredoxin 1	oxidative
Up	40.08	0.00168	NM_053359	Atox1	ATX1 (antioxidant protein 1) homolog 1	oxidative
Up	37.67	0.03003	NM_024351	Hspa8	heat shock protein 8	heat shock
Up	33.84	0.00608	NM_012880	Sod3	superoxide dismutase 3	oxidative
Up	28.77	0.04143	NM_017169	Prdx2	peroxiredoxin 2	oxidative
Up	28.13	0.00573	BI285700	Hspcb	heat shock protein 84	heat shock
Signal Transduction						
Up	70.50	0.01661	BG153272	Lamr1	ribosomal protein laminin receptor 1	cell-cell interactions
Up	62.87	0.00500	AI177366	Itgb1	integrin beta 1	integrin-mediated
Up	54.43	0.03739	BI277035	Gnas	GNAS complex locus	G-protein cAMP-mediated
Up	52.42	0.03068	NM_130734	Gnb2l1	guanine bindg protein, beta polypeptide 2-like 1	G-protein cAMP-mediated
Up	29.68	0.04941	AI227627	Cd9	CD9 antigen	trans-membrane
Up	25.42	0.00803	NM_030987	Gnb1	guanine nucleotide binding protein, beta 1	G-protein cAMP-mediated
Up	25.22	0.02676	AI170661	Rasa3	RAS p21 protein activator 3	protooncogene activator (RAS)
Up	15.94	0.00476	NM_031645	Ramp1	receptor (calcitonin) activity modifying protein 1	G-protein cAMP-mediated
Up	13.95	0.00195	BI277793	Ywhaq	3-,5-tyrosine monooxygenase activatn protein	small GTPase mediated
Up	4.08	0.00037	BI295783	Carhsp1	calcium regulated heat stable protein 1	calcium-mediated signaling

Table 3-4 (pg 3 of 3). **C6 cells: Annotated genes with high-fold differential expression and/or small p-value.**

Dir	Ratio	p-value	Accession	Gene ID	Gene Name	Activity
Kinases						
Up	104.72	0.00198	NM_053297	Pkm2	pyruvate kinase, muscle	carbohydrate catabolism
Up	83.55	0.00928	BF281311	Csnk2b	casein kinase II beta subunit	protein kinase
Up	68.97	0.01459	NM_053291	Pgk1	phosphoglycerate kinase 1	calmodulin regulated protein kinase activity
Up	31.44	0.01208	AA892351	Ywhae	3-,5-tyrosine monooxygenase activatn protein	protein kinase regulation
Up	17.11	0.00665	D14592	Map2k2	mitogen activated protein kinase kinase 2	phosphorylation
Up	16.96	0.00083	AI548699	Galk1	galactokinase 1	phosphorylation
Intermediate Metabolism						
Up	79.41	0.00729	NM_012495	Aldoa	aldolase A	carbohydrate catabolism
Up	73.56	0.03505	NM_017136	Sqle	squalene monooxygenase (epoxidase)	aromatic compound metabolism
Up	54.19	0.03384	NM_017025	Ldha	lactate dehydrogenase A	carbohydrate catabolism
Up	49.99	0.00118	AA800180	Txn2	thioredoxin 2	electron transport
Up	41.40	0.02785	D13374	Nme1	expressed in non-metastatic cells 1	pyrimidine ribonucleotide biosynthesis
Up	38.72	0.01656	AA799574	Hadhsc	hydroxyacyl-CoA dehydrogenase, short chain	oxidoreductase
Up	35.04	0.04298	M19044	Atp5b	ATP synthase, H+ transprtg, Mt F1 complex	purine ribonucleotide metabolism
Up	31.05	0.02580	J05266	Atp5a1	ATP synthase, H+-ATP synthase alpha subunit	purine ribonucleotide metabolism
Up	30.02	0.03682	NM_031698	Rpn2	ribophorin 2	protein amino acid glycosylation
Up	28.39	0.01651	NM_017268	Hmgcs1	3-hydroxy-3-methylglutaryl-CoA synthase 1	steroid biosynthesis
Up	27.73	0.00385	AI410703	Sdhd	succinate dehydrogenase subunit D	electron transport
Up	27.33	0.02868	NM_022392	Insig1	Insulin induced gene 1	cholesterol synthesis, suppression
Up	27.12	0.01554	D13127	Atp5o	oligomycin sensitivity conferring protein	purine ribonucleotide metabolism
Up	25.25	0.00198	NM_031000	Akr1a1	aldo-keto reductase family 1, member A1	oxidoreductase
Up	23.42	0.01359	NM_031840	Fdps	farensyl diphosphate synthase	steroid biosynthesis
Up	23.04	0.00708	NM_017202	Cox4i1	cytochrome c oxidase, subunit 4a	electron transport
Up	22.96	0.01578	NM_033235	Mdh1	malate dehydrogenase 1	malate dehydrogenase
Up	21.38	0.01390	AI231358	Ndufs7	NADH dehydrogenase (ubiQ) Fe-S protein 7	electron transport
Up	18.41	0.00132	AA848319	Ldhb	lactate dehydrogenase B	carbohydrate catabolism
Up	13.25	0.00083	NM_031841	Scd2	stearoyl-Coenzyme A desaturase 2	CoA desaturase
Up	7.36	0.00438	J02679	Ngo1	NAD(P)H dehydrogenase, quinone 1	oxidoreductase
Transport						
Up	113.92	0.01986	AI012445	Slc25a5	solute carrier family 25, member 5	adenine nucleotide
Up	73.41	0.00374	BG666999	Slc25a4	solute carrier family 25, member 4	nucleotide, mitochondria
Up	55.08	0.01833	NM_017199	Ssr4	signal sequence receptor 4	protein translocon complex
Up	53.81	0.04171	M23984	Slc25a3	solute carrier family 25, member 3	adenine nucleotide
Up	40.76	0.01246	BI303655	Atp1b3	ATPase, Na+/K+ transporting, beta 3	ion transport (monovalent inorganic cation)
Up	32.87	0.00493	AI178934	Rnp24	coated vesicle membrane protein	protein ER-golgi
Up	24.58	0.01030	NM_019226	Dnch1	dynein, cytoplasmic, heavy chain 1	microtubule tract
Up	24.26	0.00811	NM_031331	Psmd4	proteasome, macropain 26S, non-ATPase,4	fluid transport
Up	21.76	0.00942	BG663051	Atp6ap2	ATPase, H+ transprtg, lysosomal accesry prot 2	ion transport
Up	20.94	0.01277	BI285910	Ssr3	signal receptor 3, TRAP-complex gamma	protein translocon complex
Up	19.78	0.00507	AW253880	Kifc1	kinesin family member C1	microtubule tract
Up	15.25	0.00121	NM_053864	Vcp	valosin-containing protein	protein golgi-ER
Ion Handling						
Up	39.29	0.03690	M19261	Clta	clathrin, light polypeptide (Lca)	calcium binding
Up	33.64	0.00511	D28875	Sparc	secreted acidic cysteine rich glycoprotein	calcium binding
Up	27.96	0.01107	AJ001929	Rcn	reticulocalbin	calcium binding
Up	26.68	0.03170	NM_019905	Anxa2	calpactin I heavy chain	calcium binding
Up	12.99	0.00061	AW918443	MGC93921	calcyclin binding protein (similar)	calcium binding
Up	12.33	0.00072	NM_053968	Mt3	metallothionein 3	ion homeostasis, metal cations
Up	11.97	0.00230	AF268468	Vdac2	voltage-dependent anion channel 2	ion channel

* Discussed in text.

Table 3-5. C6 cells: z-score report for differentially expressed genes

Gene Ontology (GO) Name	Number Changed	Number Up	Number Down	Number Measured	z-score up	z-score down
Under-represented GO biological process nodes						
cell surface receptor linked signal transduction	27	27	0	517	-4.67	na
G-protein coupled receptor protein signaling pathway	12	12	0	333	-4.63	na
ion transport	22	22	0	397	-3.81	na
cell communication	103	103	0	1207	-3.61	na
metal ion transport	9	9	0	221	-3.48	na
potassium ion transport	1	1	0	102	-3.33	na
signal transduction	74	74	0	893	-3.21	na
monovalent inorganic cation transport	7	7	0	169	-3.00	na
cell-cell signaling	11	11	0	214	-2.92	na
cation transport	14	14	0	249	-2.91	na
sodium ion transport	1	1	0	65	-2.50	na
transmission of nerve impulse	9	9	0	168	-2.48	na
response to chemical substance	3	3	0	89	-2.39	na
synaptic transmission	9	9	0	163	-2.37	na
cellular process	256	256	0	2452	-2.22	na
defense response	20	20	0	270	-2.08	na
neuropeptide signaling pathway	1	1	0	48	-2.03	na
Over-represented* GO biological process nodes						
protein biosynthesis	44	44	0	153	6.97	na
protein metabolism	150	150	0	834	6.88	na
metabolism	294	294	0	2035	6.45	na
modification-dependent protein catabolism	16	16	0	36	6.32	na
ubiquitin-dependent protein catabolism	15	15	0	35	5.93	na
macromolecule biosynthesis	67	67	0	314	5.87	na
biosynthesis	78	78	0	396	5.58	na
microtubule-based process	16	16	0	42	5.52	na
cytoplasm organization and biogenesis	47	47	0	206	5.37	na
translational elongation	6	6	0	9	5.26	na
cell organization and biogenesis	55	55	0	265	5.04	na
cell cycle	52	50	0	241	5.00	na
DNA replication and chromosome cycle	13	13	0	35	4.86	na
microtubule cytoskeleton organization and biogenesis	7	7	0	13	4.86	na
microtubule nucleation	3	3	0	3	4.86	na
physiological process	409	409	0	3290	4.85	na
sterol biosynthesis	8	8	0	17	4.67	na
mitotic cell cycle	22	22	0	80	4.63	na
ribosome biogenesis	11	11	0	29	4.55	na
ribosome biogenesis and assembly	11	11	0	30	4.41	na
translation	11	11	0	31	4.28	na
sterol metabolism	12	12	0	36	4.20	na
cholesterol biosynthesis	7	7	0	16	4.11	na
intracellular transport	41	41	0	204	4.09	na
ubiquitin cycle	16	16	0	57	4.04	na
cell aging	3	3	0	4	4.03	na
mitotic spindle organization and biogenesis	3	3	0	4	4.03	na
microtubule-based movement	6	6	0	13	3.98	na
chaperone cofactor dependent protein folding	2	2	0	2	3.97	na
chaperonin-mediated tubulin folding	2	2	0	2	3.97	na
DNA damage response (p53 mediator)	2	2	0	2	3.97	na
transcription from Pol I promoter	2	2	0	2	3.97	na
tubulin folding	2	2	0	2	3.97	na
organelle organization and biogenesis	35	35	0	169	3.96	na
DNA replication	10	10	0	29	3.96	na
cytoskeleton organization and biogenesis	28	28	0	128	3.85	na
aging	4	4	0	7	3.84	na
S phase of mitotic cell cycle	10	10	0	30	3.83	na
cytoskeleton-dependent intracellular transport	6	6	0	14	3.74	na
cell proliferation	61	61	0	347	3.70	na

* GO nodes with a z-score greater than zero and less than 3.5 (155 nodes) are omitted from this table for brevity.

Table 3-6 (pg 1 of 2). C6 cells: Genes linked to protein metabolism

Dir	Ratio	p-value	Gene Identifier	Gene Name	Gene ID
Cellular Ribosomal Proteins (protein synthesis)					
Up	410.08	0.00233	BI279866	L18a (similar)	Rpl18
Up	171.80	0.00115	NM_017150	L29	Rpl29
Up	143.37	0.03382	NM_031101	L13	Rpl13
Up	136.52	0.00277	BI282255	S5	Rps5
Up	129.18	0.00992	BG668512	S19 (similar)	Rps19
Up	117.30	0.04083	AI170643	L12 (similar)	Rpl12
Up	99.75	0.02747	AA799501	S4, X-linked	Rps4x
Up	79.49	0.00222	NM_022510	L4	Rpl4
Up	72.84	0.00831	BG665124	S3	Rps3
Up	72.58	0.00216	BI297634	L24	Rpl24
Up	70.68	0.00473	AW914090	acidicP1 (similar)	Rplp1
Up	68.20	0.03742	NM_053971	L6	Rpl6
Up	67.71	0.01613	NM_031065	L10a	Rpl10a
Up	62.99	0.02073	AA799768	S9 (similar)	Rps9
Up	57.09	0.00499	NM_022402	acidic P0	Arbp
Up	54.13	0.04365	BI284252	L11 (similar)	Rpl11
Up	53.01	0.01492	NM_017151	S15	Rps15
Up	50.89	0.02497	NM_031102	L18	Rpl18
Up	36.04	0.00792	NM_031109	S10	Rps10
Up	35.05	0.00079	AI409193	L8 (similar)	Rpl8
Up	31.14	0.02893	BM388719	L7 (similar)	Rpl7
Up	26.46	0.01832	BF281221	L7 (similar)	Rpl7
Up	25.47	0.04944	NM_053597	S27	Rps27
Up	23.82	0.00233	NM_031100	L10	Rpl10
Up	23.65	0.02049	AA944861	S2	Rps2
Up	23.18	0.00232	NM_031110	S11	Rps11
Up	22.64	0.00437	BF281388	S18, cytosolic	Rps8
Up	21.69	0.03651	AA892367	L3	Rpl3
Up	21.61	0.00241	AA800007	L15	Rpl15
Up	21.29	0.00326	BG666872	S16 (similar)	Rps16
Up	20.88	0.00602	AW919054	acidic P2 (similar)	Rplp2
Up	20.74	0.03195	AW142090	L36a (similar)	Rpl36
Up	19.33	0.03927	NM_022697	L28	Rpl28
Up	18.59	0.03910	NM_031706	S8	Rps8
Up	18.18	0.02375	BF281215	L37 (similar)	Rpl37
Up	17.71	0.01539	NM_022672	S14	Rps14
Up	17.17	0.03062	BI281697	L7a	Rpl7
Up	16.70	0.03202	BE110642	S6 (similar)	Rps6
Up	10.39	0.00269	BI850152	L8 (similar)	Rpl8
Up	6.03	0.01976	NM_053330	L21	Rpl21
Up	6.01	0.02605	BI296190	RNA processing 42 (similar)	Rrp42
Mitochondrial Ribosomal Proteins (protein synthesis)					
Up	16.53	0.02099	BI294944	S12 precursor (similar)	Mrps12
Up	14.05	0.03367	BE110549	L37 (similar)	Mrpl37
Up	13.85	0.04109	BI294860	L51 (similar)	Mrpl51
Up	13.79	0.01274	BI287857	L21 (similar)	Mrpl21
Up	9.81	0.04140	AI175327	L22 (similar)	Mrpl22
Up	8.61	0.03865	AW254612	S15 precursor (similar)	Mrps15
Up	6.51	0.00765	AI639387	S6 (similar)	Mrps6
Up	6.40	0.02024	AI103129	L15 (similar)	Mrpl15
Up	6.29	0.03073	BI289416	28S S25 (similar)	Mrps25
Up	5.86	0.00720	BI279024	L3 (similar)	Mrpl3
Up	5.58	0.01832	AI170354	L10 (similar)	Mrpl10
Up	4.79	0.02877	NM_022529	L23	Mrpl23
Up	3.57	0.04337	AI575434	L12 (similar)	Mrpl12
Up	2.96	0.04371	BF408394	L35 (similar)	Mrpl35
Up	2.51	0.04283	BE097240	28S S28 (similar)	Mrps28

Table 3-6 (pg 2 of 2). **C6 cells: Genes linked to protein metabolism**

Dir	Ratio	p-value	Gene Identifier	Gene Name	Gene ID
Proteasome Subunits (protein catabolism)					
Up	63.45	0.02415	AI169273	beta type 3	Psmb3
Up	39.63	0.01713	NM_053590	beta type 1	Psmb1
Up	24.26	0.00811	NM_031331	26S, non-ATPase, 4	Psmd4
Up	23.66	0.02739	NM_053532	beta type 7	Psmb7
Up	19.96	0.01050	NM_080767	beta type 8	Psmb8
Up	18.45	0.02483	NM_031595	26S, ATPase, 3	Psmc3
Up	16.07	0.01910	NM_017264	28S, alpha	Psme1
Up	13.10	0.00037	NM_031629	beta type 4	Psmb4
Up	10.18	0.04926	NM_017280	alpha type 3	Psma3
Up	9.78	0.01314	NM_017284	beta type 2	Psmb2
Up	8.47	0.02777	NM_017257	28S, beta	Psme2
Up	7.92	0.00520	BG378826	26S, ATPase, 4	Psmc4
Up	6.88	0.00074	BF282262	alpha type 7	Psma7
Up	6.29	0.01786	NM_017278	alpha type 1	Psma1

H4IIE Cells

The array intensity scatter plot for H4IIE treatment and control arrays (Figure 3.22) demonstrates differentially expressed genes are distributed between activation and suppression. Less than ten of these genes were found in KEGG molecular interaction pathways, suggesting modes by which these gene products interact are not yet characterized. A representative list of differentially expressed H4IIE genes is presented in Table 3-6 and includes 121 annotated genes identified in significance plots (Figure 3.21) as having high-fold differential regulation and/or high measurement precision (i.e., large $-\log s_{10}p$).

Classic transcriptional induction of cytochrome P450 1A1 and 1A2 was clearly observed in H4IIE hepatoma cells (+4,300 and +228, respectively); *CYP1B1* was also substantially induced (+23). Induction of these cytochrome P450 isoforms is consistent with previous studies of AhR-mediated effects of halogenated aromatic hydrocarbons in liver (Schmidt *et al.*, 1996) . No transcripts of the AhR were detected. Other than *CYP* genes, the most highly expressed transcript was an unannotated transcribed sequence (+11.5) (GenBank, BE107848). Consistent with xenobiotic challenge by an aryl hydrocarbon, the z-score analysis (Table 3-7) reveals H4IIE cells treated with PCB126 over-expressed transcriptionally activated genes correlated with xenobiotic and aromatic compound metabolism, specifically the TCDD metabolic response. Also noteworthy, is overrepresentation of transcriptionally activated electron transport associated genes. Over-represented genes suppressed by PCB 126 were generally linked to transcription, actin cytoskeleton, and signal transduction. The most highly expressed transcript related

to gene expression was *EIF3S3* (+ 6.7), a eukaryotic translation initiation factor observed to be substantially over-expressed in large hepatocellular carcinomas in humans (Okamoto *et al.*, 2003). Also transcriptionally activated, were the mitogenic genes *epiregulin* (+3.3) and *amphiregulin* (+4.2). Substantially suppressed transcription factors included a fork-head related protein (-5.3) and a one-cut domain family member (-3.6). The most highly suppressed gene associated with cytoskeleton was a gene for procollagen (-5.9).

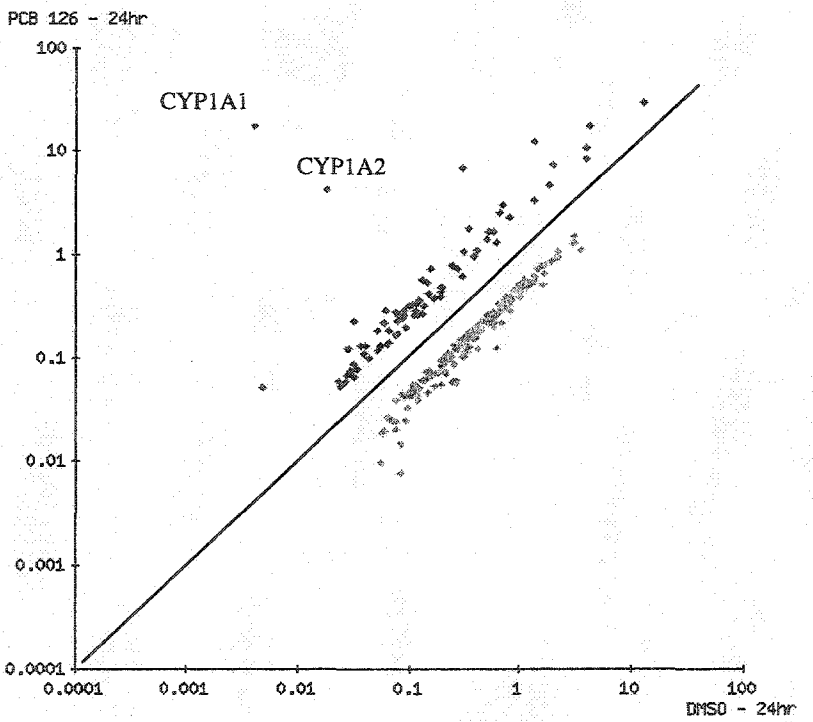

Figure 3.23. H4IIE rat hepatoma cells: Scatter plot of scanned microarray intensities for differentially expressed gene transcripts following PCB 126 treatment ($p < 0.05$, fold-change > 2).

Table 3-7 (pg 1 of 4). **H4IIE cells: Function of annotated genes with relatively high fold differential expression and/or small p-value**

Dir	Ratio	p-value	Accession	Gene ID	Gene Name	Activity
Xenobiotic Metabolism						
Up	4292.6	0.00001	X00469	Cyp1a1	cytochrome P450, 1a1	aromatic compound metabolism
Up	227.4	0.00004	K02422	Cyp1a2	cytochrome P450, 1a2	aromatic compound metabolism
Up	22.6	0.00001	NM_012940	Cyp1b1	cytochrome P450, 1b1	aromatic compound metabolism
Up	8.7	0.00000	NM_017013	Gsta2	glutathione-S-transferase, alpha type2	alkyl/aryl transferase
Up	2.7	0.00001	AI234527	Gst8	glutatione S-transferase 8 (similar)	stress response
Dn	1.2	0.00001	M20406	Cyp2b3	cytochrome P450, 2b3	monooxygenase activity
Transcription/Translation/Replication/Repair						
* Up	6.9	0.00909	BI292573	Eif3s3	eukaryot. transln init. factr 3, sub 3 gamma, 40kDa	hepatocellular carcinoma associated
Up	3.6	0.03584	AW528096	Asf1	anti-silencing function 1 homolog A (similar)	chromosome stability
Up	3.1	0.00568	NM_139186	Mki67ip	spermatogenesis-related protein	condensed chromosome protein binding
Up	2.2	0.00047	BF561716	Miz1	Msx-interacting-zinc finger	transcription - DNA dependent
Up	1.2	0.00000	BF411100	-	zinc finger protein (similar)	DNA/RNA interaction
Up	1.2	0.00000	BI273897	-	dJ310O13.3 (novel protein) (similar)	p53 and DNA damage-regulated protein
Up	1.2	0.00004	BF398121	-	zinc finger protein 277 (similar)	DNA/RNA interaction
Up	1.2	0.00000	BI283124	Sra1	steroid receptor RNA activator 1	transcriptoin cofactor
Dn	5.3	0.01710	AW144081	-	fork head-related protein like A (simmilar)	transcription factor
Dn	4.2	0.04667	BI290218	Exc7	excretory canal abnormal (similar)	RNA binding protein
Dn	3.8	0.00217	AI535239		HMG-box transcription factor TCF4E (similar)	transcription factor
* Dn	3.3	0.00000	BF396189	Onecut1	one cut domain, family member 1 (hepatocyte NF-6)	transcriptional activator
Dn	3.3	0.00021	BF284014	Ccnk	cyclin K	regulation of transcription, DNA-dependent
Dn	3.3	0.04950	NM_017103	Tceb3	transcription elongat factr B (SIII), polyptd 3	regulation of transcription, DNA-dependent
Dn	3.0	0.03716	NM_138975	Wbp2	WW domain binding protein 2	transcription factor adapter molecule
Dn	2.5	0.00044	BF397805	Atrx	alpha thalasma./mental retardn syndrm (similar)	DNA repair
Dn	2.3	0.00005	BI278651	Lyl1	lymphoblastic leukemia derived seq. 1 (similar)	negative regulation of transcription
Dn	2.1	0.00031	AY066016	Nr3c1	nuclear receptor subfamily 3, group C, member 1	regulation of transcription, DNA-dependent
Dn	2.0	0.00004	BE106199	-	nuclear orphan receptor/transcription factor (similar)	transcription factor
Dn	2.0	0.00003	NM_024388	Nr4a1	immediate early gene transcription factor NGFI-B	regulation of transcription, DNA-dependent
Dn	1.7	0.00002	BF408990	-	splicng coactivtr SRm300 AT-rich elemnt bindg factr (similar)	exonic splicing enhancer
Dn	1.6	0.00004	BE109884	-	forkhead-related transcription factor 1A (similar)	transcription factor
Dn	1.6	0.00000	BE111631	Cntf	ciliary neurotorpic factor (similar)	adipocyte gene regulation
Dn	1.5	0.00007	BF281184	Bmyb	B-myb (similar)	transcription factor repressed in G0/early G1
Dn	1.4	0.00004	AI715835	Gtf2i	general transcription factor II I	transcription factor
Dn	1.3	0.00006	AF267197	Lcp1	epidermal Langerhans cell protein LCP1	regulation of transcription, DNA-dependent
Dn	1.2	0.00002	BI290172	E2F-4	E2F transcription factor 4 (similar)	tumor suprsr - uracil-DNA glycosylase prolif. depend.
Dn	1.2	0.00009	BG375714	Nop1	nucleolar protein 1 (similar)	homologous with autoimmune antigen fibrillarin
Dn	1.1	0.00005	AI071906	-	pre-mRNA cleavage factor I, 68kD subunit (similar)	pre-mRNA 3'-end processing
Dn	1.1	0.00008	BI295122	-	MHR23B (similar)	nucleotide excision repair
Dn	1.1	0.00000	AI599066	NonO	non-POU-domain-containing, octamer binding protein (similar)	single stranded RNA/DNA binding

Table 3-7 (pg 2 of 4). **H4IIE cells: Function of annotated genes with relatively high fold differential expression and/or small p-value**

Dir	Ratio	p-value	Accession	Gene ID	Gene Name	Activity
Morphogeneisis/Organogenesis/Differentiation						
Up	10.6	0.00244	AI600057	Crim1	cysteine-rich repeat-containing protein (similar)	morphogenesis
Dn	1.7	0.00006	BF416343	NIPBL	delangin	morphogenesis
Dn	1.4	0.00005	NM_021849	Rfng	radical fringe gene homolog	inhibits notch signaling
Dn	1.4	0.00000	U44948	Csrp2	cysteine rich protein 2	cell differentiation
Dn	1.2	0.00004	AI600019	Pja2	praja 2, RING-H2 motif containing	morphogenesis
Cytoskeleton						
Up	3.4	0.02097	NM_057208	Tpm3	tropomyosin isoform 6	actin binding
Up	2.5	0.00026	NM_012975	Lgals4	lectin, galactose binding, soluble 4	heterophilic cell adhesion
Dn	5.9	0.01871	BM391350	Col11a2	procollagen, type XI, alpha 2	cell adhesion/ATP binding
Dn	3.3	0.00048	U15425	-	membrane and microfilament-associated protein p58	cytoskeleton organization and biogenesis
Dn	3.0	0.00222	AF021936	Cdc42bpb	Cdc42-binding protein kinase beta	cytoskeleton organization and biogenesis
Dn	2.1	0.00016	BE111847	Smarca4	SWI/SNF reltd actin depndt regulr chromatin sub a memb 4	chromatin remodeling
Dn	1.3	0.00008	BM383443	Ap1g1	adaptor protein complex AP-1, gamma 1 subunit	microtubule-based process
Cell Growth and Proliferation						
* Up	4.2	0.00028	NM_017123	Areg	amphiregulin	growth factor, can stimulate or inhibit growth
Up	4.2	0.04375	AI044807	Zrf2	zuotin related factor 2	negative regulation of cell growth
* Up	3.2	0.00196	NM_021689	Ereg	epiregulin precursor	positive regulation of cell proliferation - mitogenic
Up	1.2	0.00004	BG666773	Tbrg1	V-ros UR2 sarcoma virus oncogene homolog 1 (similar)	regulation of cell cycle
Up	1.2	0.00000	NM_030847	Emp3	epithelial membrane protein 3	cell growth
Dn	2.2	0.00050	BF563800	-	E3 ligase for inhibin receptor (similar)	cell growth
Dn	1.6	0.00002	BM392277	Ilkap	protein phosphatase 2C	negative regulation of cell cycle
Dn	1.4	0.00001	NM_053887	Map3k1	mitogen activated protein kinase kinase kinase 1	protein serine/threonine kinase activity
Dn	1.4	0.00009	AI406305	Ckip1	CK2 interacting 1; TNF intracellular domain-interactng (similar)	recruitment of PK CK2 to the plasma membrane
Dn	1.3	0.00001	AI172172	As3	androgen-induced prostate prolif. shutoff assoc AS3 (similar)	allele in tumor suppressor Chr region
Dn	1.2	0.00008	NM_022799	Nucks	nuclear ubiquitous casein kinase 2	regulation of cell cycle
Apoptosis						
Dn	3.5	0.02637	NM_053812	Bak1	BCL2-antagonist/killer 1	induction of apoptosis
Dn	1.5	0.00008	BE110671	Hip1	huntingtin interacting protein 1	regulation of apoptosis
Stress Response						
Up	4.5	0.02875	AI598451	Grp75	heat shock 70 protein (similar)	stress response
Up	4.2	0.03171	NM_130741	Lcn2	lipocalin 2	stress response infection
Up	3.7	0.02053	AB013454	Ac2-210	amino acid starvation-induced protein mRNA, 3 end	stress response
Up	3.6	0.00000	BM383531	Mt1e	metallothionein-IE (similar)	stress response
Up	2.1	0.00004	U66322	Ltb4dh	dithiolethione-inducible gene-1	response to toxin
Up	1.6	0.00002	NM_021744	Cd14	CD14 antigen	response to wounding/inflammatroy
Up	1.2	0.00002	NM_031624	Igbp1	immunoglobulin binding protein 1	B-lymphocyte activation
Up	1.1	0.00005	BF285292	Cdc37	Hsp90-associating relative of Cdc37	oncogenic - Recruitment of PKs to the Hsp90 system
Dn	3.1	0.02209	BF388819	Cap350	centrosome-associated protein 350	regln. peroxisom prolif.-activated nclr hormone receptr
Dn	1.1	0.00000	AW252670	Sfrs10	splicing factor, arg/ser-rich (transfmr 2 Drosophila homolog) 10	stress resonse / RNA processing

Table 3-7 (pg 3 of 4). **H4IIE cells: Function of annotated genes with relatively high fold differential expression and/or small p-value**

Dir	Ratio	p-value	Accession	Gene ID	Gene Name	Activity
Biosynthesis						
Up	5.2	0.00475	BM388719	Rpl7	ribosomal protein 7 (similar)	protein synthesis
Up	1.3	0.00003	AI411153	Mrps23	Mrps23 protein (similar)	protein synthesis - mitochondria
Signal Transduction						
Up	1.1	0.00008	NM_024377	Gng5	G protein gamma-5 subunit	cell surface receptor linked signal transduction
Dn	3.8	0.02035	AI136393	Pde10a	phosphodiesterase 10A	signal transduction
Dn	3.0	0.00069	AI145240	Akap9	A kinase (PRKA) anchor protein (yotiao)	PK anchoring protein
Dn	3.0	0.00011	BF407212	-	RAB5B, member RAS oncogene family (similar)	oncogene
Dn	2.4	0.00091	BE118639	-	nclr pore cmplx-assoc intranclr coiled-coil protein TPR (similar)	fusn w kinase domns met/trk/raf protooncogenes.
Dn	2.1	0.00094	L09653	Tgfbr2	transforming growth factor, beta receptor II	transmembrn. repcetr ser/thr kinase sig pathway
Dn	2.0	0.00048	BF560790	-	RAB5B, member RAS oncogene family (similar)	oncogene
Dn	2.0	0.00062	AI602501	-	LIM (Lin-11, Isl-1, Mec-3) and cysteine-rich domains 1 (similar)	protein-protein interaction
Dn	1.2	0.00003	BI290662	1lbg	vomeronasal 1 receptor, C3 (similar)	G-protein coupled receptors
Dn	1.2	0.00000	AI172465	Ptpn11	protein tyrosine phosphatase, non-receptor type 11	intracellular signaling cascade
Catabolism						
Up	3.1	0.00333	AI230371	Lamp1	lysosomal membrane glycoprotein 1	lytic vacuole
Up	3.0	0.00411	AI232085	Crbn	novel lethal gene (cereblon similar)	protease
Up	1.5	0.00009	BI285090	-	histocompatibility 13; presenilin-like protein 3 (similar)	protease
Up	1.3	0.00001	AI170666	Armet	arginine-rich, mutated in early stage tumors (similar)	metalloendopeptidase inhibitor activity
Up	1.2	0.00003	NM_053590	Psmb1	proteasome (prosome, macropain) subunit, beta type 1	protein catabolism
Dn	2.4	0.00008	AI235240	Aplp2	sperm membrane protein (YWK-II)	endopeptidase inhibitor activity
Dn	2.3	0.00014	BI300794	Agp7	myeloblastin	lysosomal protein
Dn	2.1	0.00008	BI294752	-	endosomal protein (similar)	waste processing
Intermediate Metabolism						
Up	4.0	0.00009	J02679	Nqo1	NAD(P)H dehydrogenase, quinone 1	oxidoreductase
Up	3.5	0.02023	AI113090	-	1,3-1,6-alpha-mannosidase (similar)	mannosidase
Up	2.5	0.00001	M23995	Aldh1a4	aldehyde dehydrogenase family 1, subfamily A4	oxidoreductase activity
Up	2.0	0.00063	NM_130756	Pte1	4,8-dimethylnonanoyl-CoA thioesterase	acyl-CoA metabolism
Up	2.0	0.00004	NM_031980	Ugt2b12	UDP-glucuronosyltransferase	glucuronosyltransferase
Up	1.6	0.00003	AI170570	Coq6	Coq6 protein (similar)	CoQ biosynthesis
Up	1.6	0.00004	AI029729	Gldc	glycine decarboxylase	decarboxylase
Up	1.4	0.00003	AY083160	Mawbp	MAP activator w WD repeats (MAWD) binding protein	hydroxylase
Up	1.3	0.00005	AI172192	Pig-x	GPI-mannosyltransferase subunit	transferase
Up	1.2	0.00009	D13921	Acat1	acetyl-coenzyme A acetyltransferase 1	acetyltransferase
Up	1.1	0.00000	U09386	Fkbp1a	FK506-binding protein 1a	isomerase
Up	1.1	0.00009	J05266	Atp5a1	mitochondrial H+-ATP synthase alpha subunit	purine synthesis
Dn	2.1	0.00076	AI511367	-	beta-galactosidase (similar)	galactosidase
Dn	1.7	0.00004	NM_017072	Cps1	carbamoyl-phosphate synthetase 1	nitrogen metabolism

Table 3-7 (pg 4 of 4). **H4IIE cells: Function of annotated genes with relatively high fold differential expression and/or small p-value**

Dir	Ratio	p-value	Accession	Gene ID	Gene Name	Activity
Transport						
Up	3.2	0.02916	NM_053584	-	golgi SNAP receptor complex member 1	protein transport
Up	1.2	0.00009	AB006450	Timm17a	translocator of inner mitochondrial membrane 17a (similar)	protein translocase
Dn	4.8	0.03637	NM_057136	*Epn1*	*epsin 1*	vesicle-mediated transport/lipid binding
Dn	3.5	0.00058	NM_133602	Marta1	MAP2 RNA trans-acting protein	nucleocytoplasmic transport
Dn	3.0	0.03203	AI639159	Yslp1	YSPL-1 form 1 (similar)	ascorbate transporter
Dn	1.4	0.00007	BM383757	Rab1b	Ras-related protein Rab-1B (similar)	ER to Golgi transport
Ion Handling						
Up	4.1	0.00000	NM_080892	Selenbp1	selenium binding protein 2	selenium binding
Up	2.3	0.00011	AF411318	Mt1a	metallothionein	metal ion homeostasis
Up	1.8	0.00004	NM_031740	-	UDP-Gal:betaGlcNAc beta 1,4-galactosyltransfrse, polyptd 6	glycosphingolipid metabolism (membrane)
Up	1.6	0.00009	NM_031546	Rgn	regucalcin	calcium ion binding
Up	1.4	0.00003	BF403759	Cacna1d	calcium channel, voltage-dependent, L type, alpha 1D subunit	second-messenger-mediated signaling
Dn	1.5	0.00007	NM_131906	Slc21a5	solute carrier family 21 (organic anion transporter), member 5	organic anion transport
Unknown - high-fold suppression						
Dn	11.5	0.00036	BE107848	-	transcribed sequence	unknown - suppressed
Dn	6.0	0.02309	BE107090	-	transcribed locus	unknown - suppressed
Dn	4.4	0.01160	BF393118	-	hypothetical protein A530094D01 (similar)	unknown - suppressed

* Discussed in text

Table 3-8. H4IIE cells: z-score report for differentially expressed genes

Gene Ontology (GO) Name	Number Changed	Number Up	Number Down	Number Measured	z-score up	z-score down
Under-represented GO biological process nodes						
none						
Over-represented GO biological process nodes						
dibenzo-p-dioxin metabolism	1	1	0	1	13.4	
zinc ion homeostasis	1	1	0	1	13.4	
purine ribonucleoside salvage	1	1	0	2	9.4	
nitric oxide mediated signal transduction	1	1	0	3	7.7	
tRNA processing	1	1	0	3	7.7	
response to xenobiotic stimulus	2	2	0	16	6.5	
xenobiotic metabolism	2	2	0	16	6.5	
ER to Golgi transport	1	1	0	6	5.3	
acyl-CoA metabolism	1	1	0	7	4.9	
tRNA metabolism	1	1	0	7	4.9	
nucleic acid transport	2	1	1	8	4.6	3.59
RNA transport	2	1	1	8	4.6	3.59
RNA-nucleus export	2	1	1	8	4.6	3.59
RNA localization	2	1	1	9	4.3	3.35
response to toxin	1	1	0	9	4.3	
cell fate determination	1	1	0	10	4.0	
nucleoside metabolism	1	1	0	10	4.0	
transition metal ion homeostasis	1	1	0	10	4.0	
electron transport	4	4	0	145	3.7	
response to chemical substance	4	3	1	89	3.6	0.28
cytolysis	1	1	0	13	3.5	
aromatic compound metabolism	2	2	0	52	3.2	
nucleobase, nucleoside, nucleotide and nucleic acid transport	2	1	1	16	3.1	2.35
regulation of muscle contraction	2	1	1	16	3.1	2.35
negative regulation of cell growth	1	1	0	16	3.1	
regulation of growth	1	1	0	16	3.1	
regulation of neuronal synaptic plasticity	1	1	0	17	3.0	
cell fate commitment	2	1	1	18	2.9	2.18
central nervous system development	2	2	0	70	2.6	
response to abiotic stimulus	5	3	2	146	2.5	0.69
cytoskeletal anchoring	1	0	1	1		10.79
RNA elongation from Pol II promoter	1	0	1	1		10.79
synaptic vesicle maturation	1	0	1	1		10.79
Rho protein signal transduction	3	0	3	11		9.54
adult somatic muscle development	1	0	1	2		7.56
chromatin remodeling	1	0	1	4		5.26
metabotropic glutamate receptor signaling pathway	1	0	1	4		5.26
neuromuscular junction development	1	0	1	4		5.26
non-covalent chromatin modification	1	0	1	4		5.26
synaptic vesicle endocytosis	1	0	1	4		5.26
mRNA-nucleus export	1	0	1	5		4.66
actin cytoskeleton organization and biogenesis	3	0	3	40		4.6
actin filament-based process	3	0	3	42		4.46
endoderm development	1	0	1	6		4.22
small GTPase mediated signal transduction	5	1	4	89	0.7	3.78
negative regulation of cell adhesion	1	0	1	8		3.59
odontogenesis (sensu Vertebrata)	1	0	1	8		3.59
transforming growth factor beta receptor signaling pathway	2	0	2	31		3.4
chromatin modification	1	0	1	9		3.35
transmembrane receptor protein ser/thr kinase signaling pathway	2	0	2	34		3.2
JAK-STAT cascade	1	0	1	10		3.15
membrane fusion	1	0	1	10		3.15
protein secretion	1	0	1	10		3.15

IV. DISCUSSION

A. OVERVIEW

The dissertation clearly demonstrates PCB 126 causes a wide spectrum of biological effects. Effects reported by others including hyperplasia, tumor promotion, or hepatocarcinogenicity, are unambiguous toxic responses, while other responses such as changes in blood chemistry or hormone levels may be little more than secondary compensatory responses. Regardless, two points were made exceeding clear by this dissertation project. First, the primary literature sources reviewed in Section II demonstrate that PCB 126 is pro-inflammatory and causes dysmorphic cell growth in certain tissues. Second, novel research presented in Section III, demonstrates that PCB 126 exerts a substantial effect on the expression of genes in different tissues. Although the literature review provides a context for research on the effects of PCB 126, its essential purpose is to provide clues for interpreting the large database generated from gene expression experiments in this dissertation. For this reason, research by other investigators will be considered putative, and are interpreted only to the extent prior data are relevant to differential gene expression results.

B. PCB 126 AND DIFFERENTIAL GENE EXPRESSION

The differential gene expression results provided in Section III illustrates major differences in the transcriptional signatures of different xenobiotic-metabolizing tissues following exposure to PCB 126. Despite the putative requirement of AhR-mediated

transcriptional activation of *CYP1A1/2*, and high-fold induction of the latter in hepatoma cells, no transcripts of the AhR were detected. This suggests the AhR is a highly efficient receptor that does not require transcriptional activation, despite its role in mediating four-thousand-fold induction of *CYP1A1* observed in this study. If the universal mechanism for coplanar PCB toxicity is AhR-mediated transcriptional activation, including substantial induction of CYP1A1/2 activity, we should have observed transcripts for *CYP1A1/2* genes in C6 astrocytic cells. This observation reemphasizes the notion of unique responses to toxicants by different tissues and brings into question the assumption that the AhR has a universal role in mediating the toxicity of TCDD and coplanar PCBs. In previous work with relatively weak AhR ligands (benzo(a)anthracine and phenobarbital), it was found that half-lives of *CYP1A1/2* mRNA in C6 cells was $1/10^{th}$ that of liver (Geng *et al.*, 1998). Perhaps transcripts of these CYP isoforms are rapidly degraded in C6 cells. This is plausible if transcriptional activation observed in C6 cells is also reflected as increased rates of mRNA catabolism. The observation that different tissues respond differently to PCB 126 is completely consistent with *in vivo* observations in rodents. PCB 126 is a known liver carcinogen in rats (NTP, 2004), yet effects on the developing rat brain range from learning and memory deficits (Eriksson *et al.*, 1998), to little or no effect (Bushnell *et al.*, 1999; Rice *et al.*, 1998; Rice, 1999; Rice *et al.*, 1999), to improved learning performance (Schantz *et al.*, 1996).

1. Distribution and Metabolism

In this study we demonstrated uniquely different tissue responses to PCB 126 at the genetic level, a finding that emphasizes the need for tissue-specific risk assessment. In addition to different tissue responses, it is also important to remain cognizant of major

differences in the metabolism and pharmacokinetics of toxicants in different organs. Metabolism and clearance of PCB 126 is exceedingly slow (Koga *et al.*, 1990) and the pharmacokinetic behavior of PCBs is explained by a simple two-compartment model consisting of fat and liver (Ryan *et al.*, 1993). Indeed, PCB 126 was shown to accumulate in the liver through selective binding to constitutively expressed CYP1A2 (Chen *et al.*, 2001). The brain however, appears to be largely protected from exposure to PCB 126. Rat dams dosed with PCB 126 beginning 5 weeks before gestation and continuing through lactation, had pups with PCB 126 brain concentrations $1/100^{th}$ of the levels found in fat at weaning (Rice, 1999) and furthermore, PCB 126 has not been detected in brains of offspring from exposed dams after weaning(Bernhoft *et al.*, 1994; Holene *et al.*, 1995; Holene *et al.*, 1998; Rice *et al.*, 1999). These data suggest a short window of exposure for developing brain tissues, during which the brain would receive relatively small doses of PCB 126.

2. C6 Glioma Cells

Histone Deacetylase Activity

Other than genes for two ribosomal proteins, the most highly activated C6 gene in this study was *LGALS1* (+174), which encodes β-galactoside-binding protein galectin-1 (Barondes *et al.*, 1994). Similar to our present findings with PCB 126 treatment, large-fold induction of *LGALS1* transcription is reported for murine embryonal carcinoma cells treated with sodium butyrate (Lu *et al.*, 1999) and P19 embryocarcinoma cells and whole mouse embryos exposed to valproic acid (VPA) (Kultima *et al.*, 2004). *In vivo*, VPA was observed to relieve histone deacetylase (HDAC)-dependent transcriptional repression

resulting in hyperacetylation of histones; VPA also promotes differentiation of carcinoma cells and transformed hematopoietic progenitor cells (Gottlicher *et al.*, 2001). It is noteworthy that, like embryonic mouse tissues responding to VPA and butyrate, C6 cells are relatively undifferentiated and exhibit biological characteristics of both astroglia and oligodendroglia (Lee *et al.*, 1992). As with VPA and butyrate, our study identifies potent induction of *LGALS1* by PCB 126. HDAC inhibition, that was previously associated with over-expression of this soluble lectin, offers a reasonable explanation for the generalized transcriptional activation we observed for C6 glioma cells.

DNA Methylation

PLAGL1 is interesting because it is the only gene transcript out of more than 1500 differentially expressed genes in C6 cells that was significantly suppressed by PCB 126 treatment (-2.5). PLAGL1 is a zinc-finger nuclear transcription factor with cell-cycle arrest activity (Cvetkovic *et al.*, 2004) and biallelically, it positively controls histone acetylation and negatively controls DNA methylation (Abdollahi *et al.*, 2003). If induction of LGALS1 by PCB 126 resulted only in prolonged histone acetylation, then PLAGL1 expression would be increased, but not suppressed as we observed in this study. It thus appears PCB 126 treatment not only increases transcription through LGALS1 induced HDAC inhibition, but may also inhibit transcription of certain genes by increased DNA methylation.

Cognitive Function

There is substantial evidence that the S100B protein may exert either neurotropic or neurotoxic effects, depending on its concentration. At nM concentrations, S100B

stimulates neurite outgrowth (Kligman *et al.*, 1985; Winningham-Major *et al.*, 1989) and astrocyte proliferation (Selinfreund *et al.*, 1991). At μM concentrations, S100B causes astrocyte and neuronal apoptosis (Fulle *et al.*, 2000; Hu *et al.*, 1996; Hu *et al.*, 1997; Huttunen *et al.*, 2000; Mariggio *et al.*, 1994). In our study, *S100B* transcripts were expressed 9-fold higher in C6 cells after treatment with PCB 126. Under the plausible assumption that there is a dose-response relationship between PCB 126 concentrations reaching the brain and the level of *S100B* transcription and translation, both diminished and improved cognitive function previously observed in animal studies could be accounted for by different levels of S100B caused by dose-dependent induction of S100B by PCB 126.

C6 Summary

In summary, PCB 126 exposure results in a transcriptional profile in C6 glioma cells that is uniquely different from H4IIE hepatoma cells. Activation of genes in C6 cells by PCB 126 is better explained by generalized histone deacetylase inhibition than by the classic aryl-hydrocarbon receptor mediated gene responsiveness described in liver. As indicated by suppression of biallelically controlled *PLAGL1*, PCB 126 may also repress transcription of some genes. Activation or suppression by these mechanisms could explain the up/down-regulation of genes observed in hepatoma cells. Diminished PCB 126 partitioning to the brain during development, would partially explain the variability in cognitive effects observed after perinatal exposure to PCB 126. Under the plausible assumption that transcriptional activation of S100B protein observed in this study depends on PCB 126 tissue dose, the wide range of neuro-cognitive effects may also be

due to the dual ability of S100B to dose-dependently induce either neuronal outgrowth or apoptosis.

3. H4IIE Hepatoma Cells

Carcinogenesis is regarded as a multi-step process requiring numerous epigenetic factors and genetic alterations that occur sequentially in a cell lineage. The list of genes differentially expressed in H4IIE cells following PCB 126 exposure is a "who's who" list of genes reported to be involved in carcinogenic processes. Given that H4IIE cells are neoplastic, it is indeterminate whether PCB 126 exposure or the transformed phenotype is primarily responsible for altered gene expression by PCB 126.

Mitogenicity

Mitogenesis is an epigenetic response thought to play an important role in carcinogenesis (Ames *et al.*, 1990). In the liver, PCB 126 exposure activates a mitogenic response that causes hepatomegaly (Yoshimura *et al.*, 1979) and that probably facilitates tumor promotion. In this study we found PCB 126 activates the expression of the autocrine growth factor epiregulin (*EREG*) (+3.2). *EREG* is believed to play an essential role in hepatocyte proliferation and it produces prolonged activation of epidermal growth factor receptor and mitogen activated protein kinase in rat hepatocytes (Komurasaki *et al.*, 2002). Activation of *EREG* by PCB 126 appears to contribute to both hepatomegaly and to mitogenesis, and hence is likely to play a role in both the tumor promoting ability and hepatocarcinogenicity of PCB 126 in rats.

Altered Transcription

PCB 126 caused altered expression of numerous H4IIE genes associated with transcription (Table 3-6). Although it appears there are more transcription factors suppressed than activated, the biological meaning of this observation is unclear. We did note relatively high transcriptional activation of *EIF3S3* (+6.9), a translation initiation factor that is over-expressed in human large hepatocellular carcinomas (Okamoto *et al.*, 2003) and advanced stage prostate cancer (Saramaki *et al.*, 2001). Finally, 3.25-fold suppression of the developmental one-cut factor HNF-6 (*ONECUT1*) gene was identified. *ONECUT1* is a gene that regulates transcription in the endoderm and later becomes restricted to activity in pancreas and liver (Pierreux *et al.*, 2004).

H4IIE Summary

PCB 126 causes generalized down-regulation of genes in H4IIE cells related to cytoskeleton organization and biogenesis and signal transduction (large z-scores for suppressed genes) while increasing expression of a key growth factor known to causes hepatocyte proliferation. Taken together, the cellular effects of PCB 126 on H4IIE cells are consistent with those needed for tumor progression, and if similar effects occur in normal hepatocytes, these effects are also consistent with those necessary for hepatocarcinogenesis.

C. MICROARRAYS AND SAGE

Numerous investigators have commented on the technical challenges of the SAGE protocol (Angelastro *et al.*, 2000; Bertelsen *et al.*, 1998; Diatchenko *et al.*, 1996; Powell, 1998; Powell, 2000). Without question, these challenges contribute significantly to the

success of alternate microarray technology. While genome-wide microarray technology is investigator-friendly, the technology is in its infancy and data analysis is non-trivial and literally millions of human hours have been spent developing the large microarray technology used in this project (Affymetrix, 2004a).

While datasets produced by SAGE or genome-wide microarrays will intersect, they information generated about gene expression is not the same. It is common for a SAGE library to contain more than 350,000 different SAGE tags, of which only 30,000 may actually map to known expressed sequences, with fewer sequences mapping to known genes (Hough *et al.*, 2000). SAGE does not require any *a priori* sequence information. This is in contrast to "transcriptome-wide" microarrays that contain about 30,000 known expressed sequences, each of which must be synthesized *a priori*. SAGE libraries consist of tags derived from any RNA having both a poly-adenylated 3'-end (i.e., putative messenger RNA) and a *Nla*III restriction site. SAGE is insensitive to whether the RNA it truly a gene transcript or whether it has undergone post-transcriptional modification. SAGE clearly has probative value not available with microarrays, but since much of the SAGE library information does not map to known gene sequences, much of data can not be interpreted.

In the present research, the greatest technical difficulty with SAGE appears to be the presence of contaminants that interfere with concatemer synthesis. Powell suggested that adapters present after *Nla*III cleavage that are not completely removed by gel isolating ditags, could inhibit concatemer synthesis (Powell, 1998). This conclusion is reasonable

because adapters and ditags have complementary sticky ends so adapters could block repetitive tag ligation and prevent concatemer synthesis. To address this problem, Powell suggested using biotinylated primers during large-scale PCR that in turn, would produce biotinylated adapters. Following *Nla*III digestion and initial gel purification, remaining adapters could be removed by adding streptavidin-coated magnetic beads that would bind biotinylated adapters and remove them by magnetic separation. Despite problems with the SAGE method, microarray technology was able to provide data sufficient to address the research hypothesis.

D. FUTURE DIRECTIONS

As previously discussed, human PCB body burdens are decreasing in parallel with slowly decreasing environmental levels. From an environmental health perspective, the fact PCBs are banned on a world-wide basis, means human risk from exposure will diminish. Thus, it appears resources used to clarify the environmental health risks of PCB 126 to humans would be better spent elsewhere.

While conventional environmental toxicology seeks to identify adverse health effects of chemical exposure and quantify the risk, it is naive to embrace a mindset that toxicants only produce adverse effects. The success in treating Alzheimer's disease with acetyl cholinesterase inhibiting drugs that resemble organophosphate insecticides (donepezil hydrochloride) or treating certain cancers with antimicrotubule agents (paclitaxel), exemplifies the role of dose, route of delivery, and context of use in determining toxicity. Unlike novel drug leads, classic environmental toxicants such as organophosphates already have massive epidemiological, mechanistic and effects databases in place.

In this context, perhaps the most intriguing and accessible avenue for future research, relates to the novel observation that PCB 126 may be acting as a histone deacetylase (HDAC) inhibitor in brain tissue. Both acetylation and deacetylation of histone proteins is know to play a critical role in regulating gene expression in a host of biological processes including cellular proliferation, development, and differentiation (Langley *et al.*, 2005). Altered acetylation and deacetylation resulting from the misregulation of histone acetyltransferases (HATs) and/or HDACs is linked to clinical disorders such as leukemia and is believed associated with neurodegeneration during acute and chronic neurological diseases such as stroke, Huntington's disease, amyotrophic lateral sclerosis and Alzheimer's disease; additionally, numerous studies examining HDAC inhibitors suggest that maintaining histone acetylation and transcriptional activation *in vitro* and *in vivo* has beneficial effects in a range of central nervous system disorders and some cancers (Langley *et al.*, 2005). If PCB 126 is indeed a selective HDAC inhibitor that targets neuronal tissues as this dissertation research suggests, it would be a candidate chemical for use in investigating the role of HDAC inhibition in nerve regeneration following ischemic or traumatic injury. Along these lines, it would also be instructive to determine the role of *LGALS1* in HDAC inhibition using RNA interference (RNAi) gene silencing techniques.

V. REFERENCES

1. Abdollahi, A., Pisarcik, D., Roberts, D., Weinstein, J., Cairns, P., and Hamilton, T. C. (2003). LOT1 (PLAGL1/ZAC1), the candidate tumor suppressor gene at chromosome 6q24-25, is epigenetically regulated in cancer. J Biol.Chem **278**, 6041-6049.

2. Affymetrix, Inc. GeneChip® Expression Analysis Data Analysis Fundamentals. 5. 2004a. Santa Clara, CA.

3. Affymetrix, Inc. GeneChip® Expression Analysis Technical Manual. 5. 2004b. Santa Clara, CA.

4. Ames, B. N. and Gold, L. S. (1990). Too many rodent carcinogens: mitogenesis increases mutagenesis. Science **249**, 970-971.

5. Andersson, L., Nikolaidis, E., Brunstrom, B., Bergman, A., and Dencker, L. (1991). Effects of polychlorinated biphenyls with Ah receptor affinity on lymphoid development in the thymus and the bursa of Fabricius of chick embryos in ovo and in mouse thymus anlagen in vitro. Toxicol.Appl.Pharmacol. **107**, 183-188.

6. Angelastro, J. M., Klimaschewski, L. P., and Vitolo, O. V. (2000). Improved NlaIII digestion of PAGE-purified 102 bp ditags by addition of a single purification step in both the SAGE and microSAGE protocols. Nucleic Acids Res. **28**, E62.

7. Aoki, Y. (2001). Polychlorinated biphenyls, polychlorinated dibenzo-p-dioxins, and polychlorinated dibenzofurans as endocrine disrupters--what we have learned from Yusho disease. Environ.Res. **86**, 2-11.

8. Ashburner, M., Ball, C. A., Blake, J. A., Botstein, D., Butler, H., Cherry, J. M., Davis, A. P., Dolinski, K., Dwight, S. S., Eppig, J. T., Harris, M. A., Hill, D. P., Issel-Tarver, L., Kasarskis, A., Lewis, S., Matese, J. C., Richardson, J. E., Ringwald, M., Rubin, G. M., and Sherlock, G. (2000). Gene ontology: tool for the unification of biology. The Gene Ontology Consortium. Nat.Genet. **25**, 25-29.

9. ATSDR. Toxicological Profile for Polychlorinated Biphenyls (PCBs). 2000. Atlanta. Agency for Toxic Substances and Disease Registry, Toxicological Profiles.

10. Atuma, S. S, Hansson, L, Johnsson, H, Slorach, S, and LindstroK m, G. Organochlorine pesticides, polychlorinated biphenyls and dioxins in human milk from Swedish mothers. Food Add.Contam. 15, 142-150. 1998.

11. Aulerich, R. J., Yamini, B., and Bursian, S. J. (2001). Dietary exposure to 3,3',4,4',5-pentachlorobiphenyl (PCB 126) or 2,3,7,8-tetrachlorodibenzo-p-dixon (TCDD) does not induce proliferation of squamous epithelium or osteolysis in the jaws of weanling rats. Vet.Hum.Toxicol. **43**, 170-171.

12. Bager, Y., Hemming, H., Flodstrom, S., Ahlborg, U. G., and Warngard, L. (1995). Interaction of 3,4,5,3',4'-pentachlorobiphenyl and 2,4,5,2',4',5'-hexachlorobiphenyl in promotion of altered hepatic foci in rats. Pharmacol.Toxicol. **77**, 149-154.

13. Bager, Y., Kenne, K., Krutovskikh, V., Mesnil, M., Traub, O., and Warngard, L. (1994). Alteration in expression of gap junction proteins in rat liver after treatment with the tumour promoter 3,4,5,3',4'-pentachlorobiphenyl. Carcinogenesis **15**, 2439-2443.

14. Baker, J. and Eisenreich, S. (1990). Concentrations and fluxes of polycyclic aromatic hydrocarbons and polychlorinated biphenyls across the air-water interface of Lake Superior. Environ Sci Technol **24**, 342-352.

15. Ballschmiter, K. and Zell, M. Analysis of polychlorinated biphenyls (PCB) by glass capillary gas chromatography. Fresenius Z.Analytical Chemistry 302, 20-31. 1980.

16. Barondes, S. H., Cooper, D. N., Gitt, M. A., and Leffler, H. (1994). Galectins. Structure and function of a large family of animal lectins. J Biol.Chem **269**, 20807-20810.

17. Behnisch, P, Allen, R, Anderson, J, Brouwer, A, Brown, D, Campbell, T, Guoyens, L, Harrison, R, Hoogenboom, R, Vanovermeire, I, Traag, W, and Malisch, R. Harmonized quality criteria for chemical and bioassay analyses of PCDDs/PCDFs in feed and food. Part 2: General considerationis, bioassay methods. Organohalogen Compds 50, 59-63. 2001.

18. Behnisch, P. A., Hosoe, K., Brouwer, A., and Sakai, S. (2002). Screening of dioxin-like toxicity equivalents for various matrices with wildtype and recombinant rat hepatoma H4IIE cells. Toxicol Sci. **69**, 125-130.

19. Benda, P., Lightbody, J., Sato, G., Levine, L., and Sweet, W. (1968). Differentiated rat glial cell strain in tissue culture. Science **16**, 370-371.

20. Benedict, W., Gielen, J., Owens, I., Niwa, A., and Nebert, D. W. (1973). Biochemical Pharmacology **22**, 2766-2769.

21. Bernard, P. and Couturier, M. (1992). Cell killing by the F plasmid CcdB protein involves poisoning of DNA-topoisomerase II complexes. J.Mol.Biol. **226**, 735-745.

22. Bernard, P., Gabant, P., Bahassi, E. M., and Couturier, M. (1994). Positive-selection vectors using the F plasmid ccdB killer gene. Gene **148**, 71-74.

23. Bernard, P., Kezdy, K. E., Van Melderen, L., Steyaert, J., Wyns, L., Pato, M. L., Higgins, P. N., and Couturier, M. (1993). The F plasmid CcdB protein induces efficient ATP-dependent DNA cleavage by gyrase. J.Mol.Biol. **234**, 534-541.

24. Bernhoft, A., Nafstad, I., Engen, P., and Skaare, J. (1994). Effects of pre- and postnatal exposure to 3,3',4,4',5-pentachlorobiphenyl on physical development, neurobehavior and xenobiotic metabolizing enzymes in rats. Environmental Toxicology and Chemistry **13**, 1589-1597.

25. Bertazzi, P. A., Bernucci, I., Brambilla, G., Consonni, D., and Pesatori, A. C. (1998). The Seveso studies on early and long-term effects of dioxin exposure: a review. Environ Health Perspect. **106 Suppl 2**, 625-633.

26. Bertelsen, A and Velculescu, V. High throughput gene expression analysis using SAGE. Drug Discovery Today 3, 152-159. 1998.

27. Betteridge, J. (2000). What is oxidative stress? Metabolism **49**, 3-8.

28. Birnbaum, L. S. (1994a). Evidence for the role of the Ah receptor in response to dioxin. Prog.Clin.Biol.Res. **387**, 139-154.

29. Birnbaum, L. S. (1994b). The mechanism of dioxin toxicity: relationship to risk assessment. Environ.Health Perspect. **102 Suppl 9**, 157-167.

30. Birnbaum, L. S., Morrissey, R. E., and Harris, M. W. (1991). Teratogenic effects of 2,3,7,8-tetrabromodibenzo-p-dioxin and three polybrominated dibenzofurans in C57BL/6N mice. Toxicol.Appl.Pharmacol. **107**, 141-152.

31. Bittinger, M., Nguyen, L., and Bradfield, C. A. (2003). Aspartate aminotransferase generates proagonists of the aryl hydrocarbon receptor. Molecular Pharmacology **64**, 550-556.

32. Bixby, j and Harris, W. Molecular mechanisms of axon growth and guidance. Annual Review of Cell Biology 7, 117-159. 1991.

33. Bowman, R. E., Heironimus, M. P., and Allen, J. R. (1978). Correlation of PCB body burden with behavioral toxicology in monkeys. Pharmacol.Biochem.Behav. **9**, 49-56.

34. Bradfield, C. A. and Bjeldanes, L. F. (1987). Structure-activity relationships of dietary indoles: a proposed mechanism of action as modifiers of xenobiotic metabolism. J.Toxicol.Environ.Health **21**, 311-323.

35. Bradlaw, J. A. and Casterline, J. J. L. (1979). Induction of enzyme activity in cell culture: a rapid screen for detection of planar polychlorinated organic compounds. J.Assoc.Off.Anal.Chemists **62**, 904-916.

36. Brix, A. E., Jokinen, M. P., Walker, N. J., Sells, D. M., and Nyska, A. (2004). Characterization of bronchiolar metaplasia of the alveolar epithelium in female Sprague-Dawley rats exposed to 3,3',4,4',5-pentachlorobiphenyl (PCB126). Toxicol.Pathol. **32**, 333-337.

37. Broccardo, C. J., Billings, R. E., Chubb, L. S., Andersen, M. E., and Hanneman, W. H. (2004). Single Cell Analysis of Switch-Like Induction of CYP1A1 in Liver Cell Lines. Toxicol.Sci. **78**, 287-294.

38. Brouwer, A., Ahlborg, U. G., Van den, B. M., Birnbaum, L. S., Boersma, E. R., Bosveld, B., Denison, M. S., Gray, L. E., Hagmar, L., Holene, E., and . (1995). Functional aspects of developmental toxicity of polyhalogenated aromatic hydrocarbons in experimental animals and human infants. Eur.J.Pharmacol. **293**, 1-40.

39. Bushnell, P. J. and Rice, D. C. (1999). Behavioral assessments of learning and attention in rats exposed perinatally to 3,3',4,4',5-pentachlorobiphenyl (PCB 126). Neurotoxicol.Teratol. **21**, 381-392.

40. Cal-EPA. Proposal for the adoption of Revised Toxicity Equivalency Factor ($TEF_{WHO\text{-}97)\ Scheme}$. Hickox, W and Denton, J. Public review draft. 2003. Sacramento, CA, California Environmental Protection Agency, Office of Environmental Protection.

41. Carlson, D. B. and Perdew, G. H. (2002). A dynamic role for the Ah receptor in cell signaling? Insights from a diverse group of Ah receptor interacting proteins. J.Biochem.Mol.Toxicol. **16**, 317-325.

42. Carver, L, Hogenesch, J, and Bradfield, C. A. Tissue specific expression of the rat Ah-receptor and ARNT mRNAs. Nucleic Acid Research 22, 3038-3044. 1994.

43. Carver, L. A. and Bradfield, C. A. (1997). Ligand-dependent interaction of the aryl hydrocarbon receptor with a novel immunophilin homolog in vivo. J.Biol.Chem. **272**, 11452-11456.

44. Chaloupka, K., Harper, N., Krishnan, V., Santostefano, M., Rodriguez, L. V., and Safe, S. (1993). Synergistic activity of polynuclear aromatic hydrocarbon mixtures as aryl hydrocarbon (Ah) receptor agonists. Chem.Biol.Interact. **89**, 141-158.

45. Chen, C. Y., Hamm, J. T., Hass, J. R., and Birnbaum, L. S. (2001). Disposition of polychlorinated dibenzo-p-dioxins, dibenzofurans, and non-ortho polychlorinated biphenyls in pregnant long evans rats and the transfer to offspring. Toxicol Appl Pharmacol. **173**, 65-88.

46. Chen, Y., Yu, M., Rogan, W., Gladen, B., and Hsu, C. (1994). A six-year follow-up of behavioral and activity disorders in the Taiwan Yu-Cheng children. Am.J Public Health **284**, 415-421.

47. Chen, Y. C., Guo, Y. L., Hsu, C. C., and Rogan, W. J. (1992). Cognitive development of Yu-Cheng ("oil disease") children prenatally exposed to heat-degraded PCBs. JAMA **268**, 3213-3218.

48. Chen, Y. H., Riby, J., Srivastava, P., Bartholomew, J., Denison, M., and Bjeldanes, L. (1995). Regulation of CYP1A1 by indolo[3,2-b]carbazole in murine hepatoma cells. J.Biol.Chem. **270**, 22548-22555.

49. Chu, I., Villeneuve, D. C., Yagminas, A., Lecavalier, P., Poon, R., Feeley, M., Kennedy, S. W., Seegal, R. F., Hakansson, H., and Ahlborg, U. G. (1994). Subchronic toxicity of 3,3',4,4',5-pentachlorobiphenyl in the rat. I. Clinical, biochemical, hematological, and histopathological changes. Fundam.Appl.Toxicol. **22**, 457-468.

50. Chubb, L. S., Andersen, M. E., Broccardo, C. J., Legare, M. E., Billings, R. E., Dean, C. E., and Hanneman, W. H. (2004). Regional induction of CYP1A1 in rat liver following treatment with mixtures of PCB 126 and PCB 153. Toxicol.Pathol. **32**, 467-473.

51. Collins, W. and Capen, C. (1980). Fine structural lesions and hormonal alterations in thyroid glands of perinatal rats exposed in utero and by the milk to polychlorinated biphenyls. Am J Pathol **99**, 125-142.

52. Conney, A. (1967). Pharmacological implications of microsomal enzyme induction. Pharmacol.Rev. **19**, 317.

53. Conney, A, Miller, E, and Miller, J. The metabolism of methylated aminoazo dyre. V. Evidence for induction of enzyme synthesis in the rat by 3-methylcholanthrene . Cancer Research 16, 540-559. 1956.

54. Cramer, P, Boggess, K, Stanley, J, Päpke, O, Olson, J, Silver, A, Schmitz, M, and Schecter, A. Intake of dioxins and related compounds from food in the U.S. population. J.Toxicol.Env.Health Part A(63), 1-18. 2001.

55. Creasey, W, Guinivan, P, and Illy, K. Review of the Literature on Herbicides, Including Phenoxy Herbicides and Associated Dioxins. US Department of Veterans Affairs VI Basic Studies Relevant to Health Effects. Induction of Cytochrome P450 and its Dependent Enzymes. 5-2-2002. Ventures, Inc.

56. Crofton, K. M. and Rice, D. C. (1999). Low-frequency hearing loss following perinatal exposure to 3,3',4,4',5-pentachlorobiphenyl (PCB 126) in rats. Neurotoxicol.Teratol. **21**, 299-301.

57. Cvetkovic, D., Pisarcik, D., Lee, C., Hamilton, T. C., and Abdollahi, A. (2004). Altered expression and loss of heterozygosity of the LOT1 gene in ovarian cancer. Gynecol.Oncol. **95**, 449-455.

58. Darnerud, P. O., Sinjari, T., and Jonsson, C. J. (1996). Foetal uptake of coplanar polychlorinated biphenyl (PCB) congeners in mice. Pharmacol Toxicol **78**, 187-192.

59. Davenport, J., Gonzalez, L., Hennies, R., and Hagquist, W. (1976). Severity and timing of early thyroid deficiency as factors in the induction of learning disorders in rats. Hor Behav **7**, 139-158.

60. Dean, C. E., Jr., Benjamin, S. A., Chubb, L. S., Tessari, J. D., and Keefe, T. J. (2002). Nonadditive hepatic tumor promoting effects by a mixture of two structurally different polychlorinated biphenyls in female rat livers. Toxicol.Sci. **66**, 54-61.

61. Degawa, M., Tanimura, S., Agatsuma, T., and Hashimoto, Y. (1989). Hepatocarcinogenic heterocyclic aromatic amines that induce cytochrome P-448 isozymes, mainly cytochrome P-448H (P-450IA2), responsible for mutagenic activation of the carcinogens in rat liver. Carcinogenesis **10**, 1119-1122.

62. DeGuise, S., Lagace, A., Beland, P., and et.al. (1995). Non-neoplastic lesions in beluga whales and other marine mammals form the St. Lawrence Estuary. J Comp Pathol **112**, 257-271.

63. delRio Gomez, I., Marshall, T., Tsai, P., Shao, Y. S., and Guo, Y. L. (2002). Number of boys born to men exposed to polychlorinated byphenyls. Lancet **360**, 143-144.

64. Denison, M. S., Fischer, R., and Whitlock, J. Inducible, receptor-dependent protein-DNA interactons at adioxin-responsive transcriptional enhancer. Proc.Natl.Acad.Sci.U.S.A 85, 2528-2532. 1988a.

65. Denison, M. S., Fisher, J, and Whitlock, J. The DNA recognition site for the dioxin-Ah receptor complex. Journal of Biological Chemistry 263, 17221-17224. 1988b.

66. Denison, M. S. and Nagy, S. R. (2003). Activation of the aryl hydrocarbon receptor by structurally diverse exogenous and endogenous chemicals. Annu.Rev.Pharmacol.Toxicol. **43**, 309-334.

67. Denison, M. S., Pandini, A., Nagy, S. R., Baldwin, E., and Bonati, L. (2002). Ligand binding and activation of the Ah receptor. Chem.Biol.Interact. **141**, 3-24.

68. DermNet New Zealand. New Zealand Dermatological Society Incorporated . 7-22-2004.

69. Desaulniers, D., Leingartner, K., Wade, M., Fintelman, E., Yagminas, A., and Foster, W. G. (1999). Effects of acute exposure to PCBs 126 and 153 on anterior pituitary and thyroid hormones and FSH isoforms in adult Sprague Dawley male rats. Toxicol.Sci. **47**, 158-169.

70. DeVito, M. J., Diliberto, J. J., Ross, D. G., Menache, M. G., and Birnbaum, L. S. (1997). Dose-response relationships for polyhalogenated dioxins and dibenzofurans following subchronic treatment in mice. I. CYP1A1 and CYP1A2 enzyme activity in liver, lung, and skin. Toxicol Appl.Pharmacol **147**, 267-280.

71. DeVito, M. J., Menache, M. G., Diliberto, J. J., Ross, D. G., and Birnbaum, L. S. (2000). Dose-response relationships for induction of CYP1A1 and CYP1A2 enzyme activity in liver, lung, and skin in female mice following subchronic exposure to polychlorinated biphenyls. Toxicol.Appl.Pharmacol. **167**, 157-172.

72. DeVito, M. J., Ross, D. G., Dupuy, A. E., Jr., Ferrario, J., McDaniel, D., and Birnbaum, L. S. (1998). Dose-response relationships for disposition and hepatic sequestration of polyhalogenated dibenzo-p-dioxins, dibenzofurans, and biphenyls following subchronic treatment in mice. Toxicol Sci. **46**, 223-234.

73. Diatchenko, L., Lau, Y. F., Campbell, A. P., Chenchik, A., Moqadam, F., Huang, B., Lukyanov, S., Lukyanov, K., Gurskaya, N., Sverdlov, E. D., and Siebert, P. D. (1996). Suppression subtractive hybridization: a method for generating differentially regulated or tissue-specific cDNA probes and libraries. Proc.Natl.Acad.Sci U.S.A **93**, 6025-6030.

74. Dolwick, K, Schmidt, H, and Bradfield, C. A. Cloning and expression of a human Ah receptor cDNA. Molecular Pharmacology 44, 911-917. 1993.

75. Doniger, SW, Salomonis, N, Dahlquist, KD, Vranizan, K, Lawlor, SC, and Conklin, BR. MAPPFinder: Using gene ontology and GenMAPP to create a global gene-expression profile from microarray data. Genome Biol 4(R7). 1-6-2003.

76. Dynal. Isolation of Nucleic Acids with Dynabeads. Dynal Biotech, LLC . 2004. 11-24-2004.

77. Enan, E. and Matsumura, F. (1996). Identification of c-Src as the integral component of the cytosolic Ah receptor complex, transducing the signal of 2,3,7,8-tetrachlorodibenzo-p-dioxin (TCDD) through the protein phosphorylation pathway. Biochem.Pharmacol. **52**, 1599-1612.

78. Engwall, M. and Hjelm, K. (2000). Uptake of dioxin-like compounds from sewage sludge into various plant species--assessment of levels using a sensitive bioassay. Chemosphere **40**, 1189-1195.

79. Eppig, J. Mouse nomenclature. Mouse Genome 91, 8. 1993.

80. Erickson, M. (1997). Analytical Chemistry of PCBs., Lewis Publishers, New York.

81. Eriksson, P. and Fredriksson, A. (1998). Neurotoxic effects in adult mice neonatally exposed to 3,3',4,4',5-pentachlorobiphenyl or 2,3,3',4,4'-pentachlorobiphenyl. Changes in brain nicotinic receptors and behaviour. Environ Toxicol Pharmacol **5**, 17-27.

82. Eriksson, P., Lundkvist, U., and Fredriksson, A. (1991). Neonatal exposure to 3,3',4,4'-tetrachlorobiphenyl: changes in spontaneous behaviour and cholinergic muscarinic receptors in the adult mouse. Toxicology **69**, 27-34.

83. Falahatpisheh, M. H. and Ramos, K. S. (2003). Ligand-activated Ahr signaling leads to disruption of nephrogenesis and altered Wilms' tumor suppressor mRNA splicing. Oncogene **22**, 2160-2171.

84. Faqi, A. S., Dalsenter, P. R., Merker, H. J., and Chahoud, I. (1998). Effects on developmental landmarks and reproductive capability of 3,3',4,4'-tetrachlorobiphenyl and 3,3',4,4',5-pentachlorobiphenyl in offspring of rats exposed during pregnancy. Hum.Exp.Toxicol. **17**, 365-372.

85. Fein, C., Jacobson, J., Schwartz, P., and Dowler, J. (1984). Prenatal exposure to polychlorinated biphenyls: effects on birth size and gestational age. J Pediatr **105**, 315-320.

86. Fernandez-Salguero, P., Hilbert, D. M., Rudikoff, S., Ward, J. M., and Gonzalez, F. J. (1996). Aryl-hydrocarbon receptor-deficient mice are resistant to 2,3,7,8-tetrachlorodibenzo-p-dioxin-induced toxicity. Toxicol.Appl.Pharmacol. **140**, 173-179.

87. Fernandez-Salguero, P., Pineau, T., Hilbert, D., McPhail, T., Lee, S. S., Kimura, S., Nebert, D. W., Rudikoff, S., Ward, J. M., and Gonzalez, F. J. (1995). Immune system impairment and hepatic fibrosis in mice lacking the dioxin-binding Ah receptor. Science **268**, 722-726.

88. Finley, W., Faux, S., Hutchenson, C., and Amstutz, L. (1985). Long-latency event-related potentials in the evaluation of cognitive function in children. Neurology **35**, 323-327.

89. Flodstrom, S and Ahlborg, U. G. Relative liver tumor promoting activity of some polychlorinated dibenzo-p-dioxin-, dibenzofuran- and biphenyl-congeners in female rats. Chemosphere 25, 169. 1992.

90. Focant, J. F., Pirard, C., Massart, A. C., and De Pauw, E. (2003). Survey of commercial pasteurised cows' milk in Wallonia (Belgium) for the occurrence of polychlorinated dibenzo-p-dioxins, dibenzofurans and coplanar polychlorinated biphenyls. Chemosphere **52**, 725-733.

91. Focant, J. F., Pirard, C., Thielen, C., and De Pauw, E. (2002). Levels and profiles of PCDDs, PCDFs and cPCBs in Belgian breast milk. Estimation of infant intake. Chemosphere **48**, 763-770.

92. Frame, G., Cochran, J., and Boewadt, S. (1996). Complete PCB congener distributions for 17 Aroclor mixtures determined by 3 HRGC systems optimized for comprehensive, quantitative, congener-specific analysis. J High Resol Chromatogr **19**, 657-688.

93. French, C. T., Hanneman, W. H., Chubb, L. S., Billings, R. E., and Andersen, M. E. (2004). Induction of CYP1A1 in Primary Rat Hepatocytes by 3,3',4,4',5-Pentachlorobiphenyl: Evidence for a Switch Circuit Element. Toxicol.Sci. **78**, 276-286.

94. Fulle, S., Pietrangelo, T., Mariggio, M. A., Lorenzon, P., Racanicchi, L., Mozrzymas, J., Guarnieri, S., Zucconi-Grassi, G., and Fano, G. (2000). Calcium and fos involvement in brain-derived Ca(2+)-binding protein (S100)-dependent apoptosis in rat phaeochromocytoma cells. Exp.Physiol **85**, 243-253.

95. Gale, R, Long, E, Schwartz, T, and Tillitt, D. E. Evaluation of planar halogenated and polycyclic halogenated and polycyclic aromatic hydrocarbons in estuarine sediments using ethoxyresorufin-O-deethylase induction of H4IIE cells. Environ Toxicol Chem 19, 1348-1359. 2000.

96. Gasiewicz,T. and Park,S. (2003). Ah Receptor: Involvement in toxic responses. In Dioxin and Health (A.Schecter and T.Gasiewicz, Eds.), pp. 491-532. John Wiley and Sons, Inc., Hoboken, NJ.

97. Geng, J. and Strobel, H. W. (1993). Identification of cytochromes P450, 1A2, 2A1, 2C7, 2E1 in rat glioma C6 cell line by RT-PCR and specific restriction enzyme digestion. Biochemical and Biophysical Research Communications **197**, 1179-1184.

98. Geng, J. and Strobel, H. W. (1995). Identification of inducible mixed function oxidase system in rat glioma C6 cell line. Journal of Neurochemistry **65**, 554-563.

99. Geng, J. and Strobel, H. W. (1998). Expression, induction and regulation of the cytochrome P450 monooxygenase system in the rat glioma C6 cell line. Brain Research **784**, 276-283.

100. Gibbs, R. A., Weinstock, G. M., Metzker, M. L., Muzny, D. M., Sodergren, E. J., Scherer, S., Scott, G., Steffen, D., Worley, K. C., and et al. (2004). Genome sequence of the Brown Norway rat yields insights into mammalian evolution. Nature **428**, 493-521.

101. Glynn, A, Atuma, S. S, Aune, M, Darnerud, P, Conney, A, and Cnattingius, S. Polychlorinated Biphenyl Congeners as Markers of Toxic Equivalents of Polychlorinated Biphenyls, Dibenzo- p-dioxins and Dibenzofurans in Breast Milk. Environmental Research Section A **86**, 217-288. 2001.

102. Goldey, E. S. and Crofton, K. M. (1998). Thyroxine replacement attenuates hypothyroxinemia, hearing loss, and motor deficits following developmental exposure to Aroclor 1254 in rats. Toxicol.Sci. **45**, 94-105.

103. Gottlicher, M., Minucci, S., Zhu, P., Kramer, O. H., Schimpf, A., Giavara, S., Sleeman, J. P., Lo, C. F., Nervi, C., Pelicci, P. G., and Heinzel, T. (2001). Valproic acid defines a novel class of HDAC inhibitors inducing differentiation of transformed cells. EMBO J **20**, 6969-6978.

104. Green, M. Nomenclature of genetically determined biochemical variants in mice. Biochemical Genetics 9, 369-374. 1973.

105. Greizerstein, H. B., Stinson, C., Mendola, P., Buck, G. M., Kostyniak, P. J., and Vena, J. E. (1999). Comparison of PCB congeners and pesticide levels between serum and milk from lactating women. Environ.Res. **80**, 280-286.

106. Guo, Y. L., Chen, Y., Yu, M., and Hsu, C. (1994). Early development of children prenatally exposed to heat-degraded PCBs born seven to twelve years after mothers' poisoning. Chemosphere **29**, 2395-2404.

107. Guo, Y. L., Hsu, C., Hsu, P., and Lambert, G. H. (2000). Sperm changes in humans prenatally exposed to polychlorinated biphenyls and dibenzofurans. Lancet **356**, 1240-1241.

108. Guo, Y. L., Lai, T. J., Chen, S. J., and Hsu, C. C. (1995). Gender-related decrease in Raven's progressive matrices scores in children prenatally exposed to polychlorinated biphenyls and related contaminants. Bull.Environ.Contam Toxicol. **55**, 8-13.

109. Guo, Y. L., Lambert, G. H., Hsu, C. C., and Hsu, M. M. (2004). Yucheng: health effects of prenatal exposure to polychlorinated biphenyls and dibenzofurans. Int.Arch.Occup.Environ.Health **77**, 153-158.

110. Gustavsson, P. and Hogstedt, C. (1997). A cohort study of Swedish capacitor manufacturing workers exposed to polychlorinated biphenyls (PCBs). Am.J.Ind.Med. **32**, 234-239.

111. Halliwell, B. (1994). Free radicals, antioxidants and human disease: Curiosity, cause, or consequence. Lancet **344**, 721-724.

112. Hanberg, A., Stahlberg, M., Georgellis, A., de Wit, C., and Ahlborg, U. G. (1991). Swedish dioxin survey: evaluation of the H-4-II E bioassay for screening environmental samples for dioxin-like enzyme induction. Pharmacol.Toxicol **69**, 442-449.

113. Hankinson, O. (1995). The aryl hydrocarbon receptor complex. Annu.Rev.Pharmacol.Toxicol. **35**, 307-340.

114. Hanneman, W. H., Legare, M. E., Tiffany-Castiglioni, E., and Safe, S. H. (1996). The need for cellular, biochemical, and mechanistic studies. Neurotoxicol.Teratol. **18**, 247-250.

115. Harper, N., Connor, K., Steinberg, M., and Safe, S. (1994). An enzyme-linked immunosorbent assay (ELISA) specific for antibodies to TNP-LPS detects alterations in serum immunoglobulins and isotype switching in C57BL/6 and DBA/2 mice exposed to 2,3,7,8-tetrachlorodibenzo-p-dioxin and related compounds. Toxicology **92**, 155-167.

116. Harries, H. M., Fletcher, S. T., Duggan, C. M., and Baker, V. A. (2001). The use of genomics technology to investigate gene expression changes in cultured human liver cells. Toxicol.In Vitro **15**, 399-405.

117. Hassoun, E. A., Li, F., Abushaban, A., and Stohs, S. J. (2000). The relative abilities of TCDD and its congeners to induce oxidative stress in the hepatic and brain tissues of rats after subchronic exposure. Toxicology **145**, 103-113.

118. Hassoun, E. A., Li, F., Abushaban, A., and Stohs, S. J. (2001). Production of superoxide anion, lipid peroxidation and DNA damage in the hepatic and brain tissues of rats after subchronic exposure to mixtures of TCDD and its congeners. J.Appl.Toxicol **21**, 211-219.

119. Hassoun, E. A., Wang, H., Abushaban, A., and Stohs, S. J. (2002). Induction of oxidative stress in the tissues of rats after chronic exposure to TCDD, 2,3,4,7,8-pentachlorodibenzofuran, and 3,3',4,4',5-pentachlorobiphenyl. J.Toxicol.Environ.Health A **65**, 825-842.

120. Hay, A. and Tarrel, J. (1997). Mortality of power workers exposed to phenoxy herbicides and polychlorinated biphenyls in waste transformer oil. Ann.N.Y.Acad.Sci. **837**, 138-156.

121. Hemming, H., Bager, Y., Flodstrom, S., Nordgren, I., Kronevi, T., Ahlborg, U. G., and Warngard, L. (1995). Liver tumour promoting activity of 3,4,5,3',4'-pentachlorobiphenyl and its interaction with 2,3,7,8-tetrachlorodibenzo-p-dioxin. Eur.J.Pharmacol. **292**, 241-249.

122. Hemming, H., Flodstrom, S., Warngard, L., Bergman, A., Kronevi, T., Nordgren, I., and Ahlborg, U. G. (1993). Relative tumour promoting activity of three polychlorinated biphenyls in rat liver. Eur.J.Pharmacol. **248**, 163-174.

123. Hennig, B., Meerarani, P., Slim, R., Toborek, M., Daugherty, A., Silverstone, A. E., and Robertson, L. W. (2002). Proinflammatory properties of coplanar PCBs: in vitro and in vivo evidence. Toxicol Appl.Pharmacol **181**, 174-183.

124. Herr, D., Goldey, E. S., and Crofton, K. M. (1996). Developmental exposure to Aroclor 1254 produces low-frequency alterations in adult rat bainstem auditory evoked responses. Fundam.Appl.Toxicol. **33**, 120-128.

125. Holene, E., Nafstad, I., Skaare, J., Bernhoft, A., Engen, P., and Sagvolden, T. (1995). Behavioral effects of pre- and postnatal exposure to individual polychlorinated biphenyl congeners in rats. Environ.Toxicol.Chem. **14**, 967-976.

126. Holene, E., Nafstad, I., Skaare, J. U., and Sagvolden, T. (1998). Behavioural hyperactivity in rats following postnatal exposure to sub-toxic doses of polychlorinated biphenyl congeners 153 and 126. Behav.Brain Res. **94**, 213-224.

127. Hollingshead, B. D., Petrulis, J. R., and Perdew, G. H. (2004). The Ah receptor transcriptional regulator XAP2 antagonizes p23 binding to Ah receptor/Hsp90 complexes and is dispensable for receptor function. J.Biol.Chem.

128. Hough, C. D., Sherman-Baust, C. A., Pizer, E. S., Montz, F. J., Im, D. D., Rosenshein, N. B., Cho, K. R., Riggins, G. J., and Morin, P. J. (2000). Large-scale serial analysis of gene expression reveals genes differentially expressed in ovarian cancer. Cancer Res. **60**, 6281-6287.

129. Hsu, S.-T., Ma, C.-I., Hsu, S.-H., Wu, S.-S., Hsu, N.-M., Yeh, C.-C., and Wu, S.-B. (1985). Discover and epidemiology of PCB poisoning in Taiwan: A four-year followup. Environ.Health Perspect. **59**, 5-10.

130. Hu, J., Castets, F., Guevara, J. L., and Van Eldik, L. J. (1996). S100 beta stimulates inducible nitric oxide synthase activity and mRNA levels in rat cortical astrocytes. J Biol.Chem **271**, 2543-2547.

131. Hu, J., Ferreira, A., and Van Eldik, L. J. (1997). S100beta induces neuronal cell death through nitric oxide release from astrocytes. J Neurochem. **69**, 2294-2301.

132. Huttunen, H. J., Kuja-Panula, J., Sorci, G., Agneletti, A. L., Donato, R., and Rauvala, H. (2000). Coregulation of neurite outgrowth and cell survival by amphoterin and S100 proteins through receptor for advanced glycation end products (RAGE) activation. J Biol.Chem **275**, 40096-40105.

133. Invitrogen (2003a). I-SAGE Long laboratory kit manual for constructing SAGE libraries, Invitrogen Life Technologies, Inc., Carlsbad, CA.

134. Invitrogen. SAGE2000 Software for the analysis of SAGE. (Serial Analysis of Gene Expression) and Long SAGE tags. (4.5E). 7-14-2003b.

135. Jacobson, J. L., Fein, G. G., Jacobson, S. W., Schwartz, P. M., and Dowler, J. K. (1984). The transfer of polychlorinated biphenyls (PCBs) and polybrominated biphenyls (PBBs) across the human placenta and into maternal milk. Am J Public Health **74**, 378-379.

136. Jacobson, J. L., Jacobson, S. W., and Humphrey, H. E. (1990). Effects of in utero exposure to polychlorinated biphenyls and related contaminants on cognitive functioning in young children. J Pediatr. **116**, 38-45.

137. Jaffe, A., Ogura, T., and Hiraga, S. (1985). Effects of the ccd function of the F plasmid on bacterial growth. J.Bacteriol. **163**, 841-849.

138. Jin, X., Kennedy, S. W., Di Muccio, T., and Moon, T. W. (2001). Role of oxidative stress and antioxidant defense in 3,3',4,4',5-pentachlorobiphenyl-induced toxicity and species-differential sensitivity in chicken and duck embryos. Toxicol.Appl.Pharmacol. **172**, 241-248.

139. Johnson, C. D., Balagurunathan, Y., Tadesse, M. G., Falahatpisheh, M. H., Brun, M., Walker, M. K., Dougherty, E. R., and Ramos, K. S. (2004). Unraveling gene-gene interactions regulated by ligands of the aryl hydrocarbon receptor. Environ.Health Perspect. **112**, 403-412.

140. Jokinen, M. P., Walker, N. J., Brix, A. E., Sells, D. M., Haseman, J. K., and Nyska, A. (2003). Increase in cardiovascular pathology in female Sprague-Dawley rats following chronic treatment with 2,3,7,8-tetrachlorodibenzo-p-dioxin and 3,3',4,4',5-pentachlorobiphenyl. Cardiovasc.Toxicol. **3**, 299-310.

141. Jones, K. and Whitlock, J. (1990). Functional analysis of the transcriptional promoter for the CYP1A1 gene. Molecular and Cellular Biology **10**, 5098-5105.

142. Kannan, N., Tanabe, S., Wakimoto, T., and Tatsukawa, R. (1987). Coplanar polychlorinated biphenyls in Aroclor and Kanechlor mixtures. J.Assoc.Off.Anal.Chemists **70**, 451-454.

143. Karoui, H., Bex, F., Dreze, P., and Couturier, M. (1983). Ham22, a mini-F mutation which is lethal to host cell and promotes recA-dependent induction of lambdoid prophage. EMBO J. **2**, 1863-1868.

144. Kashimoto, T., Miyata, H., Takayama, K., and Ogaki, J. (1987). [Levels of PCDDs, coplanar PCBs and PCDFs in patients with yusho and the causal oil by HR-GC.HR-MS]. Fukuoka Igaku Zasshi **78**, 325-336.

145. Kimbrough, R. D. (1995). Polychlorinated biphenyls (PCBs) and human health: an update. Crit Rev.Toxicol. **25**, 133-163.

146. Klaunig, J. E. and Kamendulis, L. M. (2004). The role of oxidative stress in carcinogenesis. Annu.Rev.Pharmacol Toxicol **44**, 239-267.

147. Kligman, D. and Marshak, D. R. (1985). Purification and characterization of a neurite extension factor from bovine brain. Proc.Natl.Acad.Sci U.S.A **82**, 7136-7139.

148. Kodavanti, P. R., Shin, D. S., Tilson, H. A., and Harry, G. J. (1993). Comparative effects of two polychlorinated biphenyl congeners on calcium homeostasis in rat cerebellar granule cells. Toxicol.Appl.Pharmacol. **123**, 97-106.

149. Koga, N., Beppu, M., and Yoshimura, H. (1990). Metabolism in vivo of 3,4,5,3',4'-pentachlorobiphenyl and toxicological assessment of the metabolite in rats. J.Pharmacobiodyn. **13**, 497-506.

150. Komurasaki, T., Toyoda, H., Uchida, D., and Nemoto, N. (2002). Mechanism of growth promoting activity of epiregulin in primary cultures of rat hepatocytes. Growth Factors **20**, 61-69.

151. Koopman-Esseboom, C., Huisman, M., Touwen, B. C., Boersma, E. R., Brouwer, A., Sauer, P. J., and Weisglas-Kuperus, N. (1997). Newborn infants diagnosed as neurologically abnormal with relation to PCB and dioxin exposure and their thyroid-hormone status. Dev.Med.Child Neurol. **39**, 785.

152. Kostyniak, P. J., Stinson, C., Greizerstein, H. B., Vena, J., Buck, G., and Mendola, P. (1999). Relation of Lake Ontario fish consumption, lifetime lactation, and parity to breast milk polychlorobiphenyl and pesticide concentrations. Environ.Res. **80**, S166-S174.

153. Krishnan, V and Safe, S. Polychlorinated biphenyls (PCBs), dibenzo-p-dioxins (PCDDs), and dibenzofurans (PCDFs) as antiestrogens in MCF-7 human breast cancer cells: Quantitative structure-activity relationship. Toxicology and Applied Pharmacology 120, 55-61. 1993.

154. Kultima, K., Nystrom, A. M., Scholz, B., Gustafson, A. L., Dencker, L., and Stigson, M. (2004). Valproic acid teratogenicity: a toxicogenomics approach. Environ Health Perspect **112**, 1225-1235.

155. Kuratsune, M., Morikwa, Y., Hiroshita, T., Nishizumi, M., Kohchi, S., Yoshimura, T., Matsuzaki, J., Yamaguchi, A., Saruta, N., Ishinishi, N., Kunitake, E., Shimono, O., Takigawa, K., Oki, K., Sonoda, M., Ueda, T., and Ogata, M. (1969). An epidemiologic study on "Yusho" or chlorobiphenyls poisoning. Fukuoka Igaku Zasshi **60**, 513-532.

156. Lahvis, G., Lindell, S., McCuskey, R., Murphy, C., Glover, E., Bentz, M., Southard, J., and Bradfield, C. A. (2000). Portosystemic shunts and persistent fetal vascular structures in Ah-receptor deficient mice. Proc.Natl.Acad.Sci.U.S.A **97**, 10442-10447.

157. Lan, S., Yen, Y., Yang, C., Yang, C., and Chen, E. (1987). A study of the birth weight of transplacental Yu-Cheng babies (in Chinese with English summary). Kaohsiung J Med Sci **3**, 273-282.

158. Langley, B., Gensert, J. M., Beal, M. F., and Ratan, R. R. (2005). Remodeling chromatin and stress resistance in the central nervous system: histone deacetylase inhibitors as novel and broadly effective neuroprotective agents. Curr.Drug Targets.CNS.Neurol.Disord. **4**, 41-50.

159. Lee, K., Kentroti, S., Billie, H., Bruce, C., and Vernadakis, A. (1992). Comparative biochemical, morphological, and immunocytochemical studies between C-6 glial cells of early and late passages and advanced passages of glial cells derived from aged mouse cerebral hemispheres. Glia **6**, 245-257.

160. Lee, S. K., Ou, Y. C., and Yang, R. S. (2002). Comparison of pharmacokinetic interactions and physiologically based pharmacokinetic modeling of PCB 153 and PCB 126 in nonpregnant mice, lactating mice, and suckling pups. Toxicol.Sci. **65**, 26-34.

161. Leece, B., Denomme, M. A., Towner, R., Li, S. M., and Safe, S. (1985). Polychlorinated biphenyls: correlation between in vivo and in vitro quantitative structure-activity relationships (QSARs). J.Toxicol.Environ.Health **16**, 379-388.

162. Leegwater, P, van Driel, W, and van der Vliet, P. Recognition site of nuclear factor I, a sequence-specific DNA-binding protein from HeLa cells that stimulates adenovirus DNA replication. The EMBO Journal 4, 1515-1521. 1985.

163. Li, W., Wu, W. Z., Barbara, R. B., Schramm, K. W., and Kettrup, A. (1999). A new enzyme immunoassay for PCDD/F TEQ screening in environmental samples: comparison to micro-EROD assay and to chemical analysis. Chemosphere **38**, 3313-3318.

164. Lilienthal, H., Neuf, M., Munoz, C., and Winneke, G. (1990). Behavioral effects of pre- and postnatal exposure to a mixture of low chlorinated PCBs in rats. Fundam.Appl.Toxicol. **15**, 457-467.

165. Lind, P. M., Eriksen, E. F., Sahlin, L., Edlund, M., and Orberg, J. (1999). Effects of the antiestrogenic environmental pollutant 3,3',4,4', 5-pentachlorobiphenyl (PCB #126) in rat bone and uterus: diverging effects in ovariectomized and intact animals. Toxicol.Appl.Pharmacol. **154**, 236-244.

166. Lind, P. M., Larsson, S., Johansson, S., Melhus, H., Wikstrom, M., Lindhe, O., and Orberg, J. (2000a). Bone tissue composition, dimensions and strength in female rats given an increased dietary level of vitamin A or exposed to 3,3',4, 4',5-pentachlorobiphenyl (PCB126) alone or in combination with vitamin C. Toxicology **151**, 11-23.

167. Lind, P. M., Larsson, S., Oxlund, H., Hakansson, H., Nyberg, K., Eklund, T., and Orberg, J. (2000b). Change of bone tissue composition and impaired bone strength in rats exposed to 3,3',4,4',5-pentachlorobiphenyl (PCB126). Toxicology **150**, 41-51.

168. Lind, P. M., Orberg, J., Edlund, U. B., Sjoblom, L., and Lind, L. (2004). The dioxin-like pollutant PCB 126 (3,3',4,4',5-pentachlorobiphenyl) affects risk factors for cardiovascular disease in female rats. Toxicol.Lett. **150**, 293-299.

169. Link, B., Gabrio, T., Zoellner, I., Piechotowski, I., Paepke, O., Herrmann, T., Felder-Kennel, A., Maisner, V., Schick, K. H., Schrimpf, M., Schwenk, M., and Wuthe, J. (2005). Biomonitoring of persistent organochlorine pesticides, PCDD/PCDFs and dioxin-like PCBs in blood of children from South West Germany (Baden-Wuerttemberg) from 1993 to 2003. Chemosphere **58**, 1185-1201.

170. Llobet, J. M., Bocio, A., Domingo, J. L., Teixido, A., Casas, C., and Muller, L. (2003). Levels of polychlorinated biphenyls in foods from Catalonia, Spain: estimated dietary intake. J Food Prot. **66**, 479-484.

171. Lowenfels, A. B., Maisonneuve, P., and Lankisch, P. G. (1999). Chronic pancreatitis and other risk factors for pancreatic cancer. Gastroenterol.Clin.North Am **28**, 673-85, x.

172. Lu, Y. and Lotan, R. (1999). Transcriptional regulation by butyrate of mouse galectin-1 gene in embryonal carcinoma cells. Biochim.Biophys.Acta **1444**, 85-91.

173. Lyche, J. L., Skaare, J. U., Larsen, H. J., and Ropstad, E. (2004). Levels of PCB 126 and PCB 153 in plasma and tissues in goats exposed during gestation and lactation. Chemosphere **55**, 621-629.

174. Maier, W., Kodavanti, P. R., Harry, G. J., and Tilson, H. A. (1994). Sensitivity of adenosine triphosphatases in different brain regions to polychlorinated biphenyl congeners. J Appl Toxicol **14**, 225-229.

175. Mariggio, M. A., Fulle, S., Calissano, P., Nicoletti, I., and Fano, G. (1994). The brain protein S-100ab induces apoptosis in PC12 cells. Neuroscience **60**, 29-35.

176. Mathupala, S. P. and Sloan, A. E. "In-gel" purified ditags direct synthesis of highly efficient SAGE libraries. BMC Genomics 3(20), URL. 2002.

177. Matsumura, F. (1994). How important is the protein phosphorylation pathway in the toxic expression of dioxin-type chemicals? Biochem.Pharmacol. **48**, 215-224.

178. Mayura, K., Spainhour, C. B., Howie, L., Safe, S., and Phillips, T. D. (1993). Teratogenicity and immunotoxicity of 3,3',4,4',5-pentachlorobiphenyl in C57BL/6 mice. Toxicology **77**, 123-131.

179. Michnovicz, J. J. and Bradlow, H. L. (1991). Altered estrogen metabolism and excretion in humans following consumption of indole-3-carbinol. Nutr.Cancer **16**, 59-66.

180. Micka, J., Milatovich, A., Menon, A., Grabowski, G. A., Puga, A., and Nebert, D. W. (1997). Human Ah receptor (AHR) gene: localization to 7p15 and suggestive correlation of polymorphism with CYP1A1 inducibility. Pharmacogenetics **7**, 95-101.

181. Miki, T., Yoshioka, K., and Horiuchi, T. (1984). Control of cell division by sex factor F in Escherichia coli. I. The 42.84-43.6 F segment couples cell division of the host bacteria with replication of plasmid DNA. J.Mol.Biol. **174**, 605-625.

182. Miller, C. P. and Birnbaum, L. S. (1986). Teratologic evaluation of hexabrominated naphthalenes in C57BL/6N mice. Fundam.Appl.Toxicol. **7**, 398-405.

183. Mimura, J., Yamashita, K., Nakamura, K., Morita, M., Takagi, T. N., Nakao, K., Ema, M., Sogawa, K., Yasuda, M., Katsuki, M., and Fujii-Kuriyama, Y. (1997). Loss of teratogenic response to 2,3,7,8-tetrachlorodibenzo-p-dioxin (TCDD) in mice lacking the Ah (dioxin) receptor. Genes Cells **2**, 645-654.

184. Moore, R, Bergman, A., Rudy, T, and Peterson, R. E. Effects of PCB 153, PCB 105, and PCB 126 on development of the male reproductive system in rats. Toxicologist 42(1-S), 135. 1998.

185. Moses, M., Lilis, R., and Crow, K. (1984). Health status of workers with past exposure to2,3,7,8-tetrachlorodibenzo-p-dioxin in the manufacture of 2,4,5-trichlorophenoxyacetic acid: Comparison offindings with and without chloracne. American Journal of Industrial Medicine **5**, 161-182.

186. Muangmoonchai, R., Smirlis, D., Wong, S. C., Edwards, M., Phillips, I. R., and Shephard, E. A. (2001). Xenobiotic induction of cytochrome P450 2B1 (CYP2B1) is mediated by the orphan nuclear receptor constitutive androstane receptor (CAR) and requires steroid co-activator 1 (SRC-1) and the transcription factor Sp1. Biochem.J. **355**, 71-78.

187. Mundy, W. R., Shafer, T. J., Tilson, H. A., and Kodavanti, P. R. (1999). Extracellular calcium is required for the polychlorinated biphenyl-induced increase of intracellular free calcium levels in cerebellar granule cell culture. Toxicology **136**, 27-39.

188. Muto, T., Wakui, S., Imano, N., Nakaaki, K., Takahashi, H., Hano, H., Furusato, M., and Masaoka, T. (2002). Mammary gland differentiation in female rats after prenatal exposure to 3,3',4,4',5-pentachlorobiphenyl. Toxicology **177**, 197-205.

189. Naftolin, f. (1994). Brain aromatization of androgens. Journal of Reproductive Medicine **39**, 257-261.

190. NCEH. Second national report on human exposure to environmental chemicals. NCEH 02-0716, 117. 2003. Atlanta, GA, National Center for Environmental Health, Centers for Disease Control and Prevention.

191. Nebert, D. W. (1989). The Ah locus: genetic differences in toxicity, cancer, mutation, and birth defects. Crit Rev.Toxicol. **20**, 153-174.

192. Needham, L. L., Gerthoux, P. M., Patterson, D. G., Jr., Brambilla, P., Turner, W. E., Beretta, C., Pirkle, J. L., Colombo, L., Sampson, E. J., Tramacere, P. L., Signorini, S., Meazza, L., Carreri, V., Jackson, R. J., and Mocarelli, P. (1997). Serum dioxin levels in Seveso, Italy, population in 1976. Teratog.Carcinog.Mutagen. **17**, 225-240.

193. Niwa, A., Kumaki, K., and Nebert, D. W. (1975). Molecular Pharmacology **11**, 399-408.

194. NTP. DRAFT technical report. Toxicology and Carcinogenesis Studies of 3,3',4,4',5-Pentachlorobiphenyl (PCB 126) (CAS No. 57465-28-8) in Female Harlan Sprague-Dawley Rats (Gavage Studies). National Toxicology Program, Technical Report 520 (Draft). 2004. Research Triangle Park, NC.

195. Nyska, A., Jokinen, M. P., Brix, A. E., Sells, D. M., Wyde, M. E., Orzech, D., Haseman, J., Flake, G., and Walker, N. J. (2004). Exocrine pancreatic pathology in female Harlan Sprague-Dawley rats after chronic treatment with 2,3,7,8-tetrachlorodibenzo-p-dioxin and dioxin-like compounds. Environ Health Perspect. **112**, 903-909.

196. Ogura, T. and Hiraga, S. (1983). Mini-F plasmid genes that couple host cell division to plasmid proliferation. Proc.Natl.Acad.Sci.U.S.A **80**, 4784-4788.

197. Okamoto, H., Yasui, K., Zhao, C., Arii, S., and Inazawa, J. (2003). PTK2 and EIF3S3 genes may be amplification targets at 8q23-q24 and are associated with large hepatocellular carcinomas. Hepatology **38**, 1242-1249.

198. Okey, A. B., Riddick, D. S., and Harper, P. A. (1994). The Ah receptor: mediator of the toxicity of 2,3,7,8-tetrachlorodibenzo-p-dioxin (TCDD) and related compounds. Toxicol.Lett. **70**, 1-22.

199. Okino, S. and Whitlock, J. (1995). Dioxin induces localized, graded changes in chromatin structure: implications for Cyp1A1 gene transcription. Molecular and Cellular Biology **15**, 3714-3721.

200. Ozawa, N., Yoshihara, S., Kawano, K., Okada, Y., and Yoshimura, H. (1979). 3,4,5,3',4'-Pentachlorobiphenyl as a useful inducer for purification of rat liver microsomal cytochrome P448. Biochem.Biophys.Res.Commun. **91**, 1140-1147.

201. Pantaleoni, G. C., Fanini, D., Sponta, A. M., Palumbo, G., Giorgi, R., and Adams, P. M. (1988). Effects of maternal exposure to polychlorobiphenyls (PCBs) on F1 generation behavior in the rat. Fundam.Appl.Toxicol. **11**, 440-449.

202. Pasanen, T., Saarela, J., Saarikko, I., Toivanen, T., Tolvanen, M., Vihinen, M., and Wong, G. (2003). DNA microarray data analysis, CSC - Scientific Computing Ltd, Helsinki.

203. PCB Steering Group. Interim implementaton plan for phase 2 of the multilateral cooperative project for phase-out of PCB use, and management of PCB-contaminated wastes in the Russian Federation. AMAP WG Doc 14/4/3-Add. 1. 2000. Moscow, Arctic Council.

204. Petrulis, J. R. and Bunce, N. J. (1999). Competitive inhibition by inducer as a confounding factor in the use of the ethoxyresorufin-O-deethylase (EROD) assay to estimate exposure to dioxin-like compounds. Toxicol Lett. **105**, 251-260.

205. Pierreux, C. E., Vanhorenbeeck, V., Jacquemin, P., Lemaigre, F. P., and Rousseau, G. G. (2004). The transcription factor hepatocyte nuclear factor-6/Onecut-1 controls the expression of its paralog Onecut-3 in developing mouse endoderm. J Biol.Chem **279**, 51298-51304.

206. Pitot, H. C. and Dragan, Y. P. (1993). Stage of tumor progression, progressor agents, and human risk. Proc.Soc.Exp.Biol.Med. **202**, 37-43.

207. Pitot, H. C., Peraino, C., Morse, P., and Potter, V. (1964). National Cancer Institute Monograph **13**, 229-245.

208. Pohl, H., Lados, F., Ingeman, L., Cunningham, P., Raymer, J., Wall, C., Gasiewics, T., and De Rosa, C. (2000). ATSDR Evaluation of Health Effects of Chemicals VII Chlorinated dibenzo-p-dioxins. Toxicol.Ind.Health **16**, 1-201.

209. Poland, A, Glover, E, and Kende, A. Stereospecific, high affinity binding of 2,3,7,8-tetrachlorodibenzo-*p*-dioxin by hepatic cytosol: evidence that the binding species is the receptor for induction of aryl hydrocarbon hydroxylase. Journal of Biological Chemistry 251, 4936-4946. 1976.

210. Poland, A, Glover, E, and Kende, A. Photoaffinity labeling of the Ah receptor. Journal of Biological Chemistry 261, 6352-6365. 1986.

211. Poland, A, Palen, D, and Glover, E. Analysis of the four alleles of the mutrine aryl hydrocarbon receptor. Molecular Pharmacology 46, 915-921. 1994.

212. Poland, A. and Knutson, J. C. (1982). 2,3,7,8-tetrachlorodibenzo-p-dioxin and related halogenated aromatic hydrocarbons: examination of the mechanism of toxicity. Annu.Rev.Pharmacol.Toxicol. **22**, 517-554.

213. Pollenz, R. S., Santostefano, M. J., Klett, E., Richardson, V. M., Necela, B., and Birnbaum, L. S. (1998). Female Sprague-Dawley rats exposed to a single oral dose of 2,3,7,8-tetrachlorodibenzo-p-dioxin exhibit sustained depletion of aryl hydrocarbon receptor protein in liver, spleen, thymus, and lung. Toxicol.Sci. **42**, 117-128.

214. Pongratz, I, Mason, G, and Poellinger, L. Dual roles of the 90 kDa heat shock protein Hsp 90 in modulating functional activities of the dioxin receptor. Journal of Biological Chemistry 267, 13728-13734. 1992.

215. Powell, J. (1998). Enhanced concatemer cloning-a modification to the SAGE (Serial Analysis of Gene Expression) technique. Nucleic Acids Res. **26**, 3445-3446.

216. Powell, J. (2000). SAGE. The serial analysis of gene expression. Methods Mol.Biol. **99**, 297-319.

217. Qin, H. and Powell-Coffman, J. A. (2004). The Caenorhabditis elegans aryl hydrocarbon receptor, AHR-1, regulates neuronal development. Dev.Biol. **270**, 64-75.

218. Ramos,K.S., Melchert,R.B., Chacon,E., and Acousta,D. (2001). Toxic responses of the heart and vascular systems. In Casarett and Doull's Toxicology: The Basic Science fo Poisons (C.D.Klaassen, Ed.), pp. 607-608. McGraw-Hill, Medical Publishing, New York.

219. Render, J. A., Aulerich, R. J., Bursian, S. J., and Nachreiner, R. F. (2000a). Proliferation of maxillary and mandibular periodontal squamous cells in mink fed 3,3',4,4',5-pentachlorobiphenyl (PCB 126). J.Vet.Diagn.Invest **12**, 477-479.

220. Render, J. A., Aulerich, R. J., Bursian, S. J., and Nachreiner, R. F. (2000b). Proliferation of maxillary and mandibular periodontal squamous cells in mink fed 3,3',4,4',5-pentachlorobiphenyl (PCB 126). J.Vet.Diagn.Invest **12**, 477-479.

221. Render, J. A., Bursian, S. J., Rosenstein, D. S., and Aulerich, R. J. (2001). Squamous epithelial proliferation in the jaws of mink fed diets containing 3,3',4,4',5-pentachlorobiphenyl (PCB 126) or 2,3,7,8-tetrachlorodibenzo-P-dioxin (TCDD). Vet.Hum.Toxicol. **43**, 22-26.

222. Rice, D. C. (1999). Effect of exposure to 3,3',4,4',5-pentachlorobiphenyl (PCB 126) throughout gestation and lactation on development and spatial delayed alternation performance in rats. Neurotoxicol.Teratol. **21**, 59-69.

223. Rice, D. C. and Hayward, S. (1998). Lack of effect of 3,3'4,4',5-pentachlorobiphenyl (PCB 126) throughout gestation and lactation on multiple fixed interval-fixed ratio and DRL performance in rats. Neurotoxicol.Teratol. **20**, 645-650.

224. Rice, D. C. and Hayward, S. (1999). Effects of exposure to 3,3',4,4',5-pentachlorobiphenyl (PCB 126) throughout gestation and lactation on behavior (concurrent random interval-random interval and progressive ratio performance) in rats. Neurotoxicol.Teratol. **21**, 679-687.

225. Roberts, R. J. and Halford, S. E. (1993). Nucleases, pp. 35-88. Cold Spring Harbor Laboratory Press, Cold Spring Harbor, NY.

226. Roman, B. L., Pollenz, R. S., and Peterson, R. E. (1998). Responsiveness of the adult male rat reproductive tract to 2,3,7,8-tetrachlorodibenzo-p-dioxin exposure: Ah receptor and ARNT expression, CYP1A1 induction, and Ah receptor down-regulation. Toxicol.Appl.Pharmacol. **150**, 228-239.

227. Ryan, J. J., Levesque, D., Panopio, L. G., Sun, W. F., Masuda, Y., and Kuroki, H. (1993). Elimination of polychlorinated dibenzofurans (PCDFs) and polychlorinated biphenyls (PCBs) from human blood in the Yusho and Yu-Cheng rice oil poisonings. Arch.Environ Contam Toxicol **24**, 504-512.

228. Saeki, S., Yoshihara, S., Uchino, Y., and Yoshimura, H. (1979). [Improved method of the synthesis of 3, 4, 5, 3', 4'-pentachlorobiphenyl (author's transl)]. Fukuoka Igaku Zasshi **70**, 85-87.

229. Safe, S. H. Determination of 2,3,7,8-TCDD toxic equivalent factors (TEFs): Support for the use of *in vitro* AHH induction assay. Chemosphere 16(4), 791-802. 1987.

230. Safe, S. H. Polychlorinated biphenyls (PCBs), dibenzo-p-dioxins (PCDDs), dibenzofurans (PCDFs) and related compounds: environmental and mechanistic considerations which support the development of toxic equivalency factors (TEFs). Crit Rev.Toxicol. 21, 51. 1990.

231. Safe, S. H. (1993). Development of bioassays and approaches for the risk assessment of 2,3,7,8-tetrachlorodibenzo-p-dioxin and related compounds. Environ Health Perspect. **101 Suppl 3**, 317-325.

232. Safe, S. H. (1994). Polychlorinated biphenyls (PCBs): environmental impact, biochemical and toxic responses, and implications for risk assessment. Crit Rev.Toxicol. **24**, 87-149.

233. Safe, S. H. and Krishnan, V. Polychlorinated biphenyls (PCBs), dibenzo-p-dioxins (PCDDs), and dibenzofurans (PCDFs) as antiestrogens in MCF-7 human breast cancer cancer cells: Quantitative structure-activity relationship. Toxicology and Applied Pharmacology 120, 55-61. 1993.

234. Sanderson, J. T., Aarts, J. M., Brouwer, A., Froese, K. L., Denison, M. S., and Giesy, J. P. (1996). Comparison of Ah receptor-mediated luciferase and ethoxyresorufin-O-deethylase induction in H4IIE cells: implications for their use

as bioanalytical tools for the detection of polyhalogenated aromatic hydrocarbons. Toxicol Appl.Pharmacol **137**, 316-325.

235. Saramaki, O., Willi, N., Bratt, O., Gasser, T. C., Koivisto, P., Nupponen, N. N., Bubendorf, L., and Visakorpi, T. (2001). Amplification of EIF3S3 gene is associated with advanced stage in prostate cancer. Am J Pathol. **159**, 2089-2094.

236. Sawyer, T. and Safe, S. (1982). PCB isomers and congeners: induction of aryl hydrocarbon hydroxylase and ethoxyresorufin O-deethylase enzyme activities in rat hepatoma cells. Toxicol.Lett. **13**, 87-93.

237. Schantz, S. L., Seo, B. W., Moshtaghian, J., Peterson, R. E., and Moore, R. W. (1996). Effects of gestational and lactational exposure to TCDD or coplanar PCBs on spatial learning. Neurotoxicol.Teratol. **18**, 305-313.

238. Schecter, A. and Gasiewicz, T. (2003). Dioxin and Health, John Wiley & Sons, Inc, Hoboken, NJ.

239. Schlezinger, J. J. and Stegeman, J. J. (2001). Induction and suppression of cytochrome P450 1A by 3,3',4,4',5-pentachlorobiphenyl and its relationship to oxidative stress in the marine fish scup (Stenotomus chrysops). Aquat.Toxicol **52**, 101-115.

240. Schlezinger, J. J., White, R. D., and Stegeman, J. J. (1999). Oxidative inactivation of cytochrome P-450 1A (CYP1A) stimulated by 3,3',4,4'-tetrachlorobiphenyl: production of reactive oxygen by vertebrate CYP1As. Mol.Pharmacol **56**, 588-597.

241. Schmidt, J. V. and Bradfield, C. A. AH Receptor Signaling Pathways. Annual Review fo Cellular and Developmental Biology 12, 55-89. 1996.

242. Schmidt, J. V., Carver, L, and Bradfield, C. A. Molecular characterization of the murine *Ahr* gene. Journal of Biological Chemistry 268, 22203-22209. 1993.

243. Schmitz, H, Behnisch, P, Hagenmaier, A, Hagenmaier, H, Bock, K, and Schrenk, D. CYP1A1-inducing potency in H4IIE cells and chemical composition of technical mixtures of polychlorinated biphenyls. Environ Toxicol Pharmacol 1, 73-79. 1996.

244. Schramm, K. W., Klimm, C., Hofmaier, A., and Kettrup, A. (2001). Comparison of dioxin-like-response in vitro and chemical analysis of emissions and materials. Chemosphere **42**, 551-557.

245. Schrenk, D., Lipp, H. P., Wiesmuller, T., Hagenmaier, H., and Bock, K. W. (1991). Assessment of biological activities of mixtures of polychlorinated dibenzo-p-dioxins: comparison between defined mixtures and their constituents. Arch.Toxicol **65**, 114-118.

246. Schwirzer, S. M., Hofmaier, A. M., Kettrup, A., Nerdinger, P. E., Schramm, K. W., Thoma, H., Wegenke, M., and Wiebel, F. J. (1998). Establishment of a simple cleanup procedure and bioassay for determining 2,3,7,8-tetrachlorodibenzo-p-dioxin toxicity equivalents of environmental samples. Ecotoxicol.Environ Saf **41**, 77-82.

247. Seegal, R. (1994). The neurochemical effects of PCB exposure are age-dependent. Arch Toxicol **16**, 128-137.

248. Seegal, R. F. (1996). Epidemiological and laboratory evidence of PCB-induced neurotoxicity. Crit Rev Toxicol **26**, 709-737.

249. Selinfreund, R. H., Barger, S. W., Pledger, W. J., and Van Eldik, L. J. (1991). Neurotrophic protein S100 beta stimulates glial cell proliferation. Proc.Natl.Acad.Sci U.S.A **88**, 3554-3558.

250. Seo, B. W., Li, M. H., Hansen, L. G., Moore, R. W., Peterson, R. E., and Schantz, S. L. (1995). Effects of gestational and lactational exposure to coplanar polychlorinated biphenyl (PCB) congeners or 2,3,7,8-tetrachlorodibenzo-p-dioxin (TCDD) on thyroid hormone concentrations in weanling rats. Toxicol.Lett. **78**, 253-262.

251. Shain, W., Bush, B., and Seegal, R. (1991). Neurotoxicity of polychlorinated biphenyls: structure-activity relationship of individual congeners. Toxicol.Appl.Pharmacol. **111**, 33-42.

252. Shain, W., Overmann, S. R., Wilson, L. R., Kostas, J., and Bush, B. (1986). A congener analysis of polychlorinated biphenyls accumulating in rat pups after perinatal exposure. Arch.Environ.Contam Toxicol. **15**, 687-707.

253. Shiota, K. (1976). Postnatal behavioral effects of prenatal treatment with PCBs (polychlorinated biphenyls) in rats. Okajimas Folia Anat.Jpn. **53**, 105-114.

254. Silberhorn, E, Glauert, H, and Robertson, L. Carcinogenicity of of polyhalogenated biphenyls: PCBs and PBBs. Crit Rev.Toxicol. 20, 440. 1990.

255. Slezak, B. P., Hatch, G. E., DeVito, M. J., Diliberto, J. J., Slade, R., Crissman, K., Hassoun, E., and Birnbaum, L. S. (2000). Oxidative stress in female B6C3F1 mice following acute and subchronic exposure to 2,3,7,8-tetrachlorodibenzo-p-dioxin (TCDD). Toxicol Sci. **54**, 390-398.

256. Smart, J. and Daly, A. K. (2000). Variation in induced CYP1A1 levels: relationship to CYP1A1, Ah receptor and GSTM1 polymorphisms. Pharmacogenetics **10**, 11-24.

257. Snyder, R. and Riehle, U. (1979). Classes of hepatic microsomal mixed function oxidase inducers. Pharmacol.Ther. **7**, 203.

258. Sohl, G. and Willecke, K. (2004). Gap junctions and the connexin protein family. Cardiovasc.Res. **62**, 228-232.

259. Speed, T. (2003). Statistical analysis of gene expression microarray data, Chapman & Hall/CRC, CRC Press LLC.

260. Stanton, B., DeWitt, J., Henshel, D., Watkins, S., and Lasley, B. (2003). Fatty acid metabolism in neonatal chickens (Gallus domesticus) treated with 2,3,7,8-tetrachlorodibenzo-p-dioxin (TCDD) or 3,3',4,4',5-pentachlorobiphenyl (PCB-126) in ovo. Comp Biochem.Physiol C.Toxicol.Pharmacol. **136**, 73-84.

261. Swanson, G. M., Ratcliffe, H. E., and Fischer, L. J. (1995). Human exposure to polychlorinated biphenyls (PCBs): a critical assessment of the evidence for adverse health effects. Regul.Toxicol Pharmacol **21**, 136-150.

262. Takagi, Y., Aburada, S., Hashimoto, K., and Kitaura, T. (1986). Transfer and distribution of accumulated (14C)polychlorinated biphenyls from maternal to fetal and suckling rats. Arch.Environ.Contam Toxicol. **15**, 709-715.

263. Takanaga, H., Kunimoto, M., Adachi, T., Tohyama, C., and Aoki, Y. (2001). Inhibitory effect of 2,3,7,8-tetrachlorodibenzo-p-dioxin on cAMP-induced differentiation of rat C6 glial cell line. J.Neurosci.Res. **64**, 402-409.

264. Tang, Y., Donnelly, K. C., Tiffany-Castiglioni, E., and Mumtaz, M. M. (2003). Neurotoxicity of polycyclic aromatic hydrocarbons and simple chemical mixtures. J.Toxicol.Environ.Health A **66**, 919-940.

265. Thomas, P and Hutton, J. Genetics of aryl hydrocarbon hydroxylase inducton in mice: additive inheritance in crosses between C3H/HeJ and DBA/2J. Biochemical Genetics 8, 249-257. 1973.

266. Till, M., Behnisch, P., Hagenmaier, H., Bock, K. W., and Schrenk, D. (1997). Dioxinlike components in incinerator fly ash: a comparison between chemical analysis data and results from a cell culture bioassay. Environ Health Perspect. **105**, 1326-1332.

267. Tillitt, D. and Giesy, J. P. (1991). Characterization of the H4IIE rat hepatoma cell bioassay as a tool for assessing toxic potency of planar halogenated hydrocarbons in environmental samples. Enviorn Sci Technol **25**, 87-92.

268. Tilson, H. A. and Kodavanti, P. R. (1997). Neurochemical effects of polychlorinated biphenyls: an overview and identification of research needs. Neurotoxicology **18**, 727-743.

269. Trosko, JE. Professor of Pediatrics and Human Development, Michigan State University. Scinece Advisory Baord, Toxicogenomic Teleconference. 2004.

270. Tyndale, R., Sunahara, R., Inaba, T., Kalow, W., Gonzalea, F., and Niznik, H. (1991). Neuronal cytochrome P450 IID1 (Debrisoquine/Sparteine-type): potent inhibition of activity by (-)-cocaine and nucleotide sequence identity to human hepatic P450 gene CYP 2D6. Molecular Pharmacology **40**, 63-68.

271. USEPA. Exposure and Human Health Reassment of 2,3,7,8-Tetrachlorodibenzo-p-Dioxin and Related Compounds. EPA/600/P-00/001Bb. 2000. Washington, D.C., Office of Research and Development.

272. USEPA. Polychlorinated Biphenyls (PCBs), PCB Identification, Definitions. US Environmental Protection Agency . 11-6-2003.

273. USEPA. PCB ID - Table of PCB Congeners & Other Species. USEPA . 2004.

274. van den Berg, H., Dejongh, J, and Olson, J. The toxicokinetic metabolism of polychlorinated dibenzo-p-dioxins (PCDDs) and dibenzofurans (PCDFs) and their relevance for toxicity. Crit Rev.Toxicol. 24, 1-74. 1994.

275. van den Berg, M., Birnbaum, L., Bosveld, A. T., Brunstrom, B., Cook, P., Feeley, M., Giesy, J. P., Hanberg, A., Hasegawa, R., Kennedy, S. W., Kubiak, T., Larsen, J. C., van Leeuwen, F. X., Liem, A. K., Nolt, C., Peterson, R. E., Poellinger, L., Safe, S., Schrenk, D., Tillitt, D., Tysklind, M., Younes, M., Waern, F., and Zacharewski, T. (1998). Toxic equivalency factors (TEFs) for PCBs, PCDDs, PCDFs for humans and wildlife. Environ Health Perspect **106**, 775-792.

276. Van Eldik, L. J. and Zimmer, D. B. (1987). Secretion of S-100 from rat C6 glioma cells. Brain Res. **436**, 367-370.

277. Van Melderen, L., Bernard, P., and Couturier, M. (1994). Lon-dependent proteolysis of CcdA is the key control for activation of CcdB in plasmid-free segregant bacteria. Mol.Microbiol. **11**, 1151-1157.

278. Vartiainen, T., Jaakkola, J. J., Saarikoski, S., and Tuomisto, J. (1998). Birth weight and sex of children and the correlation to the body burden of PCDDs/PCDFs and PCBs of the mother. Environ.Health Perspect. **106**, 61-66.

279. Velculescu, V. E., Zhang, L., Vogelstein, B., and Kinzler, K. W. (1995). Serial analysis of gene expression. Science **270**, 484-487.

280. Vena, J. E., Buck, G. M., Kostyniak, P., Mendola, P., Fitzgerald, E., Sever, L., Freudenheim, J., Greizerstein, H., Zielezny, M., McReynolds, J., and Olson, J. (1996). The New York Angler Cohort Study: exposure characterization and reproductive and developmental health. Toxicol.Ind.Health **12**, 327-334.

281. Vezina, C. M., Walker, N. J., and Olson, J. R. (2004). Subchronic Exposure to TCDD, PeCDF, PCB126, and PCB153: Effect on Hepatic Gene Expression. Environ Health Perspect **112**, 1636-1644.

282. Vreugdenhil, H., Slijper, F, Mulder, P, and Weisglas-Kuperus. Effects of Perinatal Exposure to PCBs and Dioxins on Play Behavior in Dutch Children at School Age. Environmental Health Perspectives 110(10), A592-A598. 2004.

283. Wang, S. L., Lin, C. Y., Guo, Y. L., Lin, L. Y., Chou, W. L., and Chang, L. W. (2004). Infant exposure to polychlorinated dibenzo-p-dioxins, dibenzofurans and biphenyls (PCDD/Fs, PCBs)--correlation between prenatal and postnatal exposure. Chemosphere **54**, 1459-1473.

284. Warner, M. and Gustafsson, J. (1995). Cytochrome P450 in the brain: neuroendocrine functions. Frontiers in Neuroendocrinology **16**, 224-236.

285. Weber, L. W. and Greim, H. (1997). The toxicity of brominated and mixed-halogenated dibenzo-p-dioxins and dibenzofurans: an overview. J.Toxicol.Environ.Health **50**, 195-215.

286. Wehler, K, Jonsson, E, Bergman, A, Brandt, I, and Darnerud, P. 3,3',4,4'-Tetrachlorobiphenyl and 3,3',4,4',5-pentachlorobiphenyl tissue-localization and metabolic fate in the mouse. Chemosphere 19(1-6), 809-812. 1989.

287. Wei, Y., Bergander, L., Rannug, U., and Rannug, A. (2000). Regulation of CYP1A1 transcription via the metabolism of tryptophan- derived 6-formylindolo[3,2-b]carbazole. Arch.Biochem.Biophys. **383**, 99-107.

288. Weisglas-Kuperus, N. (1998). Neurodevelopmental, immunological and endocrinological indices of perinatal human exposure to PCBs and dioxins. Chemosphere **37**, 1845-1853.

289. Weiss, C., Kolluri, S. K., Kiefer, F., and Gottlicher, M. (1996). Complementation of Ah receptor deficiency in hepatoma cells: negative feedback regulation and cell cycle control by the Ah receptor. Exp.Cell Res. **226**, 154-163.

290. Widholm, J. J., Clarkson, G. B., Strupp, B. J., Crofton, K. M., Seegal, R. F., and Schantz, S. L. (2001). Spatial reversal learning in Aroclor 1254-exposed rats: sex-specific deficits in associative ability and inhibitory control. Toxicol.Appl.Pharmacol. **174**, 188-198.

291. Willecke, K., Hennemann, H., Dahl, E., Jungbluth, S., and Heynkes, R. (1991). The diversity of connexin genes encoding gap junctional proteins. Eur.J.Cell Biol. **56**, 1-7.

292. Winningham-Major, F., Staecker, J. L., Barger, S. W., Coats, S., and Van Eldik, L. J. (1989). Neurite extension and neuronal survival activities of recombinant S100 beta proteins that differ in the content and position of cysteine residues. J Cell Biol. **109**, 3063-3071.

295. Yamashita, F. and Hayashi, M. (1985). Fetal PCB syndrome: clinical features, intrauterine growth retardation and possible alteration in calcium metabolism. Environ.Health Perspect. **59**, 41-45.

296. Yang, J., Shin, D., Park, S., Chang, Y., Kim, D., and Ikonomou, M. G. (2002). PCDDs, PCDFs, and PCBs concentrations in breast milk from two areas in Korea: body burden of mothers and implications for feeding infants. Chemosphere **46**, 419-428.

297. Yoshimura, H., Yoshihara, S., Ozawa, N., and Miki, M. (1979). Possible correlation between induction modes of hepatic enzymes by PCBs and their toxicity in rats. Ann.N.Y.Acad.Sci **320**, 179-192.

298. Zennegg, M, Schmid, P, Gujer, E, and Kuchen, A. PCDD, PCDF, and Dioxin-Like PCB in Fish from Swiss Lakes. 2004. Swiss Federal Office of Public Health.

299. Zhao, F., Mayura, K., Harper, N., Safe, S. H., and Phillips, T. D. (1997). Inhibition of 3,3',4,4',5-pentachlorobiphenyl-induced fetal cleft palate and immunotoxicity in C57BL/6 mice by 2,2',4,4',5,5'-hexachlorobiphenyl. Chemosphere **34**, 1605-1613.